KAPLAN, DAVID JOEL

CHANGES IN THE MACROMOLECULAR PROPERTIES OF DNA INDUCED BY MITOMYCIN C

City University of New York PH.D. 1979

PLEASE NOTE:

In all cases this material has been filmed in the best possible way from the available copy. Problems encountered with this document have been identified here with a check mark ✓.

1. Glossy photographs _____
2. Colored illustrations _____
3. Photographs with dark background ✓
4. Illustrations are poor copy _____
5. Print shows through as there is text on both sides of page _____
6. Indistinct, broken or small print on several pages ✓ throughout _____
7. Tightly bound copy with print lost in spine _____
8. Computer printout pages with indistinct print _____
9. Page(s) _____ lacking when material received, and not available from school or author _____
10. Page(s) _____ seem to be missing in numbering only as text follows _____
11. Poor carbon copy _____
12. Not original copy, several pages with blurred type _____
13. Appendix pages are poor copy _____
14. Original copy with light type _____
15. Curling and wrinkled pages _____
16. Other _____

University Microfilms International

300 N. ZEEB RD., ANN ARBOR, MI 48106 (313) 761-4700

CHANGES IN THE MACROMOLECULAR PROPERTIES OF DNA INDUCED BY MITOMYCIN C

by

David Joel Kaplan

A dissertation submitted to the Graduate Faculty in Biochemistry in partial fufillment of the requirements for the degree of Doctor of Philosophy, The City University of New York

1979

Approval Page

This manuscript has been read and accepted for the Graduate Faculty in Biochemistry in satisfaction of the dissertation requirement for the degree of Doctor of Philosophy.

8/21/79
date

Maria Tomasz
Chairman of Examining Committee

8/22/79
date

Aaron Lerner
Executive Officer

Dr. Joseph Krakow

Dr. James Wetmur

Dr. Charlotte Russell

Dr. Horst Hoyer

Supervisory Committee

The City University of New York

TABLE OF CONTENTS

TABLE OF CONTENTS

ABSTRACT

CHANGES IN THE MACROMOLECULAR PROPERTIES OF DNA INDUCED BY MITOMYCIN C

by

David Joel Kaplan

Advisor: Professor Maria Tomasz, Ph.D.

An increase in the coefficient of sedimentation, and a reduction in the reduced viscosity for unsonicated DNA occurs when it is complexed with the drug mitomycin C (MC). The altered hydrodynamic properties, when correlated with the substantial decreases seen in the electrophoretic mobilities of these complexes, indicate a coiling or bending of DNA with the resulting effect of a decrease in the radius of gyration for DNA in the complex. This interpretation of the results is supported by the direct electron microscopic observations of these DNA-MC complexes which demonstrate a significant coiling of DNA in the complex relative to the uncomplexed DNA or control. A contrast is seen when these findings are compared with the results obtained from similar experiments using DNA-MC complexes formed from the sonicated, or rod-like, form of DNA. Contrary to the results for the unsonicated complexes, sonicated complexes exhibit an increase in the reduced viscosity, marginal decreases in the electrophoretic mobilities, and no change in the coefficients of sedimentation, and in appearance under the electron microscope. These comparisons indicate, then, a molecular weight

or size dependent change in DNA properties which is acquired upon the binding of MC to DNA.

The crosslinking of DNA is implicated as the most likely cause for the increases in the melting temperatures and melting breadths observed in the DNA-MC complexes. As the binding ratio range (.10-.15) appears to be a likely saturation point for possible crosslinking sites in calf thymus DNA, it also is a leveling off point indicating maximum decreases in the viscosity and electrophoretic mobilities for the unsonicated DNA-MC complexes. The correlations between these variables suggests strongly that the bifunctional (crosslinking) binding of mitomycin C to DNA is responsible for the observed conformational changes. A likely possibility is that some molecules fix DNA into looped forms by binding distant parts of DNA together. An alternative possibility for these changes is a non-covalent self aggregation of distant heavily mitomycin C-bound segments of DNA.

Another set of findings resulted from the analysis of size-independent changes in DNA properties. It was shown that the crosslinks not only cause reversible denaturation in DNA but also cause an increase in the temperature required for DNA strand separation. It was also deduced, through flow dichroism measurements, that mitomycin C is not bound to DNA by intercalation.

ACKNOWLEDGEMENT

I would like to express my thanks to Dr. Maria Tomasz, my thesis advisor, for her help throughout the course of this study. Her continuous support and encouragement will be remembered. In regard to the late Dr. Hsueh Jei Li, my former physical biochemistry insructor, a special thanks is given for his encouragement and inspiration. The stimulating and interesting discussions with my laboratory colleagues, particularly Roselyn Lipman, Richard Pelc, Janet Weaver, and Carmen Mercado are also acknowledged.

LIST OF TABLES

page

LIST OF FIGURES

page

page

page

page

LIST OF PLATES

page

INTRODUCTION

The mitomycins are a series of chemically related antibiotics produced by Streptomyces verticillatus (Lefemine et al., 1962), and related species of yeast (Kirsh, 1967). The most studied member of the mitomycins is mitomycin C (MC)[1], a known and potent antibiotic (Iyer and Szybalski, 1963), mutagen (Szybalski, 1958), carcinogen (Kawawata et al., 1966), antitumor agent (Hata et al., 1956), lysogenic inducer (Otsuji et al., 1959; Korn and Weissbach, 1962), and agent known to stimulate the expression of inserted genes in Col E_1 plasmids (e.g. as in the case of inserted tryptophan synthetase $\propto$ gene from Salmonella (Selker et al., 1977). Mitomycin C is known also to selectively inhibit DNA synthesis (Shiba et al., 1959). This inhibition which is accompanied by DNA degradation (Kersten and Rauen, 1961) was correlated with an observed enhancement of magnesium dependent DNAase activity in MC[1]-treated cells (Reich et al., 1961). It has been shown furthermore that the template activity of DNA treated with mitomycin C is significantly reduced for both RNA and DNA polymerases in vitro (Pricer and Weissbach, 1965). Studies of DNA treated in vivo with MC, however, show a reduced template activity only for the DNA polymerases (Pricer and Weissbach, 1964).

On the molecular level it has been shown that mitomycin C is relatively inert to DNA in vitro, unless it is activated in situ by a cell free extract, in the presence of NADPH or by chemical reducing agents (e.g. sodium dithionite ($Na_2S_2O_4$), and sodium borohydride ($NaBH_4$)), demonstrating that in the cell this

drug is activated metabolically (Iyer and Szybalski, 1964). It has been demonstrated furthermore (Matsumato and Lark, 1963; Iyer and Szybalski, 1963) that exposure of bacterial cells to MC leads to the covalent crosslinking of the complementary strands of bacterial DNA. The degree of such crosslinking has been shown to increase with increasing GC content of DNA (Szybalski and Iyer, 1964b). In addition to the crosslinks, it is noted that mitomycin C binds to DNA monofunctionally (Szybalski and Iyer, 1964a; Weissbach and Lisio, 1965); a form of binding that is about ten times more prevalent than the number of crosslinking chromophores This binding is also covalent and guanine specific, as established by binding studies using synthetic polynucleotides (Tomasz et al., 1974) and DNAs of varying GC content (Lipman et al., 1978). At excessive drug concentration, however, strong electrostatic binding of mitomycin C to nucleic acids is observed in addition to the covalent binding, resulting ultimately in 1:1 drug/nucleotide ratio in the complex. No base specificity was detected for this electrostatic non-covalent binding (Lipman et al., 1978). It is also important to point out that the crosslinks were originally suggested to be the direct cause of the observed inhibition of DNA synthesis and death of bacteria upon exposure to the drug (Iyer and Szybalski, 1963). More recently the predominant monofunctional binding has also been implicated as biologically

significant in the damage to DNA (Weiss et al., 1968; Kinoshita et al., 1971; Mercado and Tomasz, 1972; Small et al., 1976).

The chemical nature of the covalent interaction between the reduced MC molecule and DNA is still largely unknown. Iyer and Szybalski (1964) presented a detailed hypothesis for the reductive activation of MC as follows:

Scheme 1:

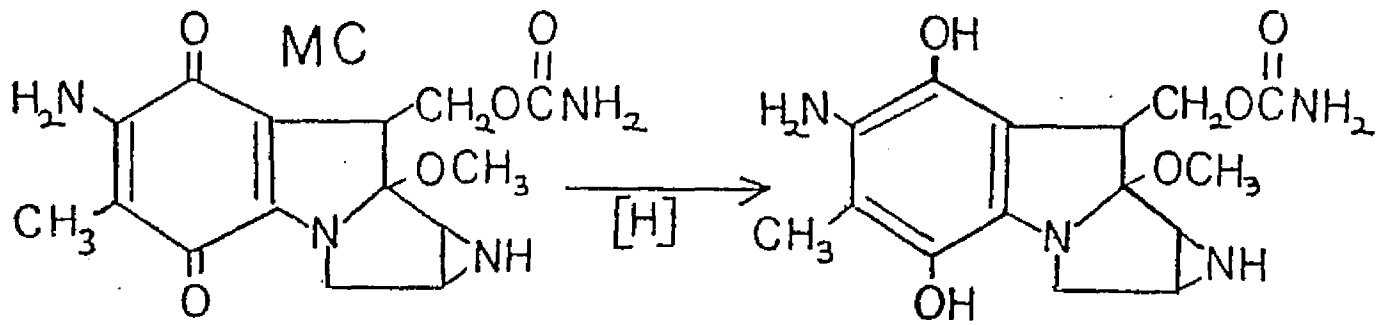

(λ_{max} 367 nm & 220 nm)

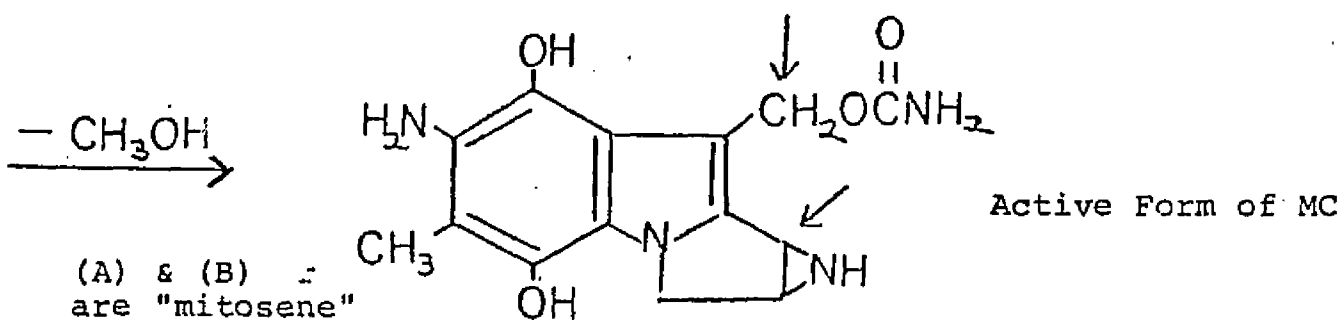

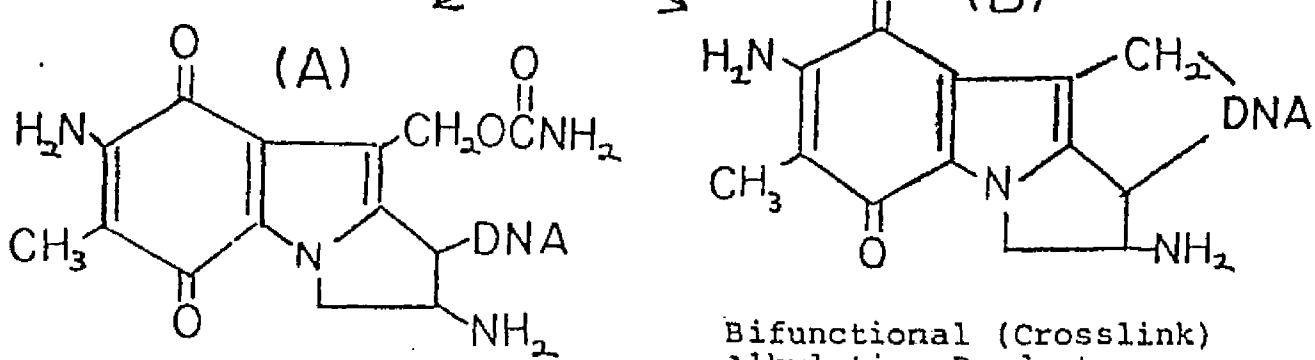

Monofunctional Alkylation Product

Bifunctional (Crosslink) Alkylation Product

According to this hypothesis, reduction and loss of CH_3OH activates the carbamate function and the aziridine ring into alkylating groups which will react with nucleophilic groups of DNA. Only the following indirect evidence exists to date for this scheme, however: DNA-bound MC has the ultraviolet spectra corresponding to the characteristic mitosene chromophore (λ_{max} 310, 248 nm) rather than to mitomycin C (λ_{max} 367, 220 nm; scheme 1(Tomasz et al., 1974)). Aziridine lacking analogs bind monofunctionally but cannot crosslink DNA (Otsuji and Maruyama, 1972; Tomasz et al., 1974; Lipman et al., 1978), indicating that one of the binding sites is absent from the drug molecule. It has also been shown that the aziridine ring is needed for the guanine specificity of the binding (Lipman et al., 1978).

While work on these chemical aspects has been in progress in our laboratory, knowledge of the physico-chemical characteristics of the DNA-MC complex is lacking. In the case of many other drug-DNA interactions the changed physico-chemical properties of DNA have given valuable information about the nature of the interaction. The case of intercalating drugs is a well known example where viscosity, helix stability, flow dichroism measurements etc. have been used to recognize intercalation. Another is the case of bleomycin where ultracentrifuge studies led to recognition of its DNA-cleaving action (Haidle, 1971). It was then the purpose of the present work

to physically characterize the DNA-MC complex with the aim of understanding better its chemical nature and to possibly relate the nature of any DNA structural changes found in these complexes to the biological phenomena caused by mitomycin C.

Materials

E.Coli K_{12} DNA was obtained from General Biochemicals, Chagrin Falls, Ohio and further purified by digestion with ribonuclease T_1 (ca. 40 units/ml in a 1 mg/ml of DNA solution in DSC[1] (1/10 SSC)[1], 1 hr. at 37°C), followed by precipitation and repeated deproteinization by $CHCl_3$ according to Marmur (1961). Calf thymus DNA (same source and also Worthington) was treated similarly. Pneumococcal DNA (gift of Alexander Tomasz, Rockefeller University) was prepared from wild type strain of Diplococcus pneumoniae as described by Hotchkiss (1957). Pneumococcal ^3H-labeled DNA was prepared by biosynthetic labeling in a medium supplemented with ^3H-thymidine. The activity of the stock sample of pneumococcus DNA was $3.9X10^8$ cpm/ml. Sonication of calf thymus DNA, where indicated, was carried out in either a Branson model W 140 sonicator at 60 power or in a Branson model W 185 sonicator at 100 watts, with a large sonicating head in a Rosette cell under cooling in an ice bath for 7 two minute intervals and 1 one minute interval with one minute intervals between sonications. By viscometry (see methods) the average molecular weight of the sonicated calf thymus DNAs depended upon the sonicator type used: when sonicated by the Branson W 185 the molecular weight was approx. $1.7X10^5$ daltons, sonication by the Branson W 140 gave molecular weights of 3.8-$5.0X10^5$ daltons. Pneumococcal DNA as prepared by the Hotchkiss

procedure had a molecular weight average of approximately 10^7 daltons. Unsonicated calf thymus DNA had a molecular weight average of approximately $5X10^6$ daltons.

Alkali denaturation of DNA was obtained by the addition of 3N NaOH to a DNA solution to pH 12.7 and stirring for 10 min., followed by neutralization with 1N HCl and dialysis into either .017 M phosphate (pH 7.4) or DSC[1]. Heat denaturation was achieved by heating a DNA solution in the latter buffer at 100°C for 10 min. and then quickly cooling in an ice bath.

Mitomycin C and Analogs: Mitomycin C was purchased from Kyowa Hakko Kogyo Co., Tokyo, Japan. Compound A (MC hydrolysis product) was prepared from MC by the procedure of Taylor and Remers (1975).

DNA-MC Complexes: As a standard method for the formation of DNA-mitomycin C complexes in vitro the following procedure of reductive activation was used: Depending upon the extent of desired binding ratio the appropriate quantity of mitomycin C was added to 2 umoles of DNA in a solution of .017 M phosphate buffer, pH 7.4. (The total volume of the reaction mixture was 3.0 ml). (See figure 1 for the binding ratio as determined by the ratio of MC to DNA in the reaction mixture.) This solution was then in turn de-

aerated by bubbling He gas (Matheson, research grade, 99.999% pure) through the solution for 20 min. Then .02 M $Na_2S_2O_4$ (sodium dithionite (a reducing agent) freshly prepared by adding the solid to H_2O deaerated by the same procedure) was added, via an appropriate Hamilton syringe, in 1.5 molar excess to the antibiotic in five equal portions, at 5 min. intervals. He bubbling continued for 5 minutes after the last addition, then the mixture (pale yellow) was exposed to air. The purple color of the reoxidized antibiotic returned quickly. The nucleic acid-antibiotic complex was isolated through gel filtration using Sephadex G-100 equilibrated in DSC.

DNA-Compound A Complexes: The procedure for the formation of DNA-compound A complexes was identical to that outlined for DNA-MC complexes except for the following: for reactions using sonicated DNA and compound A, heating of DNA and the compound separately at 37°C was necessary in order to prevent slight precipitation of DNA that tended to occur when these reactants were mixed. Despite these precautions, complexes of unsonicated DNA and compound A could not be made due to the significant precipitation that occurred when these reactants were mixed.

Binding Ratios: Binding ratios are defined as mole antibiotic bound per mole mononucleotide. The binding ratios of the complexes were determined by phosphate analysis (Ames and

Dubin, 1960) or UV absorbance at 260 nm for the nucleic acid and by UV absorbance at 310 nm for the bound drug (molar extinction coefficient for bound MC = 11,500 liters^{-1}moles^{-1}cm^{-1} and bound compound A = 11,400 liters^{-1}moles^{-1}cm^{-1} (Tomasz et al., 1974)). The Gilford 250 spectrophotometer was used for absorbance readings.

Other DNA Complexes: The formation of nitrous acid (HNO_2) crosslinked DNA was made possible by following the procedure of Geiduschek (1961).

Polyvinylsulfate-mitomycin complexes were prepared following the procedure of Lipman, Weaver, and Tomasz (1978).

Actinomycin-DNA (sonicated calf thymus) complexes were prepared by mixing predetermined proportions of actinomycin-D (Boehringer-Mannheim) and DNA together in DSC as indicated by binding isotherms of Müller and Crothers (1968).

Ethidium-DNA complexes of varying binding ratios were prepared by mixing predetermined proportions of ethidium bromide and native calf thymus unsonicated DNA in DSC as outlined Aktipis and Kindelis (1973).

DNA Complexes Formed in the presence of Catalase and Superoxide Dismutase: The procedure was the same as described for DNA-MC complexes except that 100 μg of each enzyme (Worthington) per μmole of DNA was added to the reaction mixture (pH 7.4) prior to the addition of sodium dithionite ($Na_2S_2O_4$).

DNA Complexes Formed in the Presence of Catalase (for viscosity experiments): Stock solution of catalase (5760 units/ml or 5.76 units/μl) was prepared by taking 10 mg catalase and dissolving in 2.0 ml of .0425 M phosphate buffer (pH 7.4). One ml of this solution in turn was diluted to 5 ml with distilled H_2O. The set of reactions (all requiring the 5 step reductive activation procedure as described) used in this experiment are as follows: (a) 3 μmoles $Na_2S_2O_4$ + 2 μmoles DNA + 2 μmoles MC, (b) same + 80 μl catalase, (c) same as (a) minus MC, and (d) same as (c) + 80 μl catalase.

DNA Melting and Cooling Curves, Calculation of Fraction of Crosslinked DNA: DNA melting and cooling curves were taken on a Gilford 240 spectrophotometer with heating compartment connected to a Haake heater (Haake Inst., New Jersey), liquid circulating pump and thermostat unit. A Honeywell chart recorder (Honeywell, Ft. Washington, Pa.) connected to the Gilford recorded the absorbance and temperature of 3 samples (buffer, control and DNA complex) at 3 second intervals. The fraction of crosslinked DNA was calculated from the extent of reversibility of the melting curve on cooling using 50% methanol/50% DSC buffer, pH 7.4 according to Geiduschek (1961). The equation used is:

$$\text{Fraction Crosslinked} = \frac{f_s - f_c}{1 - f_c}$$

f_s = fractional loss of hyperchromicity of melted sample (complex) upon cooling to 30°C.
f_c = fractional loss of hyperchromicity of melted control upon cooling to 30°C (Geiduschek, 1964)

The reproducibility of results was better using 50% methanol/50% DSC buffer than using aqueous buffers. However, aqueous buffer (DSC) was used for T_m (melting temperature) and m.b. (melting breadth) determinations of DNA samples. The absorbance (A_{260}) of the DNA-MC complex was corrected for bound drug absorbance at 260 nm by subtracting 1.34 X the total 310 nm absorbance of the complex from its total 260 nm absorbance (A_{260}).[2]

Chromatography: Silica gel plates (Macherey-Nagel +10 40X80 mm polygram Sil G/UV 254) for thin layer chromatography were run with either absolute methanol, or isopropanol:1% NH_4OH (2:1)

For Sephadex G-25 chromatography .01 M NH_4HCO_3 buffer was used.

Viscosity of DNA Complexes: The viscosities of various nucleic acid solutions were measured in a Zimm-Crothers (Zimm and Crothers, 1962) model A rotary viscometer (Beckman). The average shear stress for DNA solutions of 25 µg/ml was no more than .015 dynes/cm^2 (Zimm and Crothers, 1962). Measurements for turbulance (Taylor, 1936) were negative with the rotor speed and concentrations of DNA used. Constant temperature for the apparatus was provided by a MGW Lauda-thermostat and pump (Messgerate-Werk Lauda) connected via tubing to the water jacket of the viscometric apparatus. The buffer used for all viscometric experiments was DSC[1] and $9X10^{-4}$ M EDTA; pH 7.4. Concentrations of nucleic acid solutions used varied depending upon the size of

DNA sample (e.g. for sonicated DNA, the concentrations were from 0.40 to 1.20 mg/ml, where for larger DNA (unsonicated) the concentrations used were from 0.01 to 0.05 mg/ml). The intrinsic viscosity $[\eta]$ of each sample was found in the following way: The relative viscosities of an individual sample at several different concentrations were calculated (the time in seconds for 15 revolutions of the rotor for a sample divided by the time for the same number of revolutions of the rotor for buffer alone). The division of specific viscosity (relative viscosity - 1) by the DNA concentration gave the reduced viscosity (dl/gm). The plotting of the reduced viscosity (ordinate) against concentration (abscissa) in gm/dl $X10^{-4}$ for several different concentrations gave a linear plot (with the aid of linear analysis by Texas Instrument SR-51 calculator). The Y intercept of this plot, which is the reduced viscosity of the DNA sample at infinite dilution, is the intrinsic viscosity or the viscosity of the molecule itself. The molecular weights of unsonicated nucleic acid samples were calculated by the Zimm-Crothers modification (Crothers and Zimm, 1965) of the Mandelkorn-Flory equation (Mandelkorn and Flory, 1952):

$$.665 \log \text{M.W.} = 2.863 + \log([\eta] + 5)$$

The molecular weights of sonicated DNA above $3X10^5$ daltons were calculated by the equation of Doty, McGill and Rice (1958):

$$[\eta] = 1.45X10^{-6} \log \text{M.W.}^{1.12}$$

The molecular weights of sonicated DNA below $2X10^5$ daltons were calculated by the equation from Eigner and Doty (1965):

$$[\eta] = 1.05X10^{-7}M.W.^{0.132}$$

Moderate corrections for molecular weight determined by the above equations was achieved through the use of the Cox equation (Cox, 1960; Douthart and Bloomfield, 1968):

$$\frac{[\eta]}{[\eta^0]} = \left(\frac{C}{C^0}\right)^{-m}$$

$[\eta]$ = intrinsic viscosity of DNA
C = concentration of salt
m = slope from log (Na^+) vs. log$[\eta]$ plot for specific DNA (Douthart and Bloomfield, 1968)
0 = Superscript zero denotes some reference solution.

This equation allows for changes, by variations in salt concentrations, on DNA molecular length.

Fractionation of Sonicated DNA by Sucrose Density Gradient Ultracentrifugation: Fractionation of polydisperse (heterogeneous in M.W.) sonicated DNA (calf thymus) was achieved by ultracentrifugation on discontinuous sucrose gradients following the procedure of Godfrey (1976). Sucrose (ultrapure density gradient grade; Schwarz/Mann Becton) solutions of 20%, 15%, 10% and 5% were hand layered as described by Brakke and Pelt (1970) into 6 (38.5 ml) polyallomar tubes (Beckman, Spinco Division). The buffer used was .017 M phosphate, pH 7.4. One ml of sonicated DNA (conc. = 1 mg/ml) in the same buffer was then carefully layered over the discontinuous gradients. Then an

appropriate quantity of paraffin oil (Fisher) was layered over this until 1 mm below top of polyallomar tubes. All tubes were balanced to within 0.1 gm before centrifugation. The rotor used was SW 27 (Beckman, Spinco Division). The centrifuge used was an L3-50 Beckman. The speed of run was 25,000 r.p.m. at 14°C using high acceleration and deceleration as suggested (Beckman manual for L3-50) for large tubes to prevent wobbling due to velocity changes. The time of run was 48 hours. After centrifugation tubes were punctured by a Buchler piercing unit and the fractions (78 drops per tube) were collected in 30 tubes via a Gilson fraction collector. Fractions from tubes were read at 260 nm in Gilford 250 spectrophotometer. Plots of DNA concentrations (in $O.D._{260}$ units) vs. tube number gave reproducible sedimentation peaks. Appropriate peaks were pooled and dialyzed.

Ultracentrifugation of DNA-Mitomycin C Complexes in Sucrose Density Gradients: Sedimentation of DNA-MC complexes were done in continuous density gradients made by the technique as outlined by Brakke (1970). The conditions for centrifugation were the same as outlined for the fractionation of sonicated DNA except that for unsonicated DNA, the time of the runs was less (9-24 hours). The sample size was 1 ml of DNA (1 μmole/ml) solution. Via the puncturing device and fraction collector, samples were collected into 40 tubes (58 drops of sucrose per tube). Distance of peaks from the top of gradient was calculated by the relationship of 0.1 cm per

0.50 mls of sucrose collected as measured according to the SW 27 polyallomar tube. Corrections for volume difference due to the convexing at bottom of tube, where volume per distance changes, was taken into account. The concentrations of DNA in fractionated samples were measured via their optical densities at 260 nm. When ^{3}H-labeled DNA was used, the activity, in counts per minute (tritium) was measured in a Unilux Nuclear Scintillation counter. For these measurements 10 ml of New England Nuclear Aquasol-2 cocktail was mixed with 1 ml of DNA solution.

Ultracentrifugation in Alkaline Sucrose Density Gradients:

These gradients were prepared in the same manner as described for neutral gradients except that the individual stock solutions varying in sucrose concentrations were adjusted to pH 12 with NaOH prior to the formation of the gradients. The samples for sedimentation in alkali were adjusted to pH 12.7 immediately prior to their application unto the gradients. The polyallomar tubes, as previously described, were pierced and fractionated into 40 test tubes. DNA concentrations were determined spectrophotometrically at 260 nm while taking into account the slight absorption of the blank at this wavelength due to the presence of alkali.

Flow Dichroism of DNA-MC Complexes: These measurements were carried out by me in the laboratory of Dr. E. Gabbay, Univers-

ity of Florida. Flow dichroism measurements were carried out at 260 nm or 310 nm using the Cary 17D spectrophotometer with a Glan-Taylor calcite polarizing prism. DNA-MC complex solutions (1.5-1.8 mM) were allowed to flow through a quartz capillary (0.415 mm radius) via a Sage syringe pump (model 341, Sage Instruments). The shear rate for all experiments varied from 65 to 2573 sec^{-1}. Spectra were taken with polarizing beam at 0° (parallel) relative to flow of solution and at 90° (perpendicular) relative to flow of solution. The reduced dichroism in units of absorbance at either 260 nm or 310 nm was calculated according to the equation of Gabbay et al. (1976b)

(1) $$\text{Reduced Dichroism} = \frac{A\perp_\lambda - A\parallel_\lambda}{A_\lambda}$$

λ = 260 nm or 310 nm

$A\perp_\lambda$ = absorbance perpendicular to flow

$A\parallel_\lambda$ = absorbance parallel to flow

A_λ = absorbance of stationary solution

The reduced dichroism corrected for bound drug absorbance in the 260 nm region utilizes the following equation:

(2) $$\text{Reduced Dichroism} = \frac{(A\perp_{260} - 1.34\,A\perp_{310})\ (A\parallel_{260} - 1.34\,A\parallel_{310})}{(A_{260} - 1.34 A_{310})}$$

A_{310} = absorbance at 310 nm due to bound drug

$1.34 A_{310}$ = A_{260} of bound drug alone

$A_{260} - 1.34\,A_{310}$ = A_{260} of DNA alone

The shear rates for flow dichroic studies were calculated by the equation from Davidson (1959):

(3) $$\text{Shear Rate} = \frac{8V}{3\pi r^3 t}$$

r = capillary radius

V = volume of flow in time (t)

Volume (V) per time (sec.) on Sage syringe pump were at these positions:
.2167, .1117, .0517, .0233, .0117, and .0055 ml/sec.

Gel Electrophoresis: The method of gel electrophoresis used was that of Dewachter and Fiers (1971). The vertical electrophoresis slab apparatus with upper and lower reservoirs was employed. The power supply used to provide current to gels was a SP-17A Heath Schlumberger power unit. The voltage applied was 90 volts (approx. 9 volts/cm gel) with a current of approximately 15 milliamps. All electrophoresis runs were made at room temperature.

Agarose Gels: Buffer used was a 1:25 dilution of 1 M Tris, 0.5 M sodium acetate, 50 mM sodium EDTA (adjusted to pH 7.2 with acetic acid). 1.8% agarose gel was prepared by placing 1.8 gm of agarose (Seakem Marine Colloids) into 100 ml of the buffer. This mixture was then boiled until the agarose dissolved completely. Gels were ready for use approximately 1/2 to 3/4 hrs. later.

Polyacrylamide Gels: Buffer used was 1XTEB (10XTEB is 108 gm Tris, 9.3 gm disodium EDTA, and 55 gm borate per liter of solution, pH 8.3). 3.5% polyacrylamide gels were made by mixing 7.5 mls of 10XTEB, 8.75 mls of 30% acrylamide solution (29 g acrylamide + 1 g of N,N′-methylene bisacrylamide/100 ml), 3 mls of 1.6% ammonium persulfate (freshly prepared) and adding distilled water to a final volume of 75 mls. After degassing, the solution was polymerized by the addition of 25 ul of N,N,N′,N′-tetramethylethylene-diamine (TEMED, catalyst). Polymerization of this dilute gel took 1/2 to 3/4 hour. However, the gel was not used until 1.5 to 2.0 hrs. after layering gel so as to ensure complete polymerization.

Layering of Samples: 20 µl of DNA (DNA conc. = 2.0 $O.D._{260}$/ml) solution in DSC buffer was mixed with 5 ul of sucrose solution (8% sucrose + .025% bromophenol blue as indicator) and was layered over appropriate slots via capillary tubing. Both upper and lower resevoirs contained the appropriate buffer (Tris and TEB, respectively for agarose and polyacrylamide electrophoresis).

Electrophoretic Runs: Runs were commenced by turning on voltage with the anode in bottom reservoir and cathode on top and current through gel. The time of runs for unsonicated DNA was approximately 9 hrs. (the exact times were noted to calculate mobilities) and approximately 2 hrs. for sonicated DNA samples.

Staining and Photography of Gels: After terminating the run, the gel slab was placed in a glass tray containing 500 ml of TEB buffer solution and .1 ml ethidium bromide (5 g/l) for ½ hour to stain DNA. Gels were then washed with distilled water. In the dark under UV light the fluorescent DNA bands were photographed by a Polaroid Land 195 camera stand system using close-up lense and red gelatin filter. The film used was # 107 Polaroid. Exposure time depended upon brightness (as determined by distance) of UV lamp and bands, but was usually 30 seconds using f-8 stop in camera.

Distances Moved by Bands: Distances were measured by metric ruler. Relative mobility was taken as the distance traversed by sample band (midpoint of band) in millimeters divided by distance traversed in gel by control (native DNA). Mobilities were calculated in units of cm^2/volt·sec. by multiplying distance traversed by sample in centimeters by the height of gel (cm) and dividing this by the voltage and the time of run in seconds.

Molecular Weight Determination by Electrophoresis: Molecular weights of DNA samples used in electrophoresis runs were estimated by their distance migrated in gels relative to that of standard DNA fragments of known molecular weight. The standard DNA was f_1(RFI) viral DNA digested with RHae III restriction enzyme (kindly supplied by Dr. Ken Horiuchi of Rockefeller University). The molecular weights of these fragments were 1.90, 1.18, 0.59, 0.09, 0.07, and 0.05 million daltons respectively

(Horiuchi, 1975). The molecular weights of various DNA samples were estimated from the linear plot of log M.W. vs. mobility of the standard fragments (Maniatis, 1975; Peacocke and Dingman, 1971).

Electron Microscopy: These experiments were performed in the laboratory of Dr. Alexander Tomasz at Rockefeller University, New York, with the help of Ms. Maria Fazio.

The electron microscopy of DNA-MC complexes and appropriate control DNAs were performed with a Sieman's 101 electron microscope at magnifications of 25,000X to 50,000X. Davis and Hyman's version (Davis and Hyman, 1971) of the Kleinschmidt procedure (KLeinschmidt and Zahn, 1959) was used for the preparation and spreading of DNA samples for electron microscopy. DNA-MC complexes for electron microscopy were made following the standard procedure as outlined in the methods. For DNA samples prepared in the presence of the enzymes catalase and superoxide dismutase (see methods) a subsequent deproteinization by chloroform was performed (Marmur, 1961). The final concentration of DNA in the samples used in these electron microscopy procedures was 0.5 μg/ml.

RESULTS

Thermal Denaturation Experiments at 260 nm

The thermal denaturation profiles of the MC complexes of calf thymus sonicated and unsonicated DNA, and of E.Coli DNA in DSC buffer are displayed in figs. 2,3, and 4, respectively, along with controls. One of the several and distinguishing characteristics of the various DNA-MC complexes is the ability to renature spontaneously upon cooling, depending upon the extent of drug binding (binding ratio; tables 1 and 2).

A second pattern is the increase of T_m (temperature of melting or midpoint of DNA hyperchromic rise) of the complexes relative to their controls. As shown in fig.5, the ΔT_m (T_m difference between complex and control) in aqueous buffer, increases with greater binding ratio of the complex and levels off at a maximum value (between 7 and 9°C) near binding ratio 0.10-0.15 for both calf thymus and E.coli DNAs.

A third characteristic present in these melting profiles is the increase in the melting breadth (defined as the temperature interval between 10 and 90% melted DNA (Dove and Davidson, 1962)) with increasing binding ratio for these complexes relative to their controls (see fig.6 and 7). The curves for Δ m.b. vs. binding ratio (fig.7) and ΔT_m vs. binding ratio (fig.5) are quite similar.

A contrast is seen in a number of melting characteristics when one compares high and low molecular weight complexes (un-

sonicated and sonicated DNA-MC complexes, respectively; see table 1). Sonicated DNA and their complexes, exhibit lower T_m values and higher melting breadths relative to the complexes and controls of the higher molecular weight DNA forms.

An additional characteristic seen in the comparisons of the melting profiles for sonicated and unsonicated complexes (see table 1) is the diminished ability of sonicated DNA-MC complexes to renature relative to complexes formed with larger DNAs (e.g. unsonicated DNA).

Findings exceptional to the ones obtained with DNA-MC complexes are displayed by complexes of DNA made with compound A, the open aziridine derivative of mitomycin C. These complexes display no appreciable change in T_m, melting breadth or renaturability of melting profile (see figures 5, 7 and 8).

Thermal denaturation studies of native unsonicated calf thymus DNA-MC complexes similar to those completed in aqueous buffer, were also conducted in a 1:1 methanol/DSC buffer system (see figures 10 and 11, and table 3). (In figure 9 is the melting profile of a fully nitrous acid crosslinked DNA sample used as a comparision for the DNA-MC complexes in 1:1 (50/50) buffer). This system was chosen since it allows for greater reproducibility and consistency of results in DNA thermal denaturation studies (Szybalski and Menningham, 1962). While reversible denaturation was readily observed in this buffer, the increase of T_m (ΔT_m) and melting breadth (Δm.b.)at a given binding ratio was much lower than that observed in DSC (see fig.5, fig.7 and table 1B and 3).

"Double Melting Profiles"

The thermal denaturation profiles of a DNA-MC complex and its control in aqueous buffer are shown in figure 19. Both the complex and control have been thermally denatured and, upon cooling to the premelting temperature, were reheated, as in the original thermal denaturation, and then again recooled. In the DNA-MC complex there is very little change in the melting temperatures (75.0°C vs. 76.5°C), melting breadths and in the levels of renaturation between the first and second melting-cooling cycles.

Viscosity Experiments

A. Drug Complexes of Sonicated DNA: The relationship between DNA-drug complex concentration and reduced viscosity for a series of sonicated calf thymus DNA-MC complexes and control DNA is shown in figure 24. All complexes display a distinct increase of intrinsic viscosity relative to the control; an increase which becomes more apparant, as shown in figure 25, with greater binding ratio of complex. The viscosity plots for two sonicated DNA-compound A complexes of binding ratios .12 and .06 are displayed in figure 28. These complexes display increases in viscosity relative to the control comparable to those shown by DNA-MC complexes.

A plot of reduced viscosity versus concentration for an actinomycin-sonicated calf thymus DNA complex (binding ratio of

.13) and its control (in duplicate) is shown in figure 26.

In view of the fact that aggregation can lead to large viscosity increases (Eigner and Doty, 1962), the viscosity of a solution of stored (2 weeks) sonicated DNA-compound A complex which may have contained an aggregate form of its complex was measured (fig. 27) against control to demonstrate the pattern the viscosity increase would take in the presence of probable aggregation. The exceptionally large slope of the viscosity-binding ratio relationship for the complex, relative to the control, demonstrates the concentration dependent effect of aggregate formation (e.g. formation of dimers, trimers etc.) (Gabbay et al., 1976a; Zimm et al., 1971). Such adverse concentration dependent effects are not seen in the viscosity-binding ratio plots for the DNA-MC complexes (figures 24 and 28) and thus aggregation is eliminated as the cause of increased viscosity in these samples.

B. Unsonicated DNA-MC Complexes: Figure 29 shows a plot of reduced viscosity versus DNA-MC complex concentration for two unsonicated calf thymus DNA-MC complexes and control. In contrast to the marked increase in viscosity displayed by the sonicated complexes, these complexes (binding ratios .12 and .10) display a pronounced drop in viscosity (intrinsic viscosities of 34 and 35 respectively) which represents approximately 80% of that shown by control DNA ($[\eta]$=43). Since these values for the viscosity possess a precision (maximum percentage deviation) of 4.3% or less (see table 7), they represent real differ-

ences in the viscosity of the samples. The relative intrinsic viscosity (sample $[\eta]_s$/control $[\eta]_c$) for a series of unsonicated DNA-MC complexes of varying binding ratios is shown in figure 25 and table 6. In this plot it is apparent that the relative intrinsic viscosity diminishes as the DNA becomes more extensively bound with mitomycin C. (This effect is also reproduced with DNA-MC complexes made from E.coli DNA, see table 6). As shown in figure 25, furthermore, the decrease in viscosity levels off near a binding ratio of 0.10 (one drug molecule per 5 base pairs).

Viscometric measurements made in an effort to determine whether the decrease in viscosity was the result of DNA chain scission (double strand breakage) are displayed in table 6. Here the viscosities of a series of calf thymus DNA samples containing the enzyme catalase (used to prevent chain scission of DNA by catalytically converting H_2O_2 (hydrogen peroxide) to H_2O and O_2 (Morgan et al., 1976) was measured. The results show no change in the viscosities of the following samples; (1) DNA + $Na_2S_2O_4$ (reducing agent), (2) DNA + $Na_2S_2O_4$ + catalase, (3) DNA + $Na_2S_2O_4$ + MC, (4) DNA + $Na_2S_2O_4$ + MC + catalase.

Ultracentrifugation of DNA-MC Complexes in Neutral Sucrose Density Gradients

A. Sonicated DNA-MC Complexes: An analytical examination of the DNA-MC complexes was possible in these gradients since the sedimentation characteristics for all samples complied with the linear relationship (Burgi and Hershey, 1963)[7] found between sedimentation coefficients, distance and time of sedimentation for nucleic acids in sucrose gradients. The maximum average percentage deviation (a measure of precision, Skoog and West, 1965) found in any set of runs for the samples was no more than 3.5% (e.g. in fig. 31 is a triplicate run of unsonicated calf thymus native DNA whose precision was 1.4%; see also table 8).

The sedimentation profiles for two sonicated DNA-MC complexes (binding ratios 0.10 and 0.05), and a control sample in neutral sucrose are shown in fig. 32. With the exception of a slight increase in the distance of sedimentation, and an increase of peak heights (due to drug absorbance at 260 nm) for the complexes, relative to the control, there is no significant difference in the sedimentation patterns of these samples. (There is a 1.7 to 3.4% increase in the distances sedimented for these complexes (binding ratios 0.05 and 0.10, respectively) relative to the control. These increases, which are due to the added mass of bound drug in these complexes,[6] are relatively small and statistically insignificant.)

B. Unsonicated DNA-MC Complexes:

The sedimentation curves for 3 unsonicated DNA samples (in duplicate; control, and 2 DNA-MC complexes of binding ratios 0.10 and 0.05) are shown in fig. 33. The main characteristic is the difference in distances sedimented by the various samples. The change of distance sedimented (as measured by peak of curve) by complex III (b.r. = 0.10) is approximately 42% (see table 9) over that of control, while there is a 17% increase of distance sedimented by complex II (b.r. = 0.05). These increments of increase are greater than what one expects for the increased mass due to bound drug. The increase of mass of DNA due to bound drug will increase the distance of sedimentation (Bloomfield, Crothers, and Tinoco, 1974) to an extent that can be calculated depending upon the binding ratio (see table 9).

The smaller height of peak III (unsonicated complex of 0.10 b.r., see fig. 33) can be best explained by a diminishing peak compensated by curve broadening relative to the width of control peak I. This broadening becomes more significant at lower O.D.s (see fig. 33).

Sedimentation of "Mixed Unsonicated-Sonicated" DNA-MC Complexes

The sedimentation curves (in duplicate) of DNA-MC complexes made from equimolar quantities of sonicated (^{3}H-labeled) and unlabeled unsonicated DNA are shown in figure 34. (Controls: a DNA mixture of the same ratio without standard MC reaction). The purpose of these experiments was to see if labeled sonicated DNA could be "linked", via mitomycin C, to unlabeled unsonicated DNA (intermolecular crosslinks). Apparantly, from these curves, there is complete retention of label in the sonicated DNA peak (in sonicated complexes as well as with controls). The results thus show no observable "linking" or complexing between sonicated and unsonicated DNA, via the reductively activated MC reaction.

Ultracentrifugation in Alkaline Sucrose Gradients

The sedimenting peaks for several native calf thymus samples in neutral sucrose gradients are seen in figure 35. DNA treated with $Na_2S_2O_4$ displays no apparent difference in its distance of sedimentation relative to the untreated control. The DNA-MC complex of binding ratio .087 sediments, as expected, ahead of the control DNA.

The sedimenting peaks for the same samples in alkaline sucrose gradients are seen in figure 36. While the complex, as anticipated, sediments ahead of control DNA, the sodium dithio-

nite treated DNA lags behind the control in its ability to sediment, a finding which suggests the presence of single stranded breakage (see discussion).

When $Na_2S_2O_4$ treatment of DNA is carried out in the presence of catalase and superoxide dismutase the effects of $Na_2S_2O_4$ are prevented since no shift to lower sedimentation coefficient is observed, as seen in fig. 37. Catalase and superoxide dismutase have no effect on the DNA-MC complex, however (see appendix 10).

Flow Dichroism

The change observed in the reduced dichroism for several DNA (unsonicated)-MC complexes and their control versus shear rates at 260 nm and 310 nm is shown in figure 41. From these plots, several distinguishing patterns are discernable. One such pattern is the unequal reduced dichroism of opposite sign for DNA (260 nm) and bound mitomycin C (310 nm). Another characteristic is the increase and approach towards a leveling off of the reduced dichroism with increasing shear rate for the DNA samples. This pattern displays the expected behavior of the reduced dichroism of DNA with increasing shear rates (Bloomfield, Crothers and Tinoco, 1974). A third pattern displayed is the decrease in magnitude of the reduced

dichroic curves for the DNA samples with increasing binding ratio of drug. A similar pattern is also found for the 310 nm reduced dichroism of the bound drug.

Gel Electrophoresis of Unsonicated DNA-MC Complexes

In plate C2 the electrophoretic patterns in 3.5% polyacrylamide for several unsonicated calf thymus DNA-MC complexes of varying binding ratio are shown. The essential characteristic displayed in this pattern is the reduced mobility of drug-DNA complexes compared to control DNA, a characteristic which becomes more apparent in complexes with higher binding ratios. The mobility for these unsonicated complexes, as shown in figure 38 (see also table 10), decreases linearly until a binding ratio of 0.10-0.15 where a leveling off appears. A second characteristic seen is the reduction or the quenching of ethidium flourescence intensity in these complexes with increasing binding ratio of the complex. (Ethidium bromide, a fluorescent stain for DNA, has been shown by Lown (1976) to be, in some manner, sterically blocked by mitomycin C, from entering that portion of the nucleic acid responsible for the enhanced fluorescence). A third pattern seen in all electrophoretic runs with unsonicated DNA complexes is the immobile band at the top or entering portion of the gel. (Bands appear larger in photographs due to angle of U.V. light entry). These bands appear

to be large DNA (see appendix 9).

To test the possibility that the pattern of reduced mobility was unique to calf thymus DNA, the electrophoretic runs on two E.coli DNA-MC complexes were performed under identical conditions (see plate A1). The fact that the reduced relative mobilities of these two complexes (binding ratios .05 and .08) fell on the plot (fig.38) established for calf thymus DNA demonstrates that the reduction in mobility is not exclusive for calf thymus DNA.

An electrophoretic run of native calf thymus DNA treated with sodium dithionite in the absence of mitomycin C is displayed in plate A2. The results show no change in the mobility of a $Na_2S_2O_4$ treated DNA sample shown to contain single stranded breakage (see sedimentation results) relative to control. As second control a DNA-MC complex (binding ratio .087), made with MC and an identical quantity of reducing agent, was also used and displayed the expected decrease in electrophoretic mobility.

Unsonicated DNA samples crosslinked with nitrous acid show only a slight reduction in electrophoretic mobility relative to control (plate B2).

Unsonicated DNA-ethidium complexes formed from ethidium bromide, on the other hand, display (plate C1) a broadening as well as a lowering in the electrophoretic mobilities relative to controls (table 10 and figure 38).

Detection of Crosslinked DNA by Gel Electrophoresis

Crosslinked DNA renatures spontaneously to the native state after denaturation in contrast to control (linear) DNA. Denatured DNA, on the other hand, migrates more slowly and appears more smeared than native DNA in polyacrylamide gels (Lyons and Kotin, 1965). Consequently, after applying denaturing conditions, the migration of crosslinked DNA remains unchanged, while the mobility of control DNA, now denatured, is reduced. If the sample is only partially crosslinked, a heterogeneous pattern is seen. Plate E1 shows the gel patterns of a series of DNA-MC complexes which demonstrates these principles. Complex II is 100% crosslinked by MC (as established from UV assay, see methods) and shows no difference before and after submission to denaturation conditions. Complexes III and IV which are only partially crosslinked display some renatured material but mostly denatured after submission to denaturation conditions. (The small renatured bands seen here and in plate E2 indicate the presence of intrinsic crosslinks in calf thymus DNA (Alberts and Doty, 1968).) Note that thermal and alkaline denaturation give the same results. To demonstrate that these principles are true for crosslinking agents other than MC, HNO_2-crosslinked DNA was also investigated and the results shown in plate B_2 indicate that this is so: After submission to denaturating conditions, crosslinked DNA is clearly distinguishable from control.

Gel Electrophoresis of Sonicated Calf Thymus DNA-MC Complexes

For these experiments sonicated DNA was fractionated into different M.W. ranges by sucrose density gradient ultracentrifugation as described in the methods. The polyacrylamide gel patterns for two sets of fractionated sonicated DNAs with varying molecular weights are shown in plate G1. The molecular weights range from $3X10^5$ to $1X10^6$ daltons, as assessed by direct comparison to a standard M.W. reference pattern from f_1(RFI) DNA (plate F1).

Mitomycin C complexes formed from fractions of sonicated DNA were run electrophoretically against their DNA controls (see plates F1 and F2). With the binding of MC to DNA, there is the expected reduction in electrophoretic mobility for the complex relative to controls. The reductions, however, for these complexes are less drastic than those displayed by unsonicated DNA-MC complexes of comparable binding ratios (see figure 38 and table 10). In consideration of this difference it is interesting to note that the plot (fig.39) of the relative mobility vs. M.W. of different size DNA-MC complexes having an identical binding ratio of 0.09 shows clearly that the decreased electrophoretic mobility of DNA-MC complexes is a DNA size-dependent effect.

Sonicated DNA-compound A complexes, on the other hand, regardless of their binding ratio, show little or no reduction in electrophoretic mobility relative to controls (see plate G2).

The presence, however, of residual immobile bands on top of gel patterns for some of the complexes (slots 2 and 6) suggests some form of DNA breakdown or aggregation-like phenomenon in DNA-compound A complexes of higher binding ratios which prevents a fraction of the DNA (as indicated by ethidium fluoresence) from entering the gel. Furthermore, in plate G2 the bands for complex 2 (sonicated DNA-compound A complex of binding ratio .23) show a decrease in ethidium fluorescence suggesting, as already described for DNA-MC complexes, the presence of bound drug. Nevertheless, it is understandable that removal of a certain portion of DNA, in the form of an immobile band, if significant, will naturally lower the concentration of DNA in the mobile band, thus explaining its decreased flouresence.

Electron Microscopy of Unsonicated Calf Thymus DNA-MC Complexes

Plate 1 is a photograph (50,000X) of an electron microscopic grid pattern for a control (unsonicated native calf thymus) DNA sample. In this pattern several molecules of DNA are displayed whose strands are relatively smooth in contour.

In plate 2 the grid pattern (50,000X) is shown for control DNA treated with a quantity of sodium dithionite used in the standard procedure for the formation of DNA-MC complexes. (This quantity is also known to produce significant single strand breakage; see sedimentation studies.) Relative to plate 1,

the contour of the double strands of plate 2 DNAs display, overall, a slight curving or bending of strands.

Plates 3a and b represent the grid patterns (50,000X) of an unsonicated DNA-MC complex of binding ratio 0.1. In these grids a number of DNA molecules exhibit a definite coiling or bending in strand contour which cannot be explained by the natural overlap or tangling of DNA strands that may stem from variation in the techniques of spreading of DNA onto microscope grids (Beer, 1968).

In plate 4 is displayed the pattern for control DNA treated with the enzymes catalase and superoxide dismutase. The prevalent aspect observed, relative to the non-enzyme treated control (plate 1), is a jaggedness in the contour of the DNA strands. (Magnification is 50,000 X.)

In plate 5 is displayed the pattern for control DNA treated with sodium dithionite (as in grid 2) in the presence of catalase and superoxide dismutase. The contour of the DNA strands exhibited in this pattern are similar to those displayed in plate 4. (Magnification is 50,000 X.)

In plate 6 is displayed the grid pattern for a DNA-MC complex (binding ratio 0.1) formed in the presence of catalase and superoxide dismutase. A definite increase in the coiling of DNA strands for many of the molecules displayed here reproduce the patterns shown in plates 3a and 3b. (Magnification is 50,000 X.)

Electron Microscopy of Sonicated Calf Thymus DNA-MC Complexes

Electron microscope grid patterns for sonicated calf thymus control DNA and a sonicated calf thymus DNA-MC complex of binding ratio 0.10 are displayed in plates 7 and 8, respectively. A comparison of these plates indicates that there is no difference in the contour and shape of DNA strands in the complex and control. (Magnification of pattern is 50,000 X.)

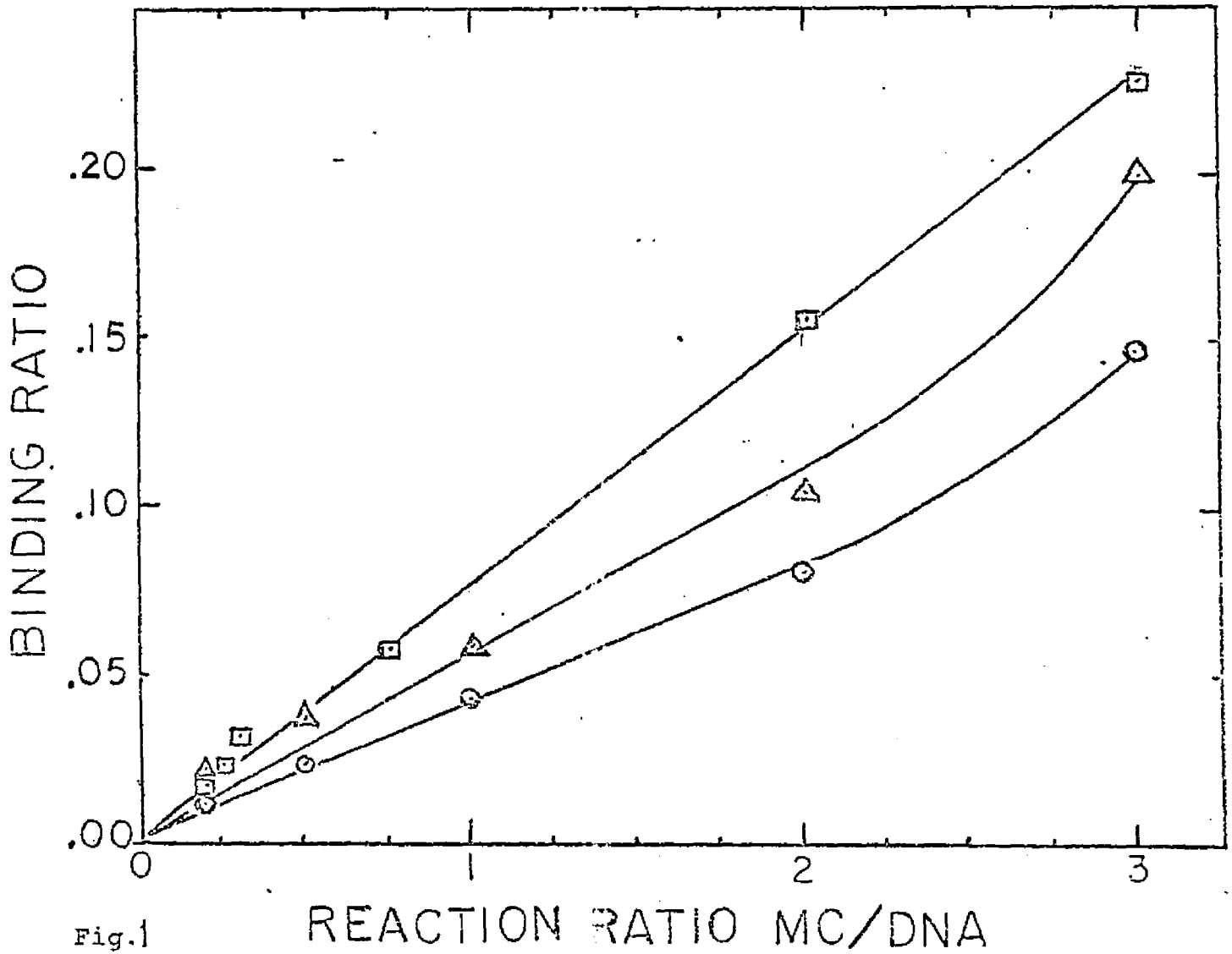

Fig.1

Legend: Binding Ratio vs. Reaction Ratio (Moles Mitomycin C / Moles DNA) for various DNA-mitomycin C complexes. Unsonicated calf thymus (⊙) and E. Coli (⊡) DNA-mitomycin C complexes. Sonic. c. thymus DNA-MC complexes (△).

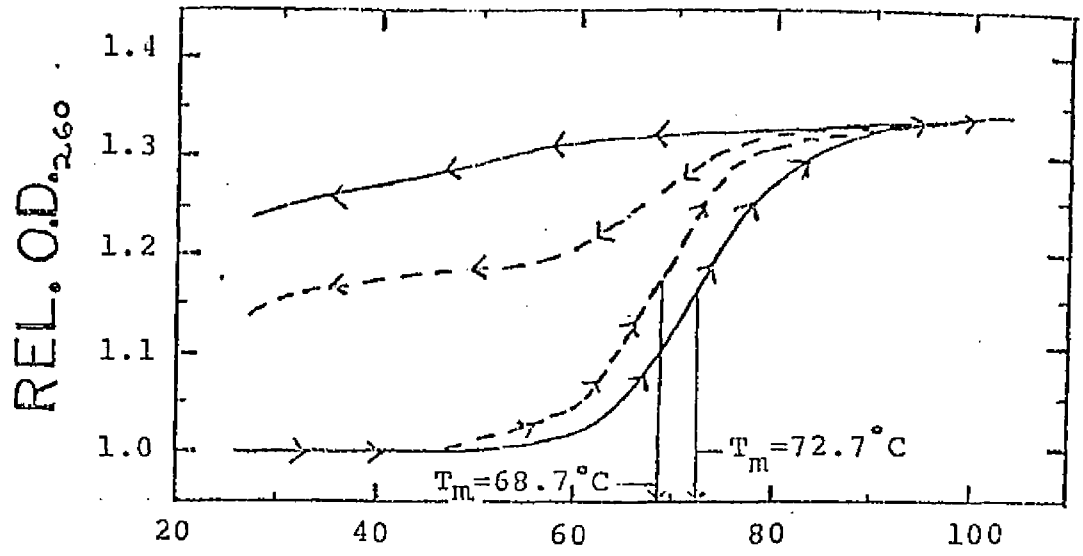

Fig.2 .

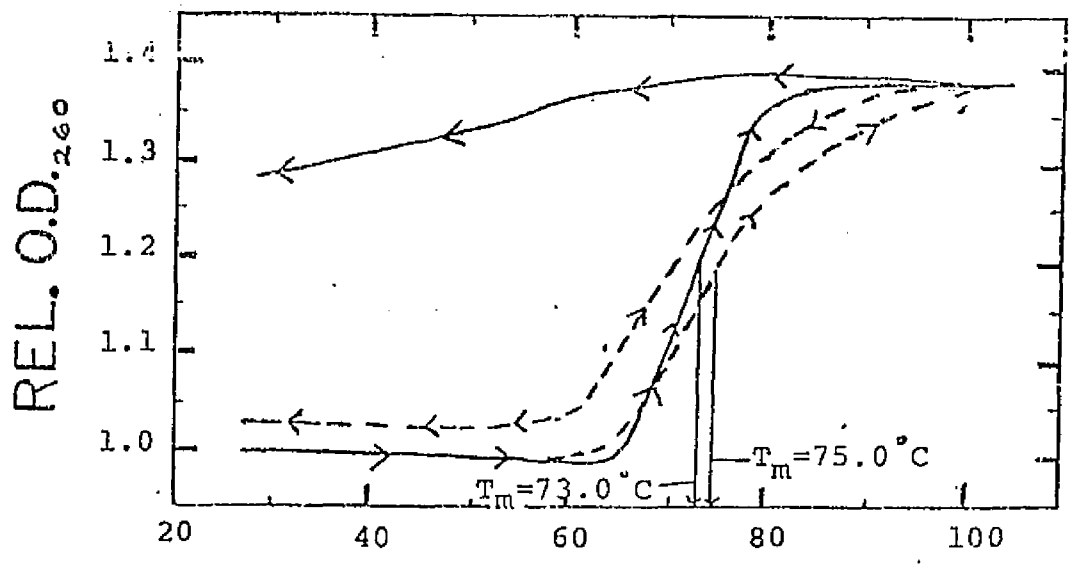

Fig.3 .

Legend: Fig.2 . Relative O.D.$_{260}$ versus Temp. for sonicated calf thymus control DNA (—) and its mitomycin C complex (b.r.=.06) in DSC (---). Fig.3 . Rel. O.D.$_{260}$ v.s. Temp. for unsonic. calf thymus control DNA (—) and it's MC-complex (b.r.=.02) in DSC (---).

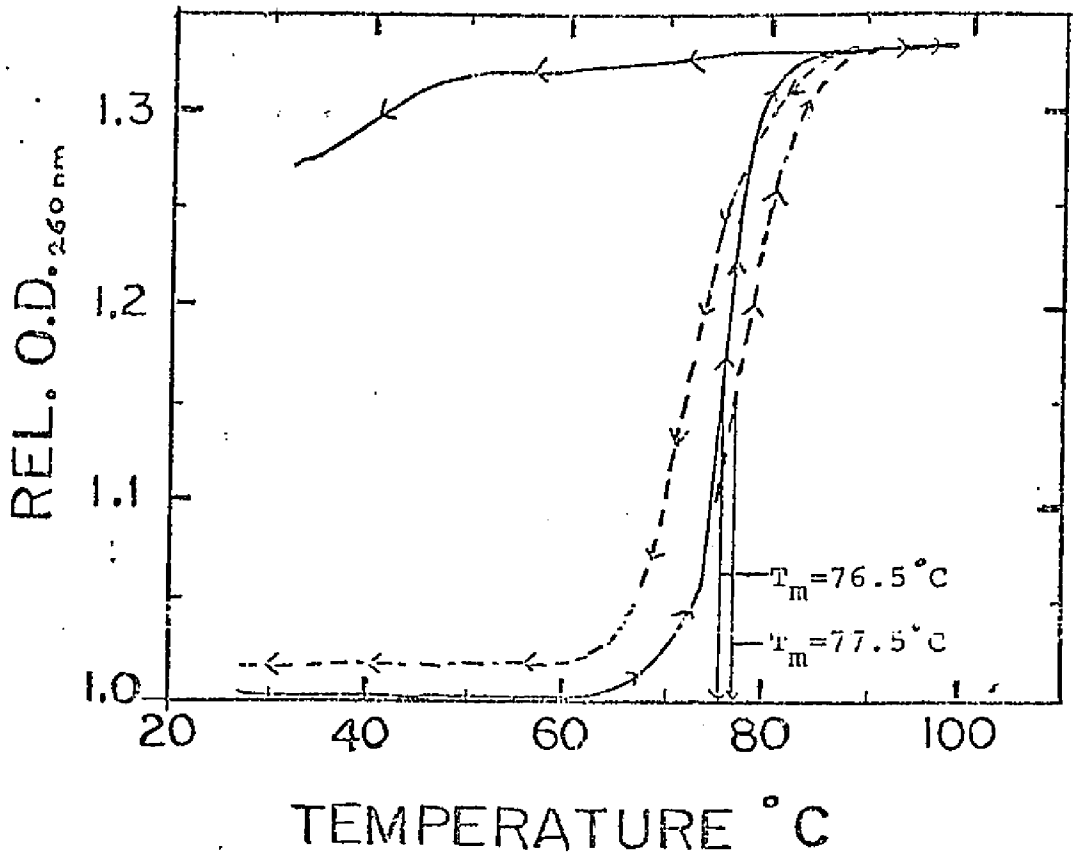

Fig.4 . Relative O.D.260 versus Temperature (melting profile) for E.Coli DNA (unsonicated) control (——) and its mitomycin C complex (- - -) of binding ratio .05 in DSC buffer.

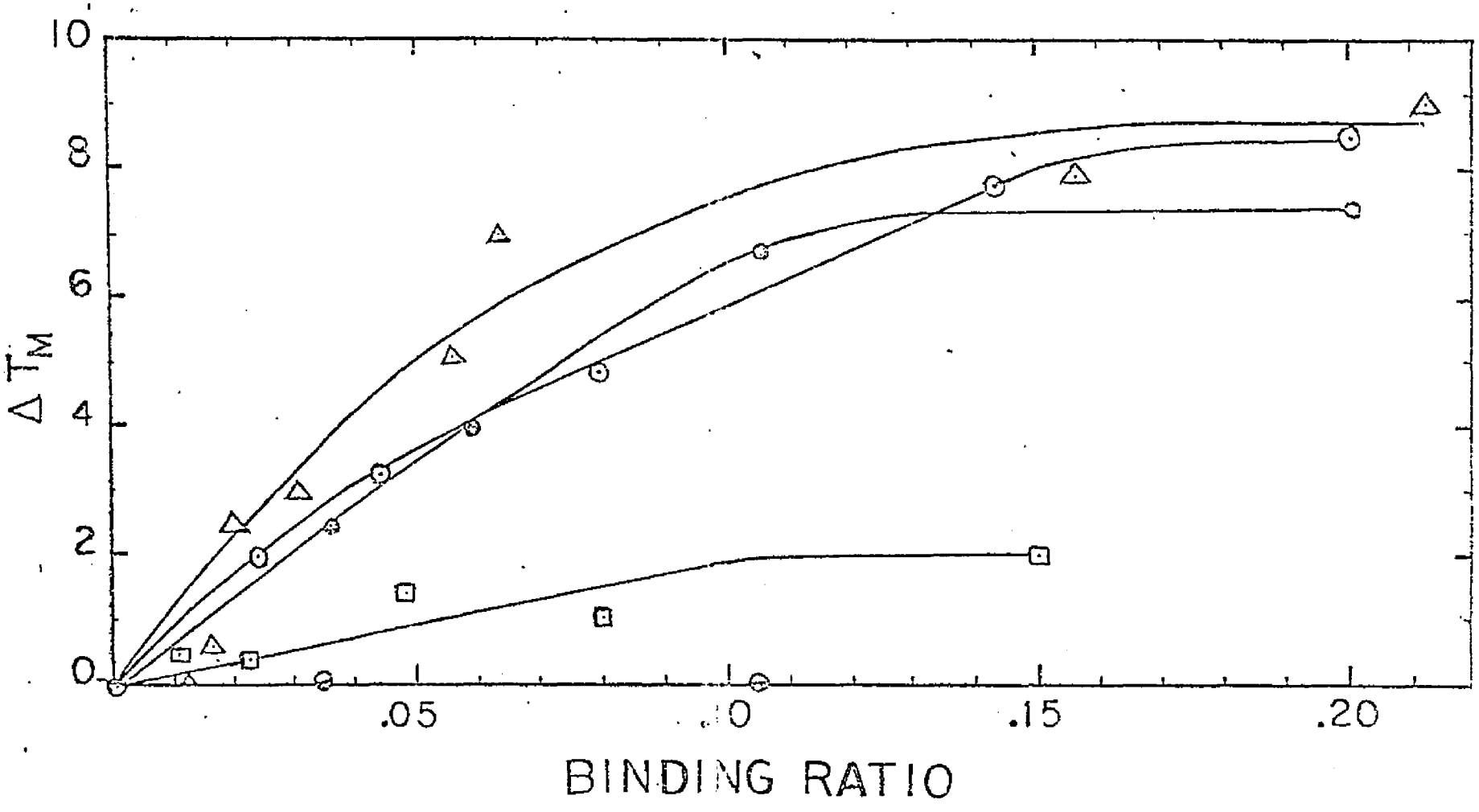

Fig.5 . ΔT_m versus Binding Ratio for a series of native DNA-mitomycin complexes. Legend is as follows: Unsonicated calf thymus DNA-mitomycin C complexes in DSC (⊙), unsonicated calf thymus DNA-mitomycin C complexes in 1:1 methanol-DSC buffer (⊡), unsonicated E.Coli DNA-mitomycin C complexes in DSC (△), sonicated E.Coli DNA-compound A complexes in DSC (⊖), and sonicated calf thymus DNA-mitomycin C in DSC (○).

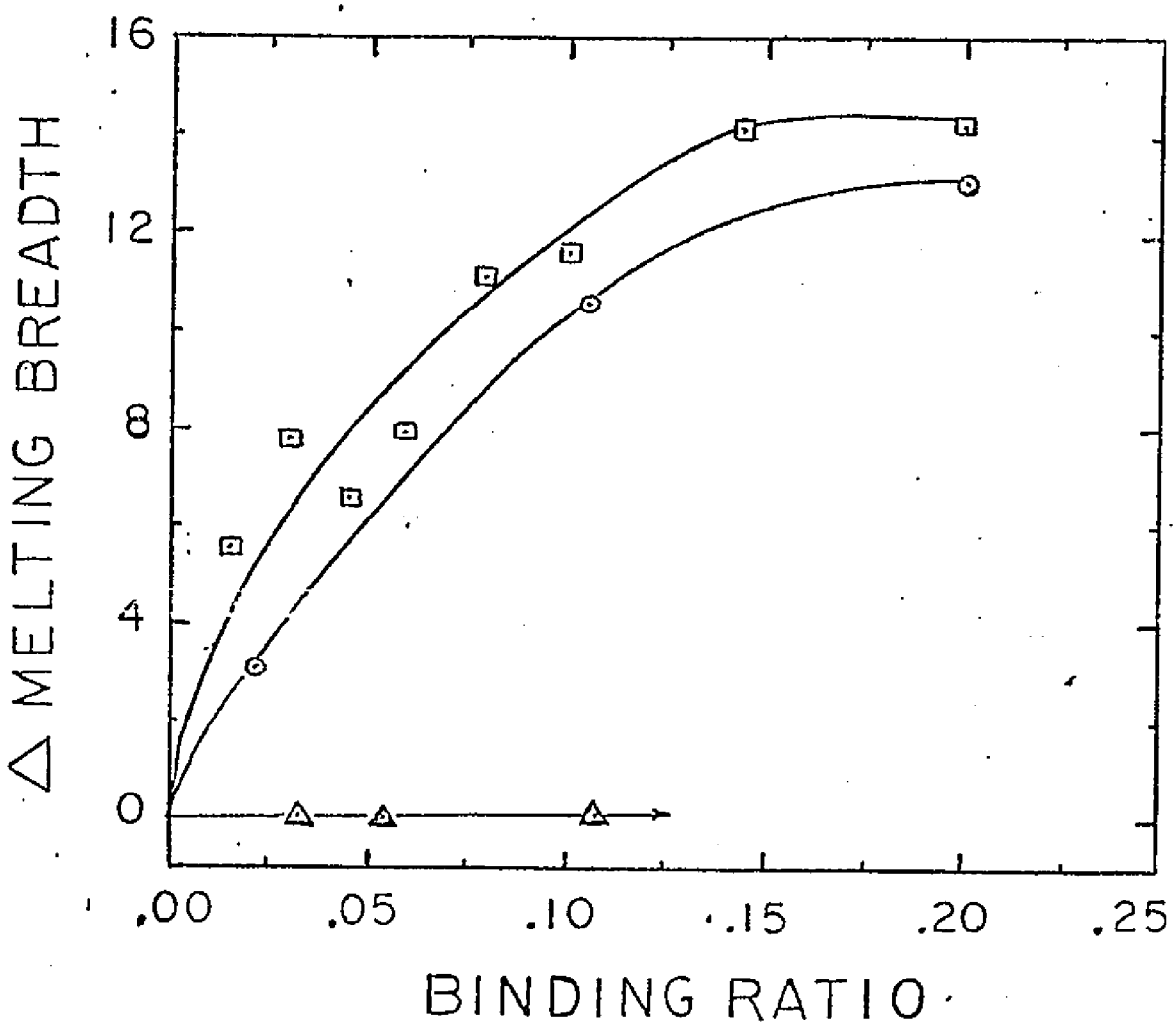

Fig.7 . Δ Melting Breadth versus Binding Ratio for DNA-mitomycin complexes. Calf thymus unsonicated (⊡) and sonicated (⊙) DNA-mitomycin C complexes. Calf thymus sonicated (▲) and E.Coli sonicated (△) DNA-compound A complexes.

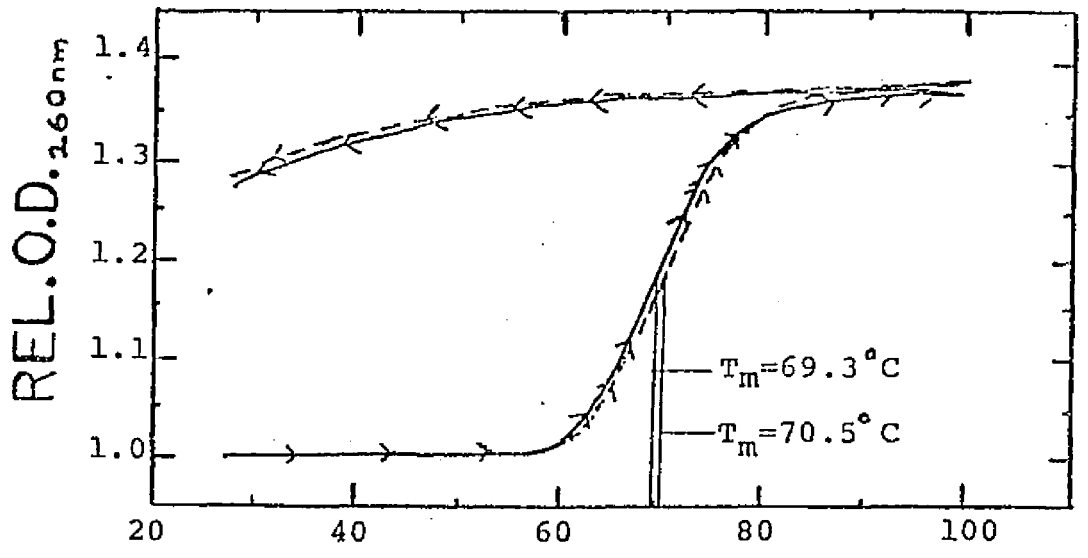

Fig.8 .

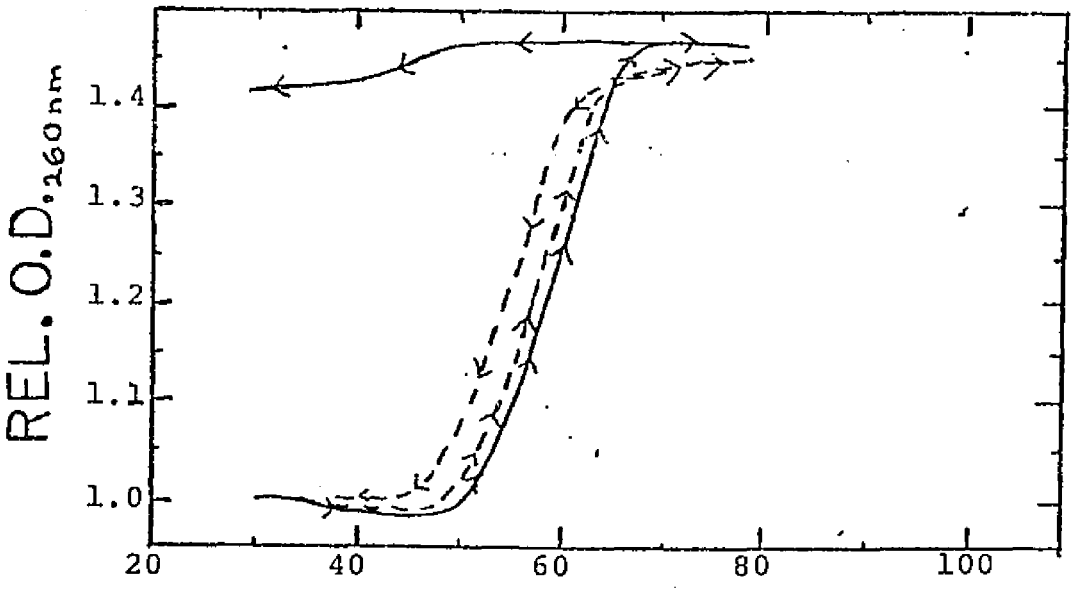

Fig.9 .

Legend: Fig.8. Relative O.D.$_{260}$ vs. Temp. for sonicated calf thymus DNA-compound A complex (b.r.=.05, (---)), and it's control (—) in DSC buffer. Fig.9 . Rel. O.D.$_{260}$ vs. Temp. for a nitrous acid crosslinked (100%) unsonic. calf thymus DNA complex (---), and it's control (—) in 1:1 methanol-DSC buffer.

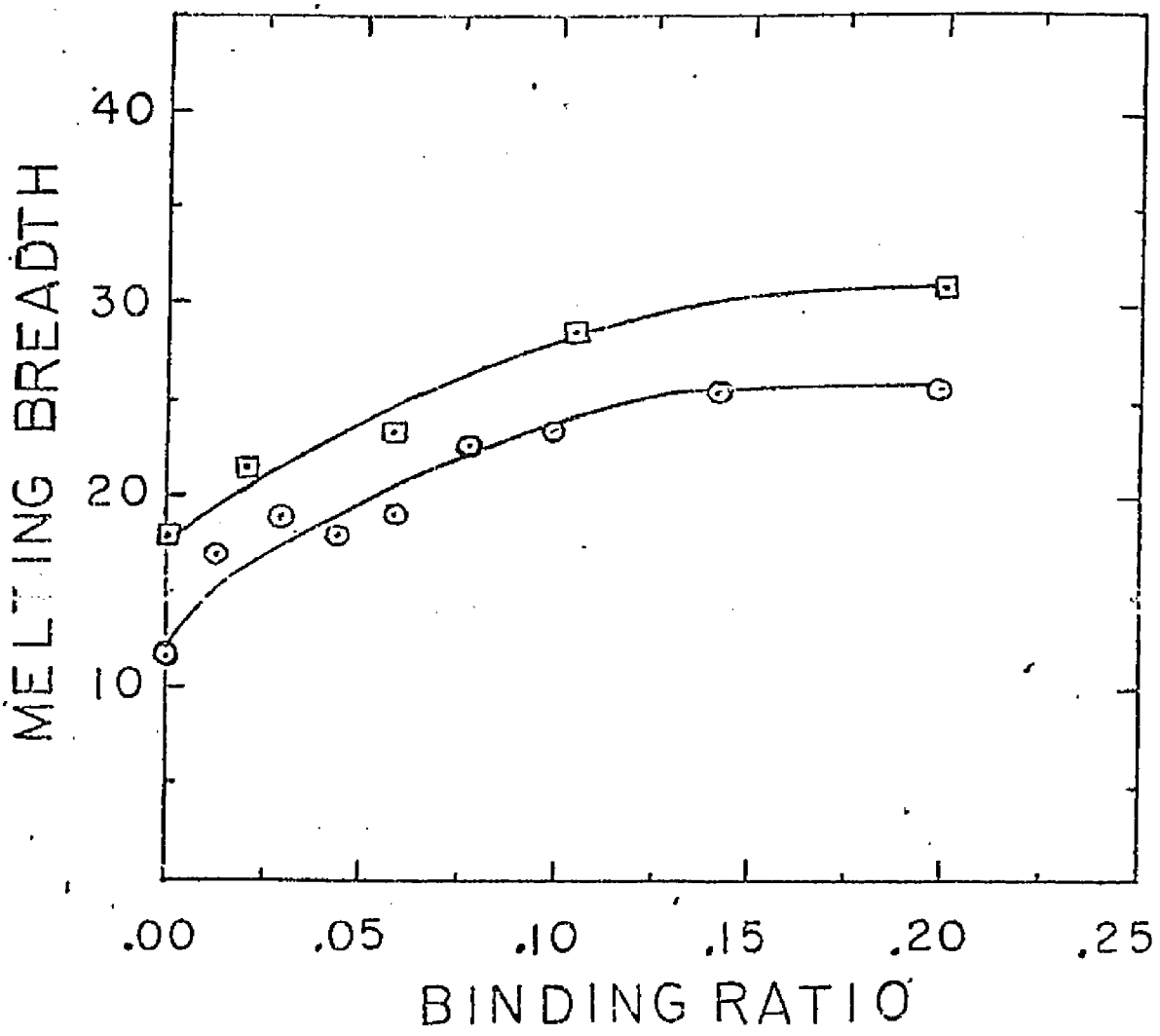

Fig.6 . Melting Breadth versus Binding Ratio for unsonicated (⊙) and sonicated (⊡) calf thymus native DNA-mitomycin C complexes.

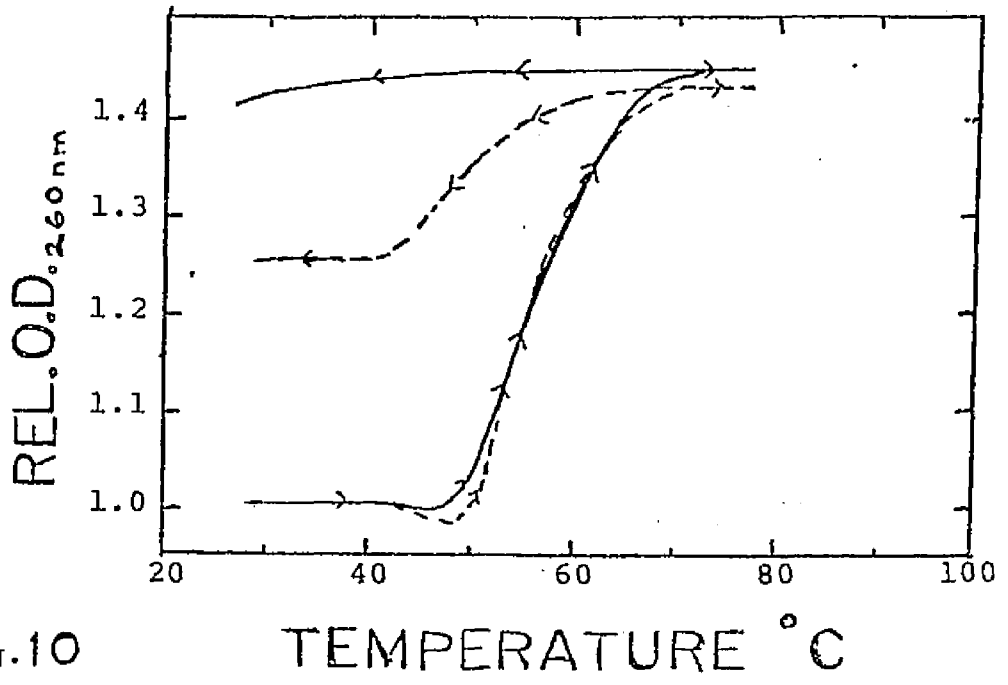

Fig.10

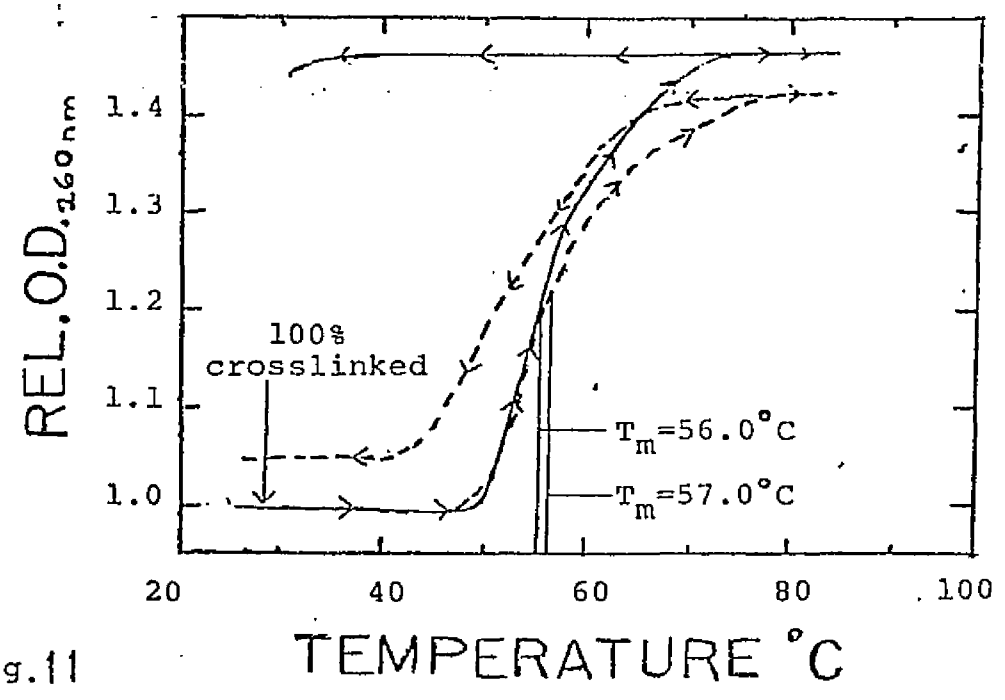

Fig.11

Legend: Fig.10 . Relative O.D.$_{260}$ Vs. Temp. for unsonicated calf thymus DNA-mitomycin C complex (b.r. >.005, (---)), and control (—) in 1:1 methanol-DSC. (Complex is 37.7% crosslinked). Fig.11. Rel. O.D. Vs. Temp. for unsonic. calf thymus DNA-MC complex (b.r.=.08, (---), and control (—) in identical buffer.

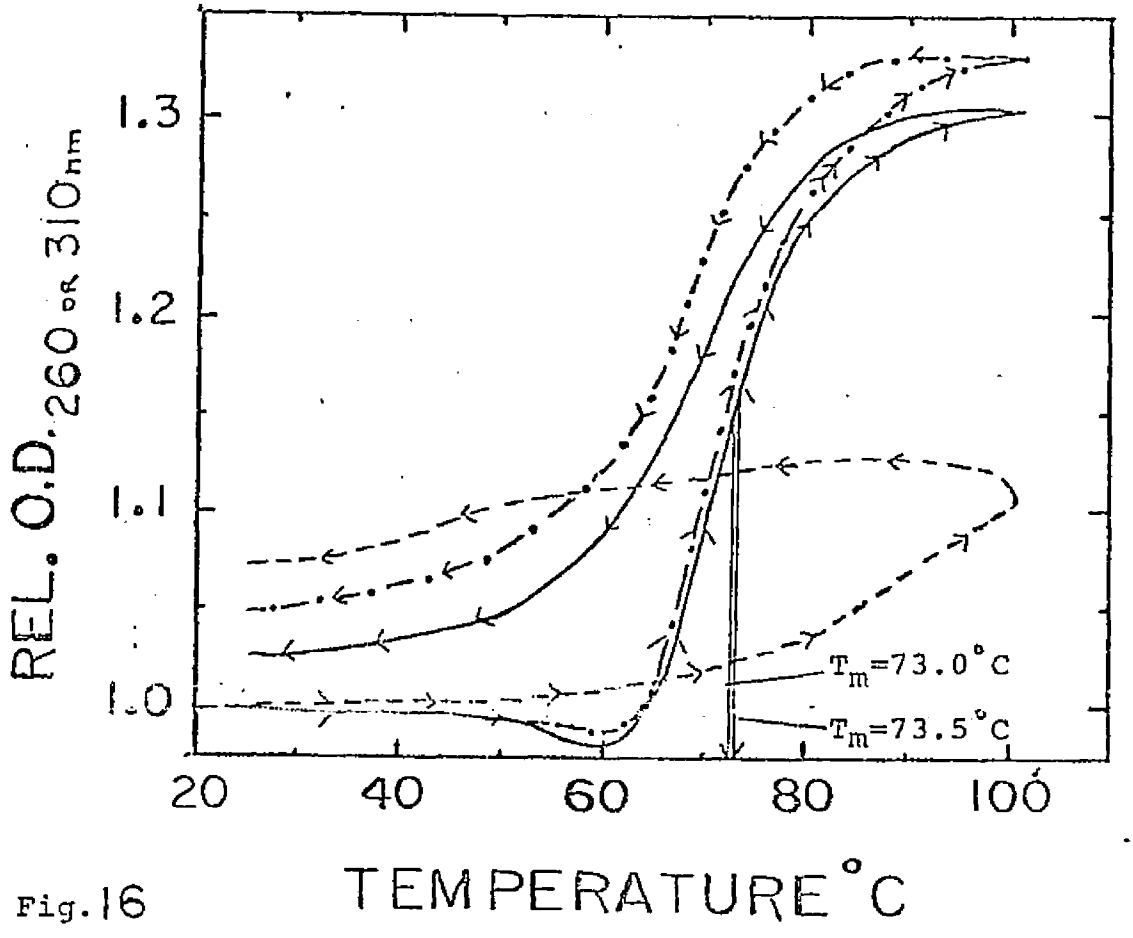

Fig.16

Legend: Relative O.D. at 260 or 310 nm versus Temperature for an unsonicated calf thymus DNA-mitomycin C complex of binding ratio .15 in DSC (—•—). Melting profile of the complex corrected for 260 nm absorbance due to bound drug's "hyperchromic effect" (——). Rel. $O.D._{310}$ v.s. Temp. for bound drug (---). The T_m and melting breadth (m.b.) for the complex is 73.5°C and 20.0°C as opposed to 73.0°C and 17.5°C for the corrected melting profile.

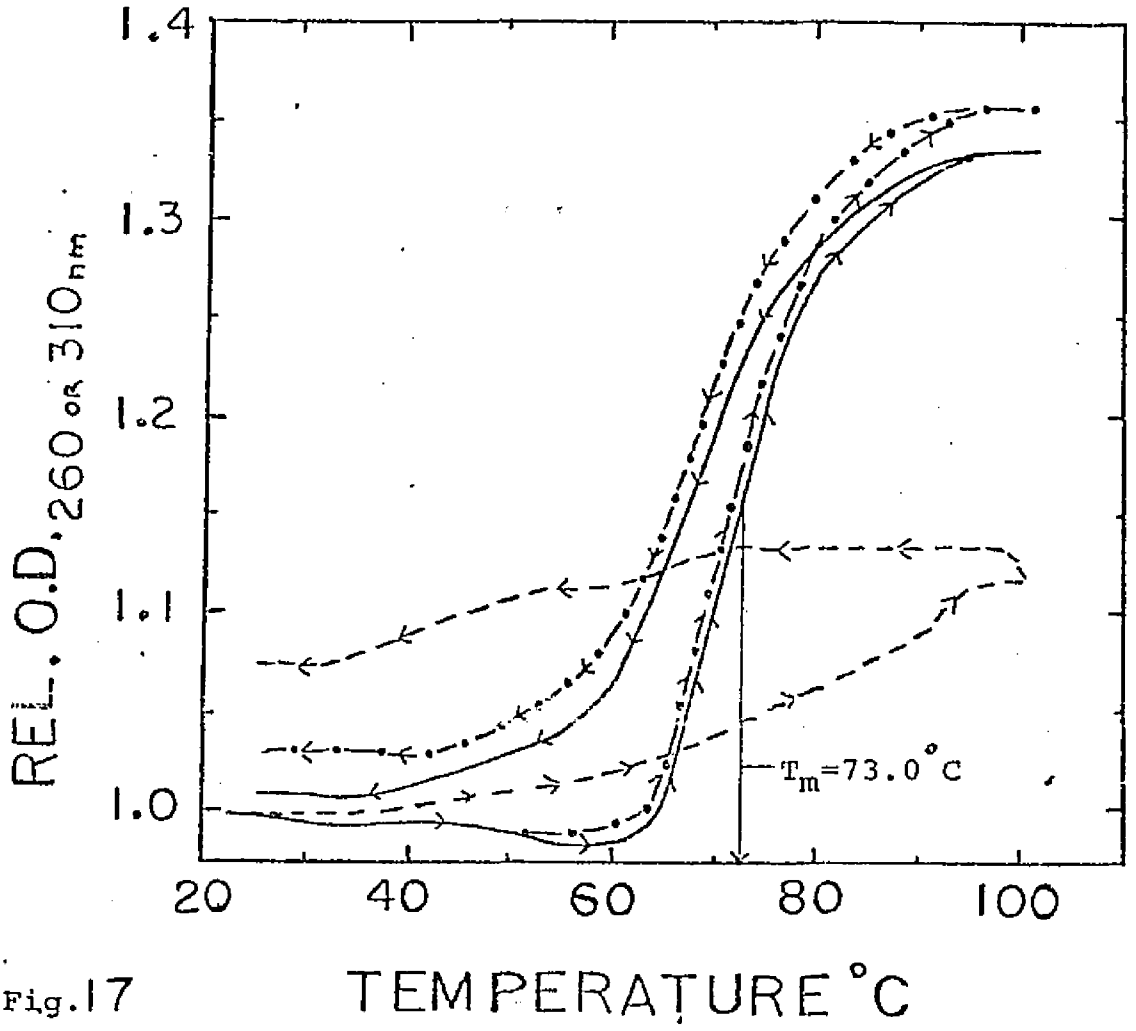

Fig.17

Legend: Relative O.D. at 260 and 310 nm vs. Temperature for an unsonicated calf thymus DNA-mitomycin C complex in DSC (binding ratio = .08, (—•—)). Melting profile of the complex corrected for the 260 nm absorbance due to the "hyperchromicity" of bound drug (——). Relative $O.D._{310}$ vs. temperature for bound mitomycin C (- - -). The T_m and melting breadth (m.b.) for the complex is 73.0°C and 19.0°C respectively. The corrected complex has a melting temp. and m.b. of 73.0°C and 18.0°C.

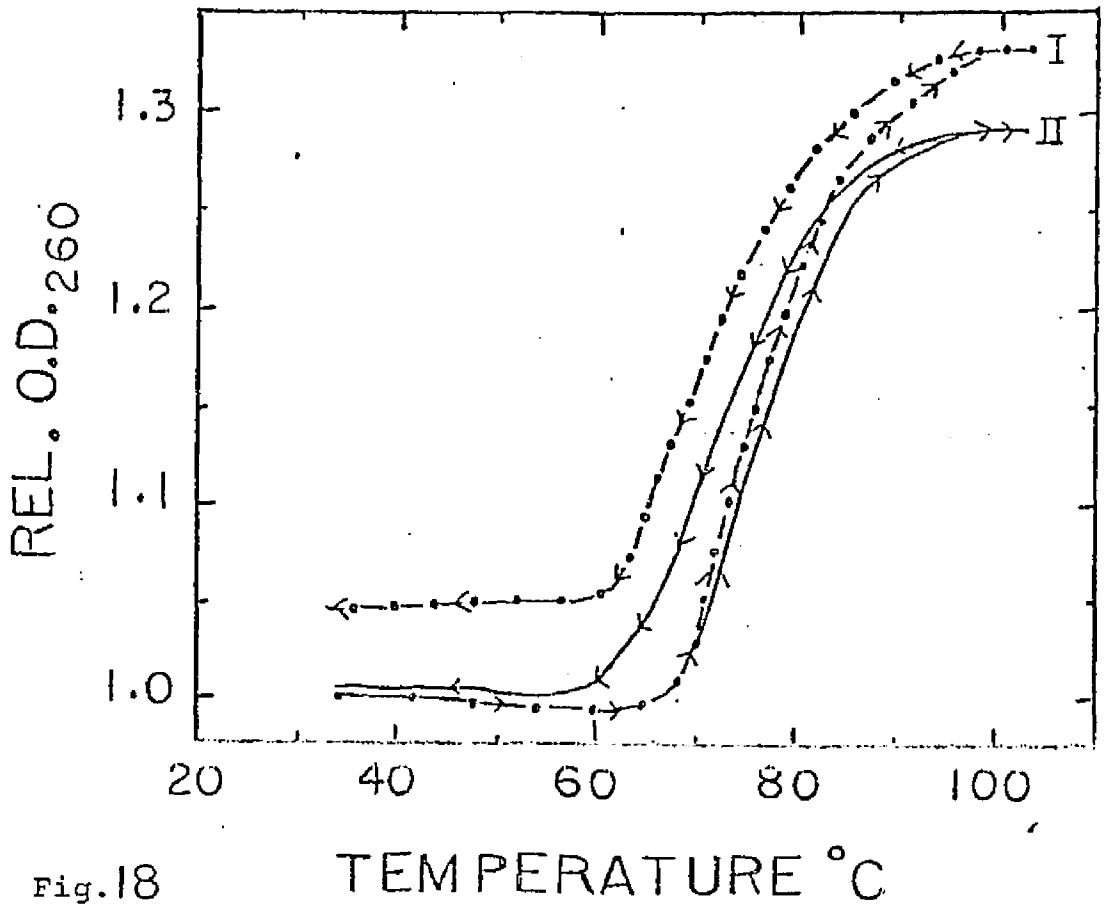

Fig.18

Legend: Relative O.D.$_{260}$ versus Temperature for an unsonicated calf thymus DNA-mitomycin C complex of binding ratio .11 in DSC (–•–), and a corrected profile (corrected for the "hyperchromic effect" associated with the 260 nm absorbance contributed by the bound drug) of the same complex (——). The T_m and melting breadth (m.b.) of the complex are 76.5°C and 19.5°C respectively. The T_m and m.b. for the corrected profile are 76.5°C and 17.0°C.

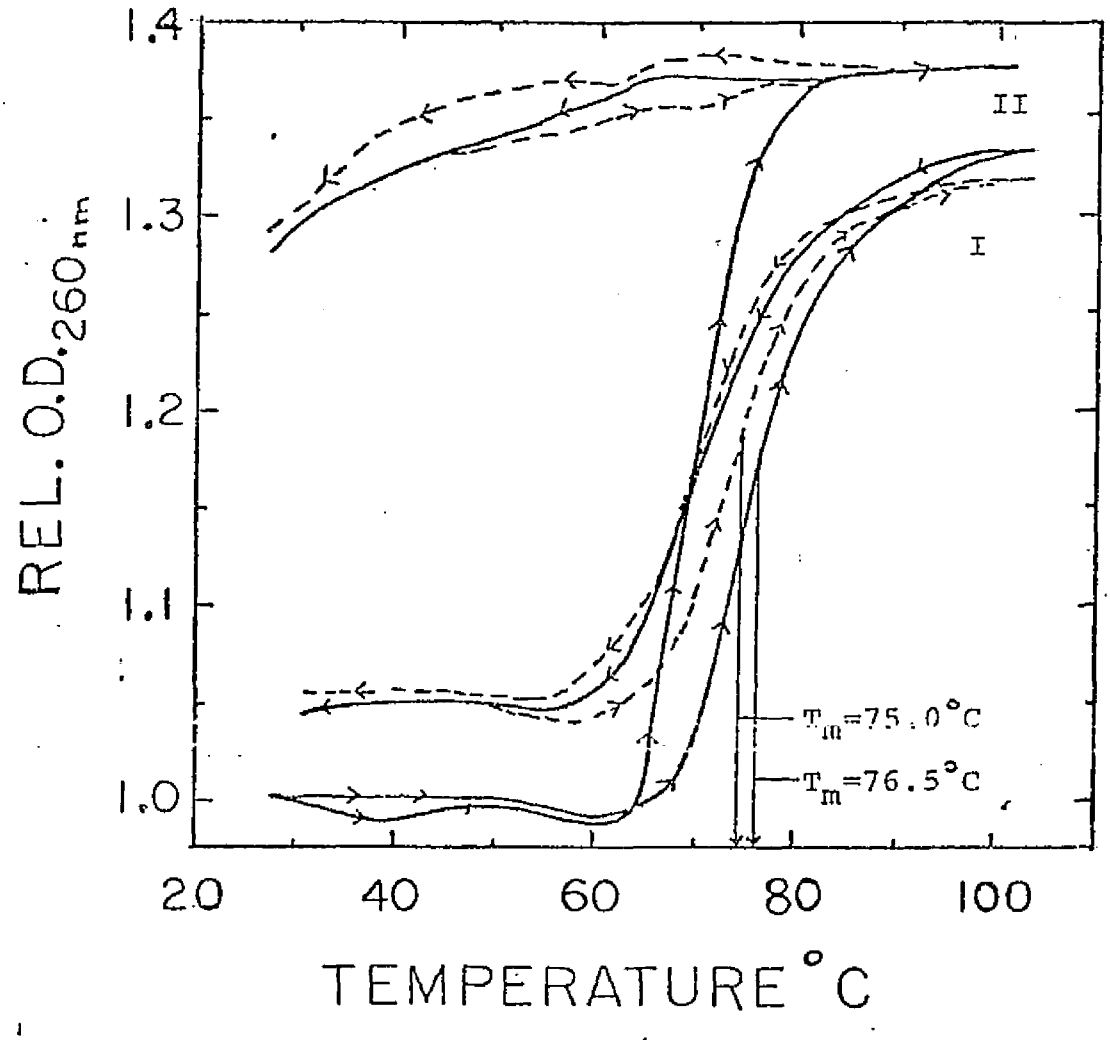

Fig.19 . Relative O.D.$_{260}$ versus Temperature for a calf thymus DNA-mitomycin C complex (I) of binding ratio .11 and it's control (II). (——) and (---), respectively, represent the 1st and 2nd melting profiles for the complex and the control. For the complex, the T_m and the melting breadth for the 1st profile are, respectively, 76.5 and 19.5°C as opposed to 75.0 and 20.0°C for the 2nd profile. The T_m for the control is 70.5°C. The buffer used is DSC.

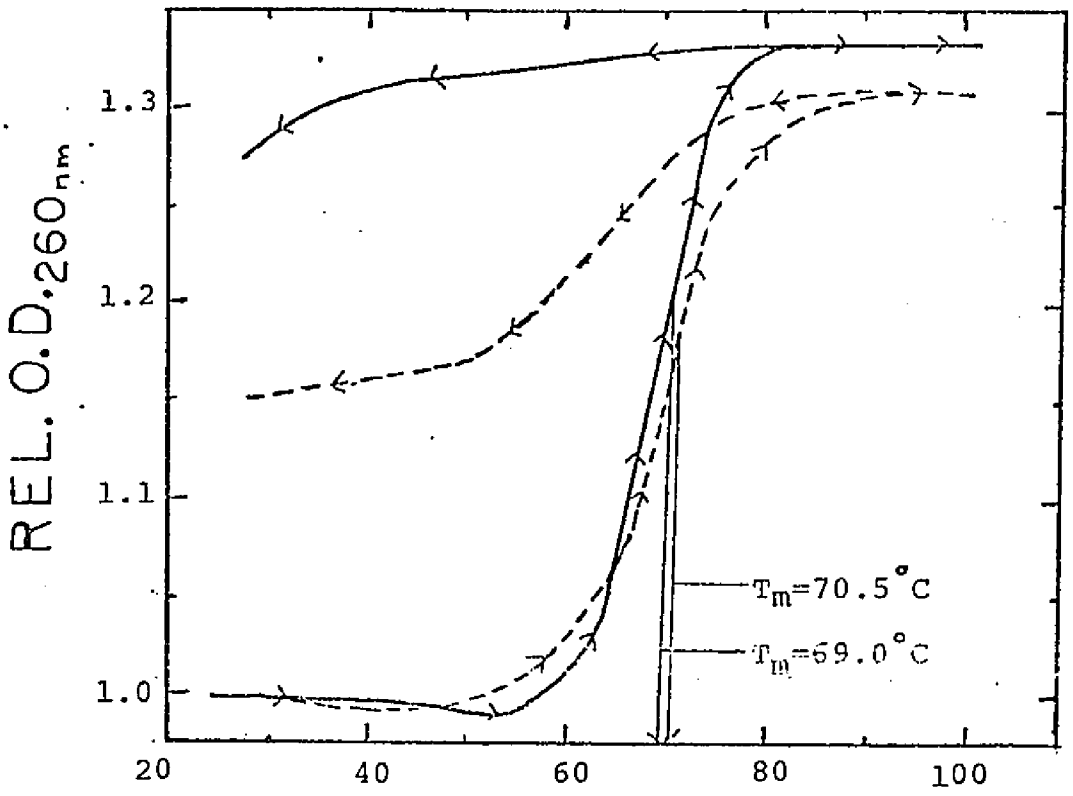

Fig.20

Legend: Relative O.D.$_{260}$ versus Temperature for a calf thymus DNA-mitomycin C complex (- - -) and it's control (——) which were sonicated. The melting breadth and temperature for the complex was, respectively 18.5° and 70.5°C, as compared to 11.5° and 69.0°C, respectively for the control. Melting profiles were taken in DSC buffer. The binding ratio of the complex was .12.

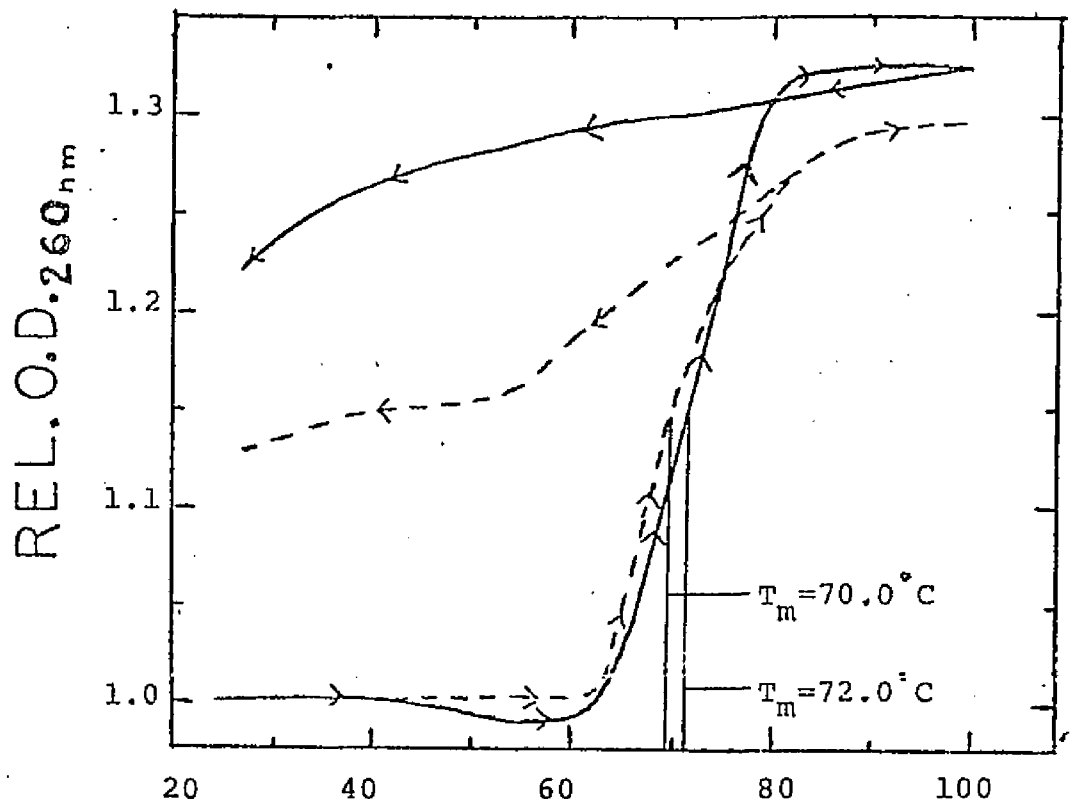

Fig.21

Legend: Relative O.D.$_{260}$ versus Temperature for a calf thymus DNA-mitomycin C complex (---) and its control (——) which were sonicated. The melting breadth and temperature for the complex was respectively 17.0 and 70.0°C as compared to 11.5 and 72.0°C for the control. Melting profiles were taken in DSC buffer. The binding ratio of the complex was .04.

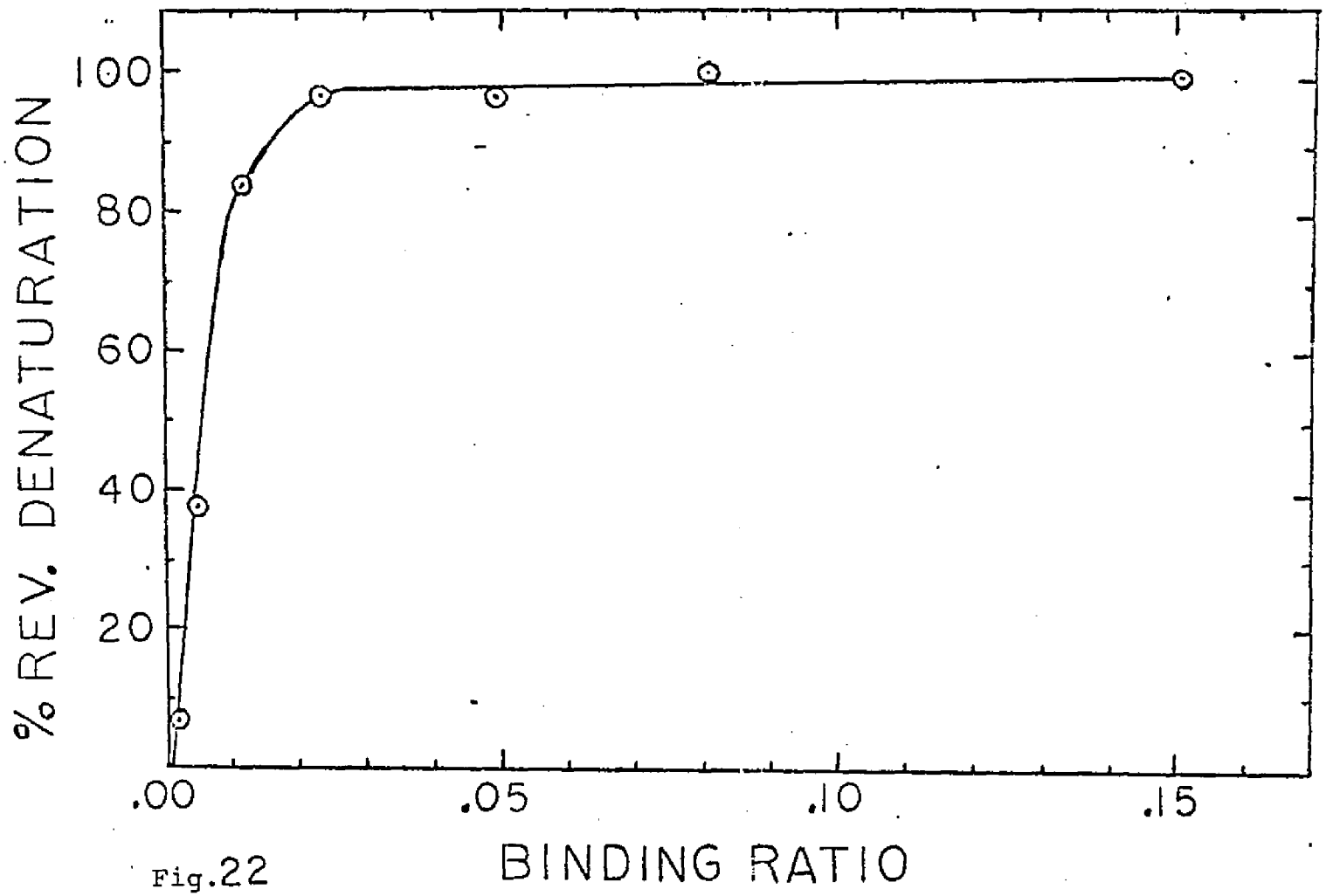

Fig.22

Legend: % Reversible Denaturation Due to Crosslinking vs. Binding Ratio for unsonicated calf thymus native DNA-mitomycin C complexes in 1:1 DSC-methanol buffer.

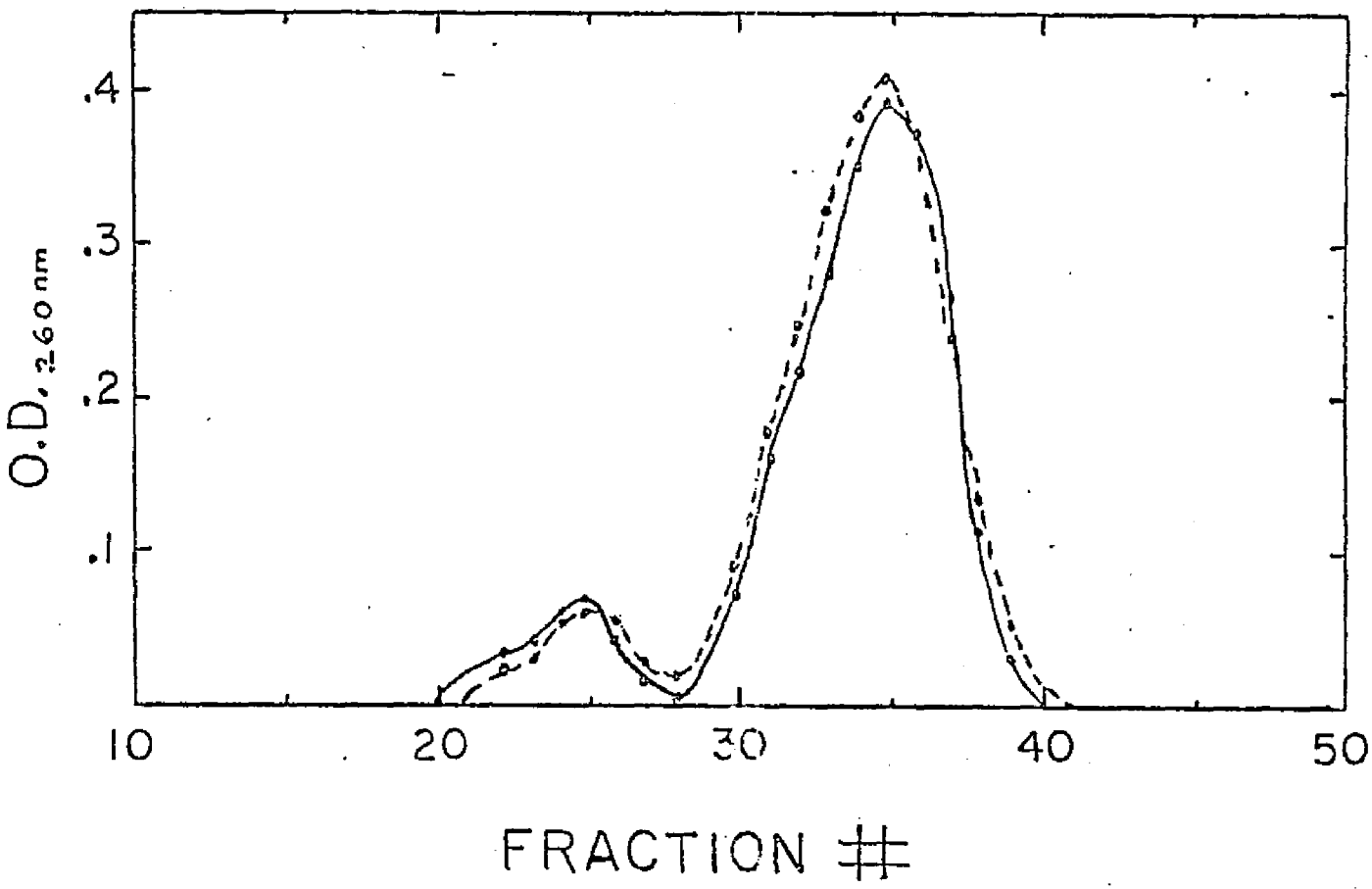

Fig.23. O.D.$_{260}$ versus Fraction Number for heated (---) and unheated (——) compound A fractionated via a G-25 Sephadex column.

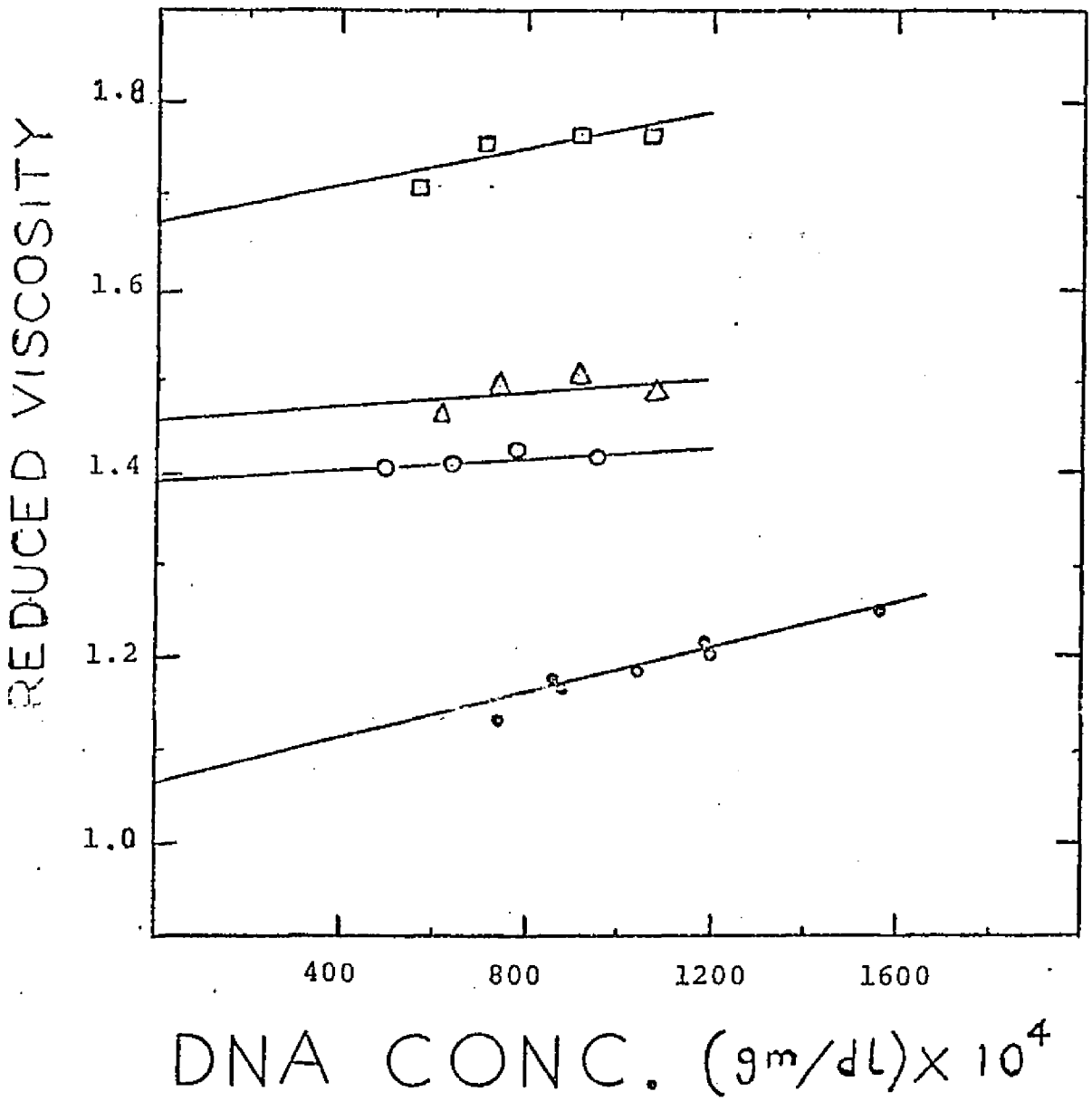

Fig.24. Reduced Viscosity versus DNA Concentration for a series of native sonicated DNA-mitomycin C complexes. In DSC-EDTA buffer at 25.0°C. M.W. of DNA used was approx. $2X10^5$ daltons. Control DNA (●), complex with b.r.= .15 (⊡), complex with b.r.= .10 (△), and complex with b.r.= .07 (⊙).

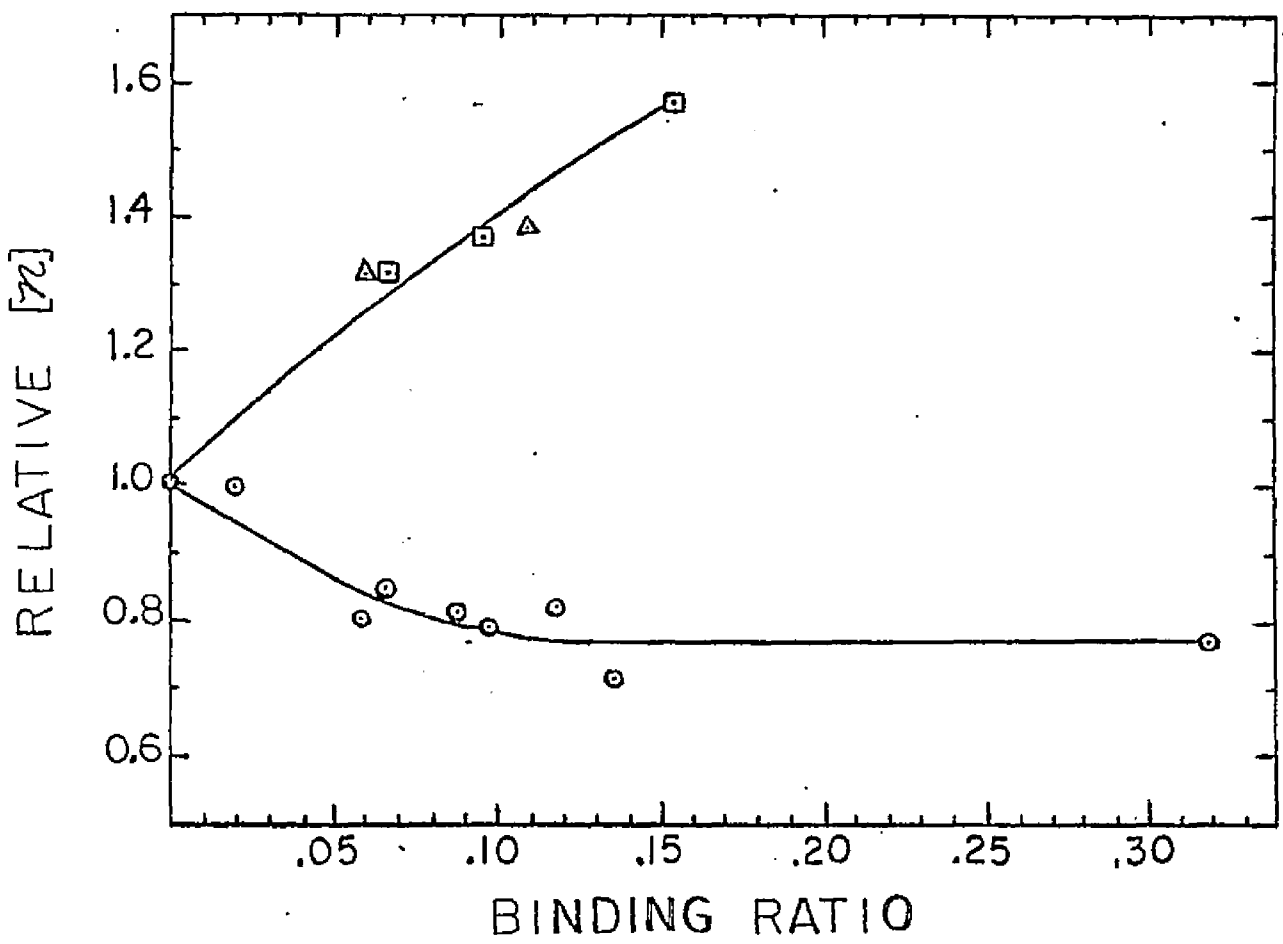

Fig.25 . Relative Intrinsic Viscosity [η] versus Binding Ratio for DNA-mitomycin complexes. (●) Control DNA, (⊙) unsonicated, and (⊡) sonicated DNA-mitomycin C complexes. (△) sonicated DNA-compound A complexes.

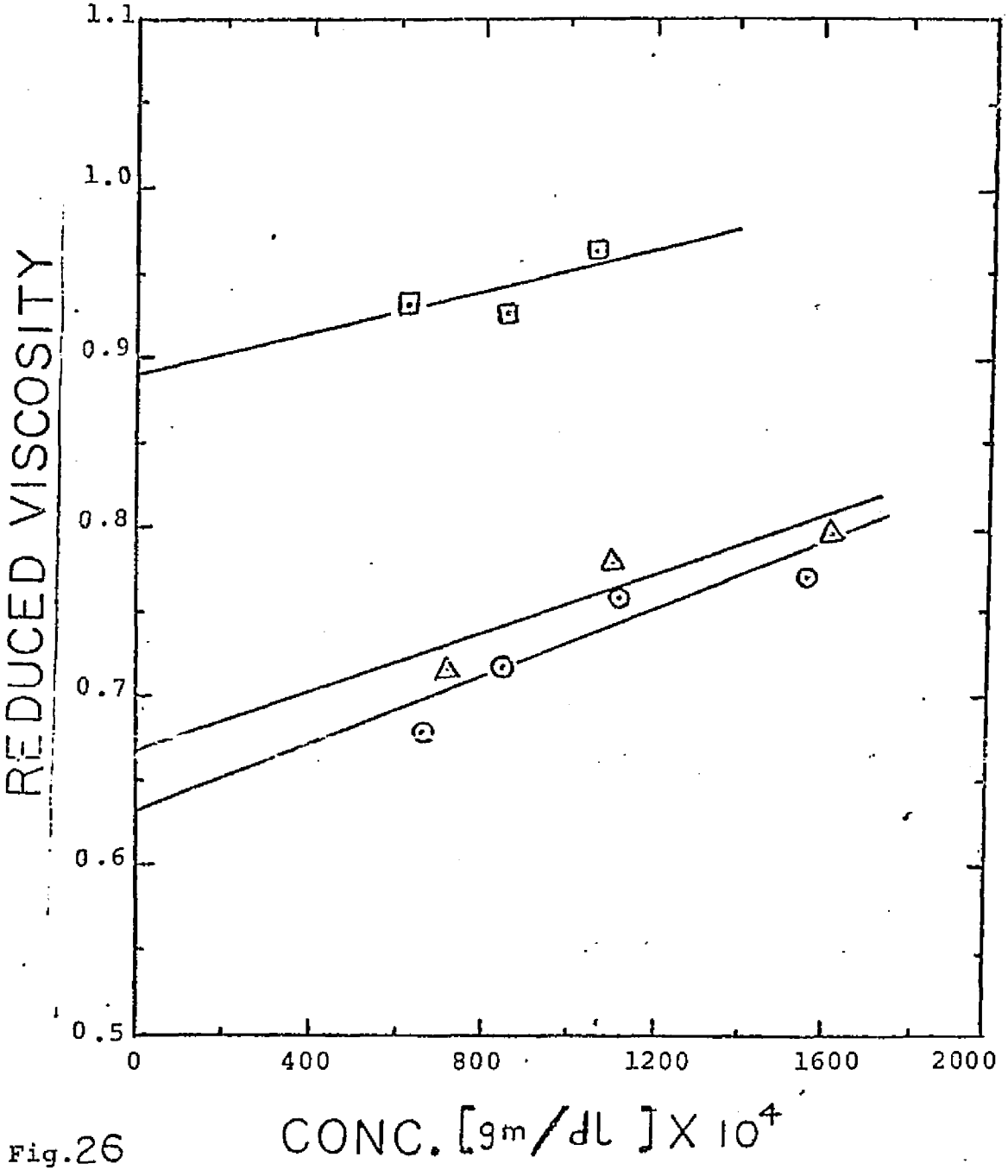

Fig.26

Legend: Reduced Viscosity versus DNA Concentration for native sonicated calf thymus DNA-actinomycin complexes in DSC-EDTA buffer at 25.0°C. Control DNA (⊙, △, 2 determinations), and a DNA-actinomycin complex (⊡) of approximate binding ratio of .125 (drug/phosphate).

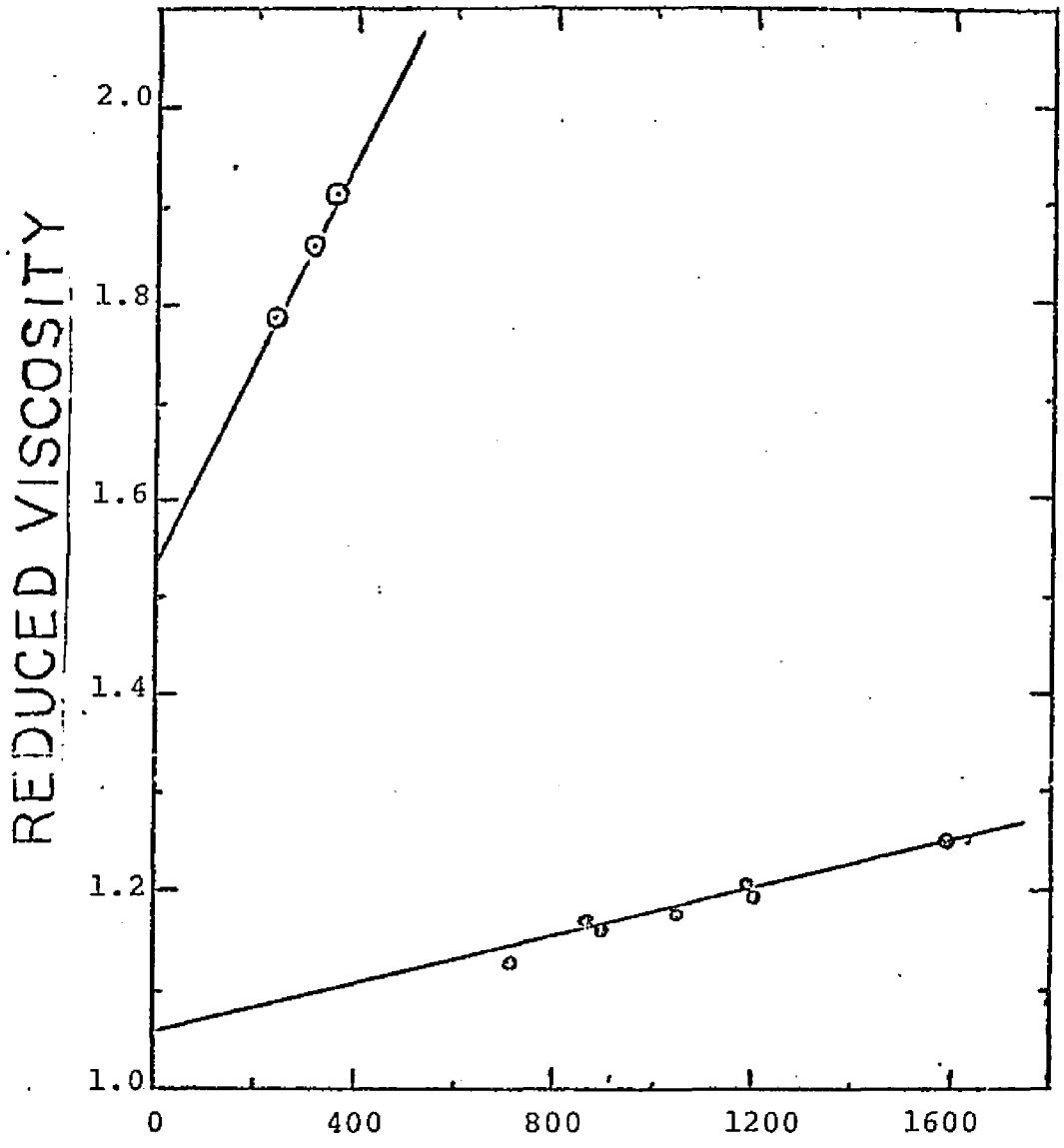

Fig.27

Legend: Reduced Viscosity versus DNA Concentration for a sonicated native calf thymus DNA-compound A complex that was stored (⊙) and its control (•). Measurements were taken in DSC-EDTA buffer at 25.0°C.

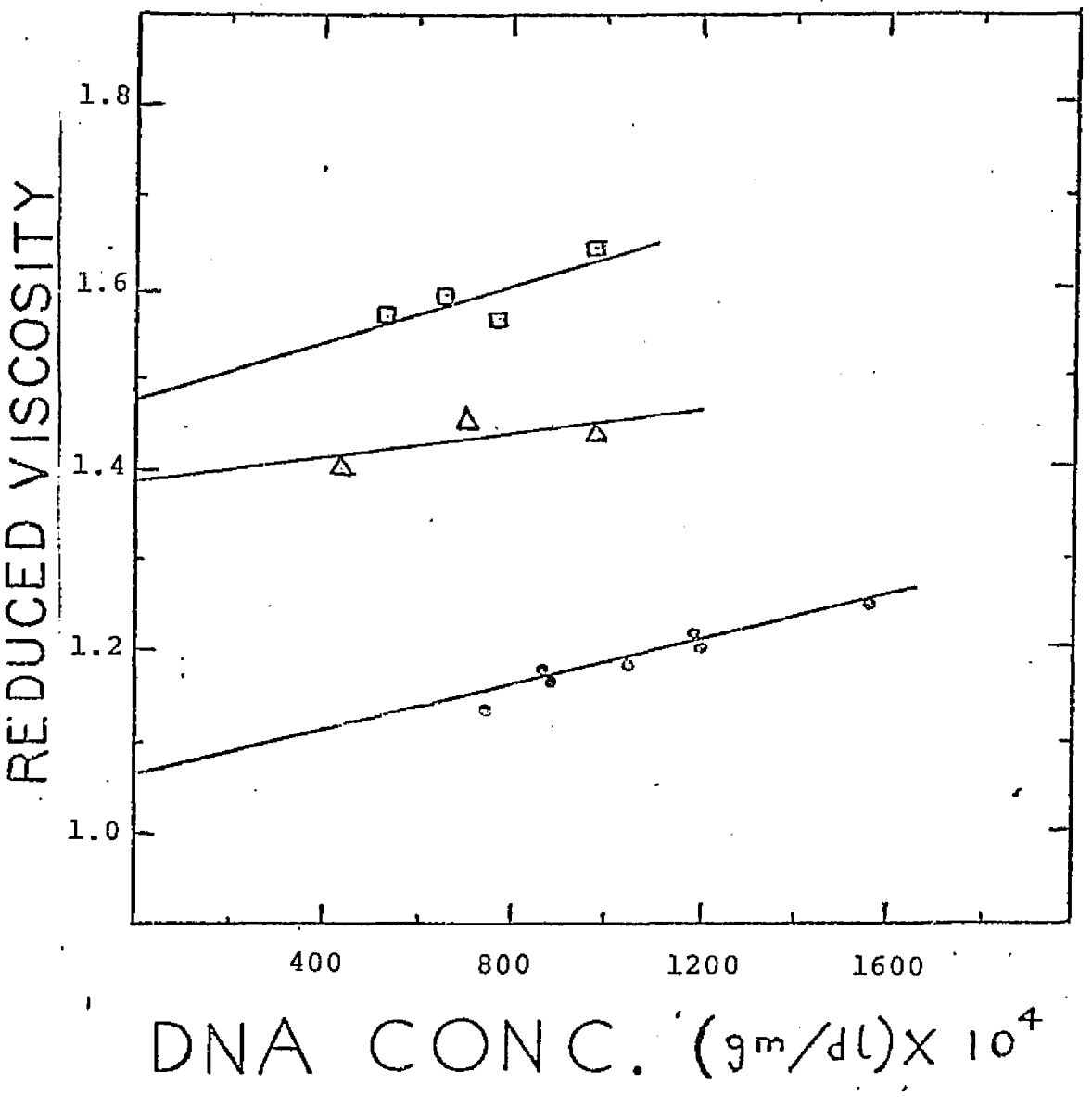

Fig.28. Reduced Viscosity versus DNA Concentration for a series of native sonicated DNA-compound A complexes in DSC-EDTA buffer at 25.0°C. M.W. of DNA was approx. 2×10^5 daltons. Control DNA (●), complex with b.r.= .11 (⊡), and complex with b.r.= .06 (△).

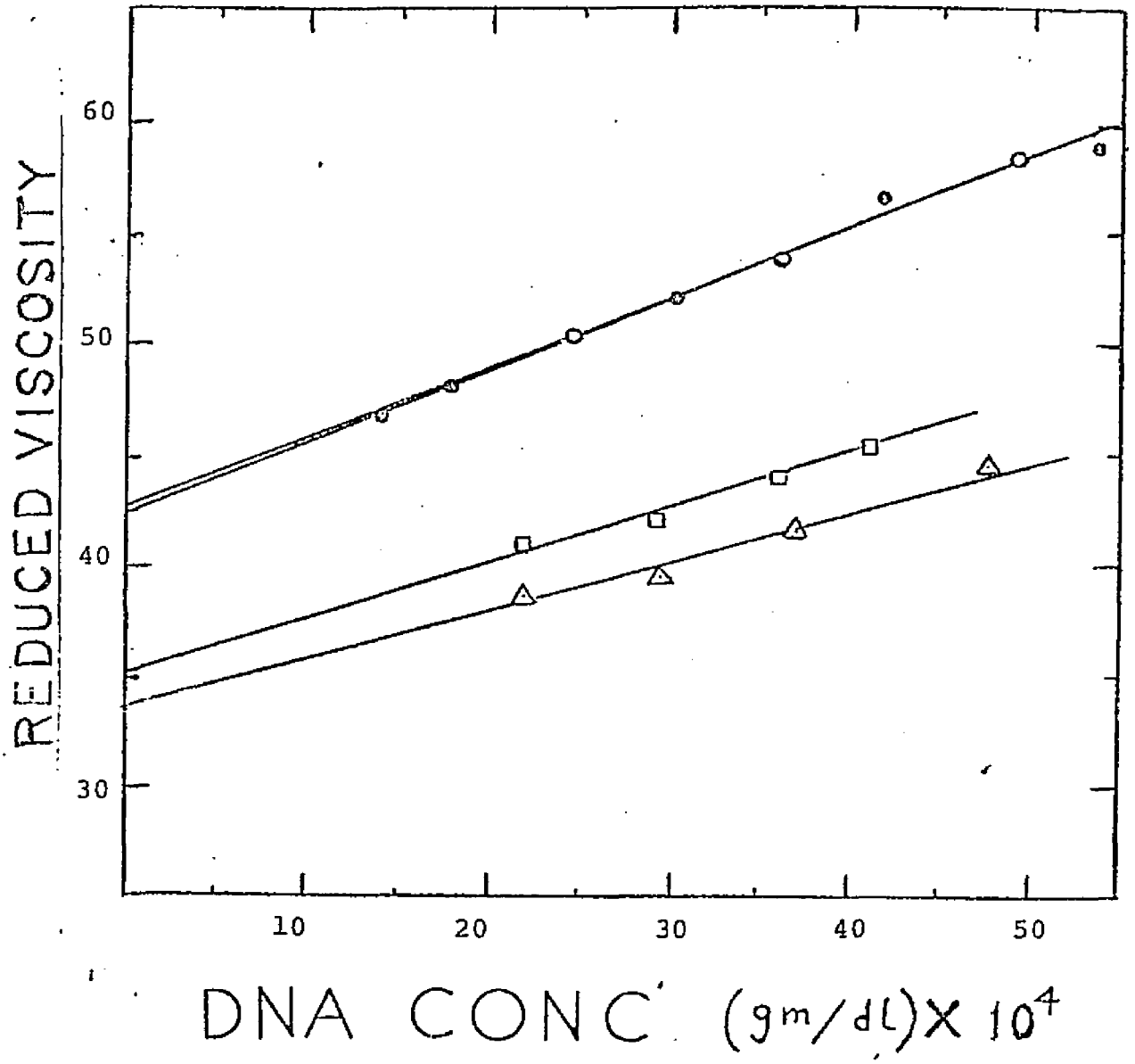

Fig.29. Reduced Viscosity versus DNA Concentration for unsonicated native DNA-mitomycin C complexes in DSC-EDTA buffer (pH 7.4) at 25.0°C. Control (2 determinations, (•) & (○)), complex with b.r.= .10 (△), and complex with b.r.= .12 (□).

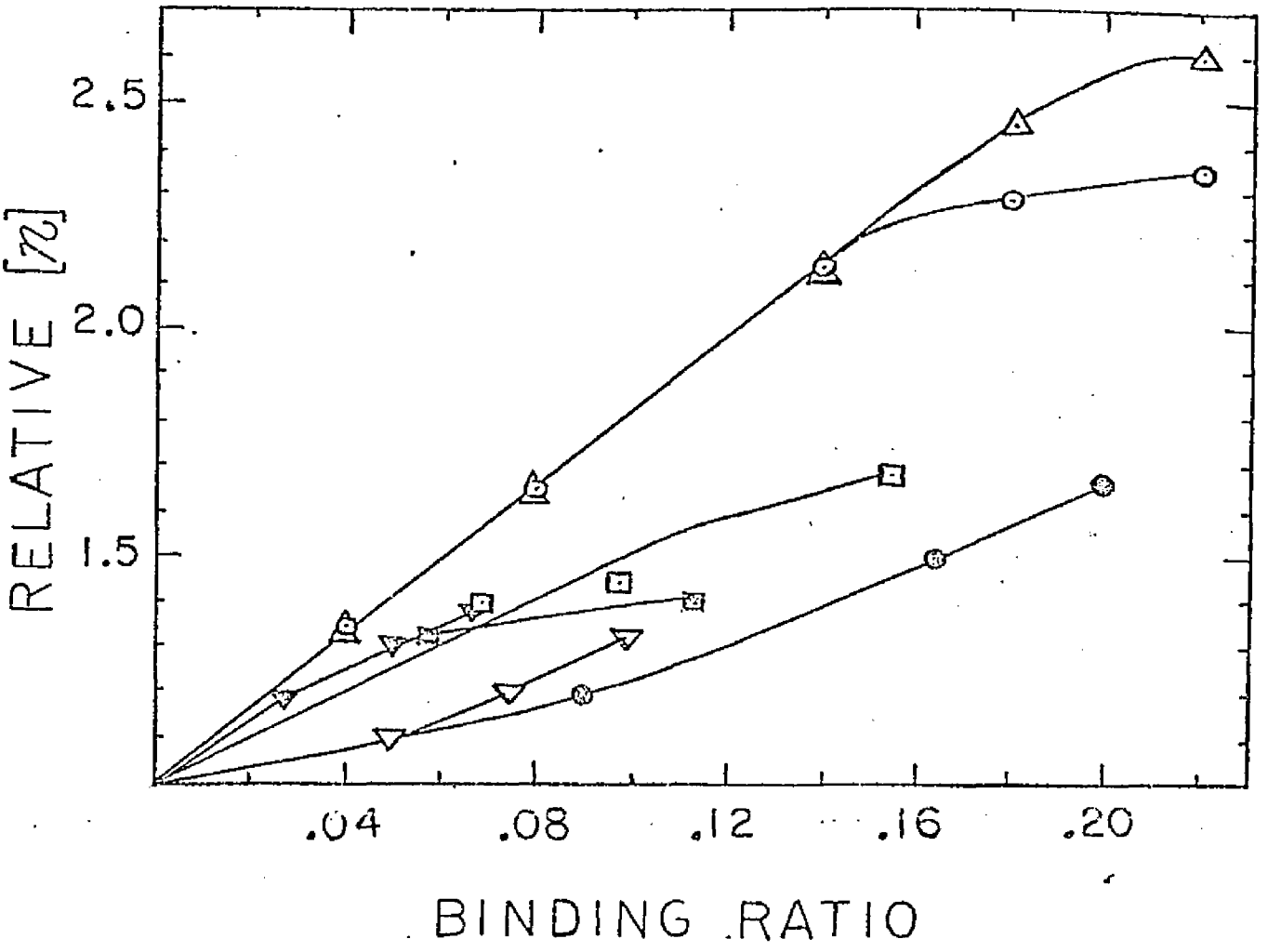

Fig.30. Relative Intrinsic Viscosity $\frac{[\eta_c]}{[\eta_o]}$ versus Binding Ratio for various DNA complexes. Complexes made with proflavine (⊙), and 9-aminoacridine (△) in .005M Na^+. (Unsonicated DNA was used. (Drummond, D.S. et al., 1966)). Complexes formed from actinomycin D (⊛), in .2M Na^+. (DNA M.W. $\simeq 10^5$ daltons. (Muller, W., and Crothers, D.M., 1968)). Complexes made with mitomycin C (⊡), and compound A (⊠) in .015M Na^+. (DNA M.W. was approx. $2X10^5$ daltons). Complexes made with adriamycin (▽), and it's β anomer (▽) in .1M Na^+. (Zunino, F. et al., 1977).

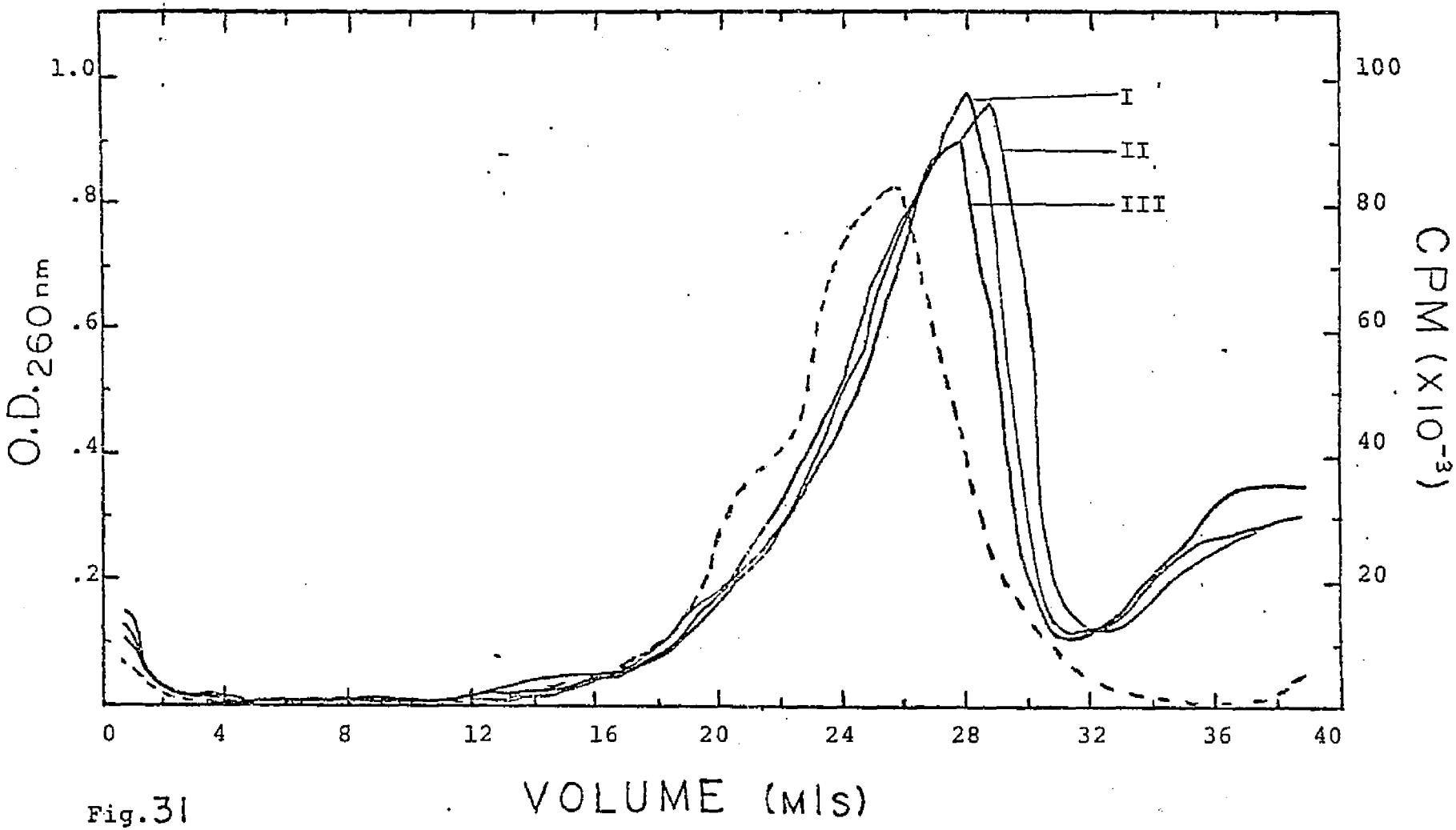

Fig.31

Legend: O.D.$_{260}$ versus Volume Sucrose Fractionated for calf thymus native unsonicated DNA in .017 M phosphate buffer (pH 7.4) in triplicate (I, II, & III, (——)). CPM (x10^{-3}) v.s. Vol. Sucrose Fractionated for unsonicated pneumococcal DNA labled with ^{3}H (- - -) which was run under identical conditions. Run conditions: 24,500 r.p.m. for 17 hrs. at 14°C.

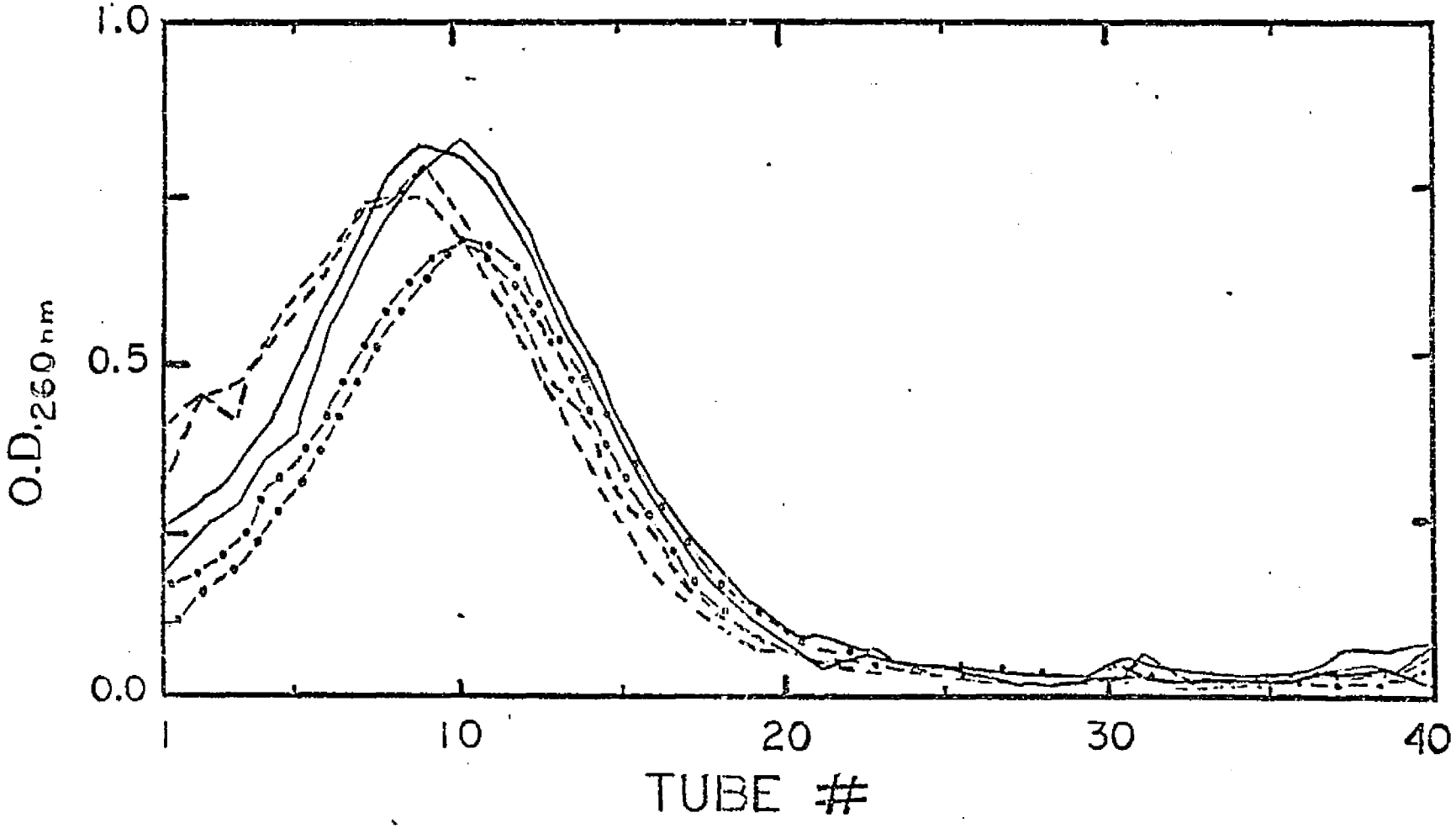

Fig.32. O.D.$_{260}$ versus Tube Number for sonicated native DNA-mitomycin C complexes in neutral sucrose gradients. Run conditions: 24,500 r.p.m. for 93 hrs. and 40 min. at 14 C. Control DNA (-•-), complex (b.r.= .05, (——)), and complex (b.r.= .11, (---)). All samples were run in duplicate.

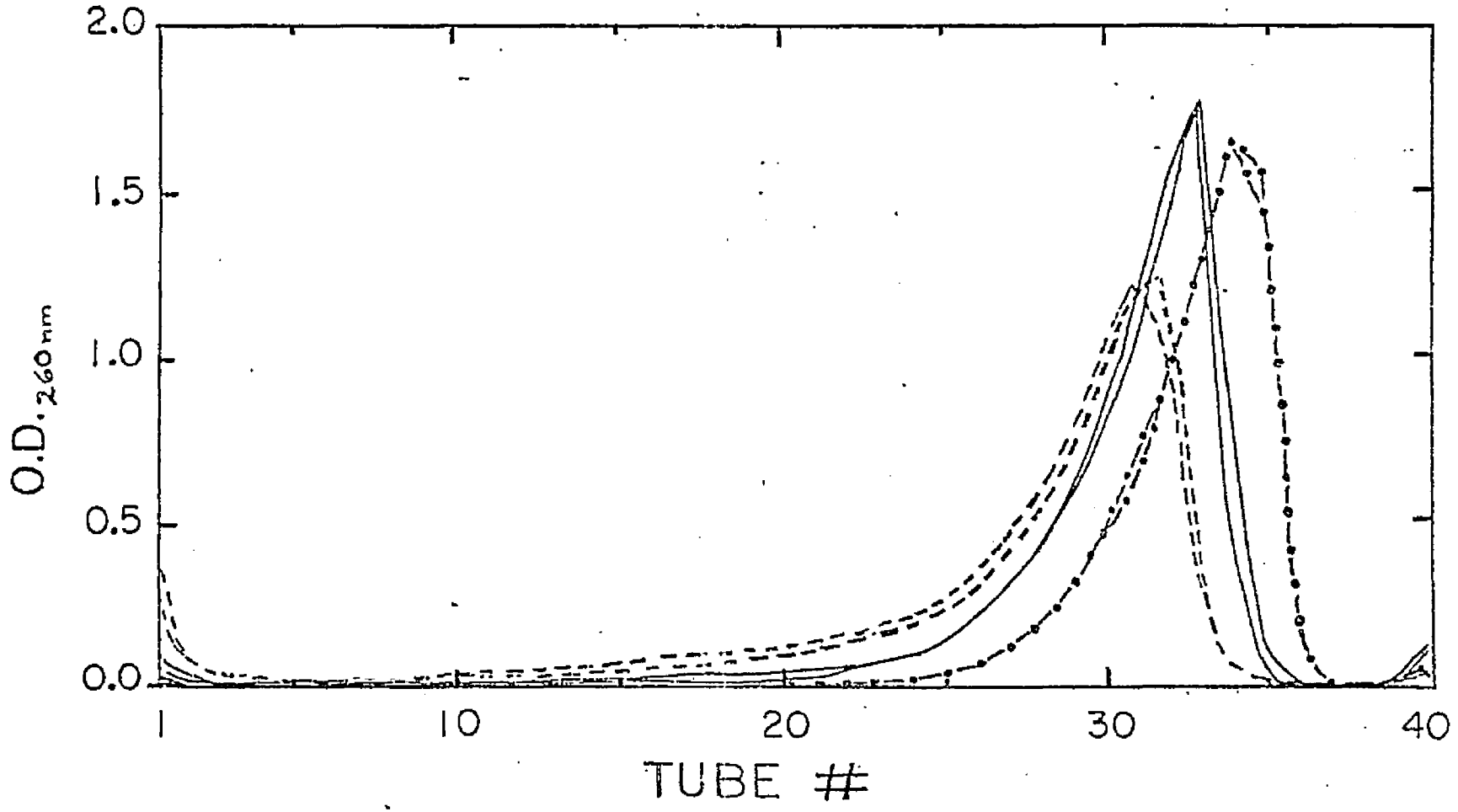

Fig.33. O.D.$_{260}$ versus Tube Number for unsonicated native DNA-mitomycin C complexes in neutral sucrose gradients. Run conditions: 24,500 r.p.m. for 9.5 hrs. at 14°C. Control DNA (-•-), complex (b.r.=.05, (——)), and complex (b.r.= .10, (---)). All samples were run in duplicate.

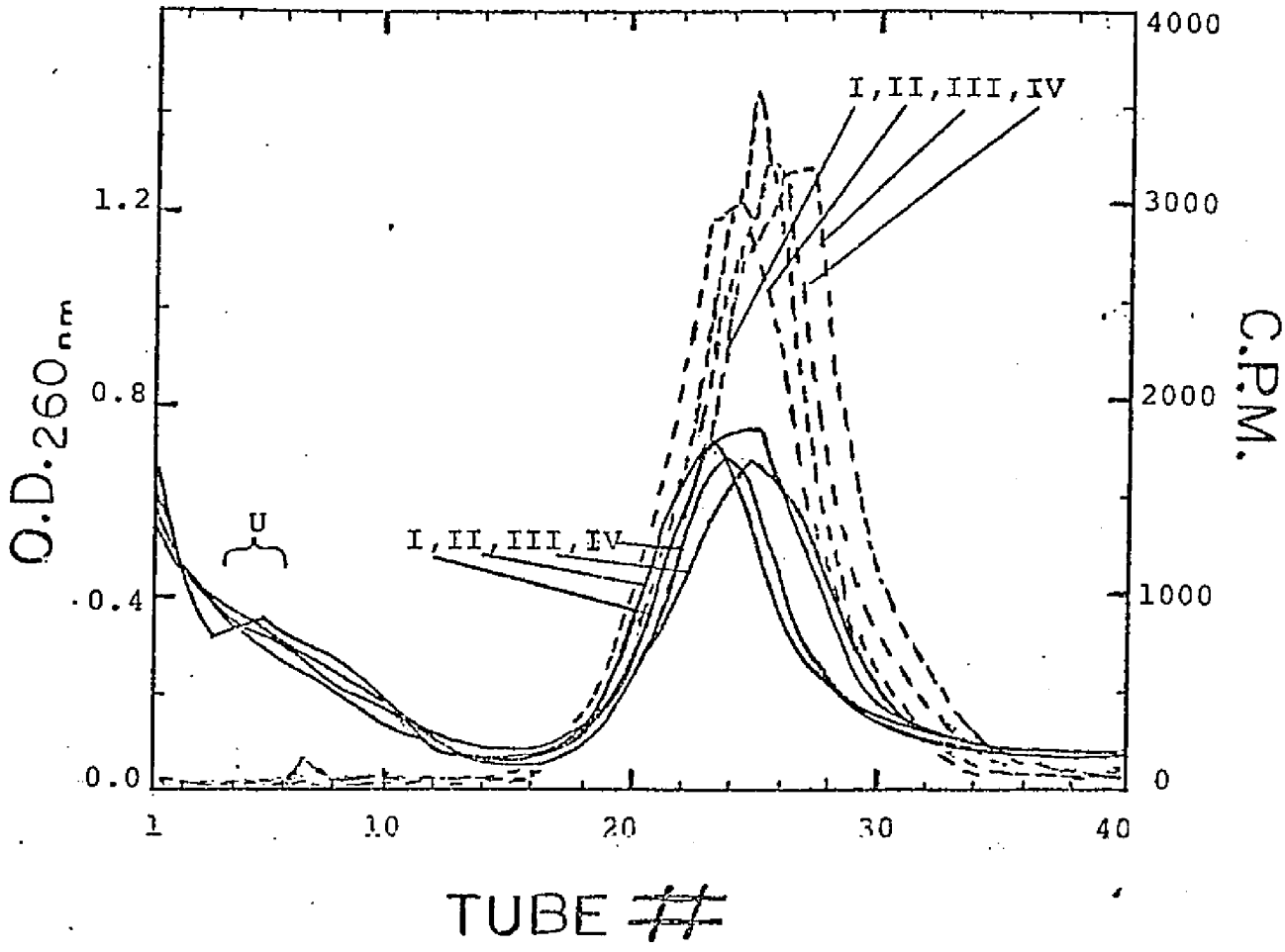

Fig.34 . O.D.$_{260}$ (——) and C.P.M. (---) versus Tube Number for native calf thymus DNA samples in neutral sucrose gradients. I and II are duplicates of labled sonicated and unlabled unsonicated DNA reacted under standard reductive activation conditions with mitomycin C (binding ratio = .08). III and IV are duplicates of controls for runs I and II (controls are a similar mixture of labled sonicated and unlabled unsonicated DNA without mitomycin C). U represents the sedimentation of the unlabled unsonicated DNA. Run conditions: 24,500 r.p.m. at 14°C for 49 hours.

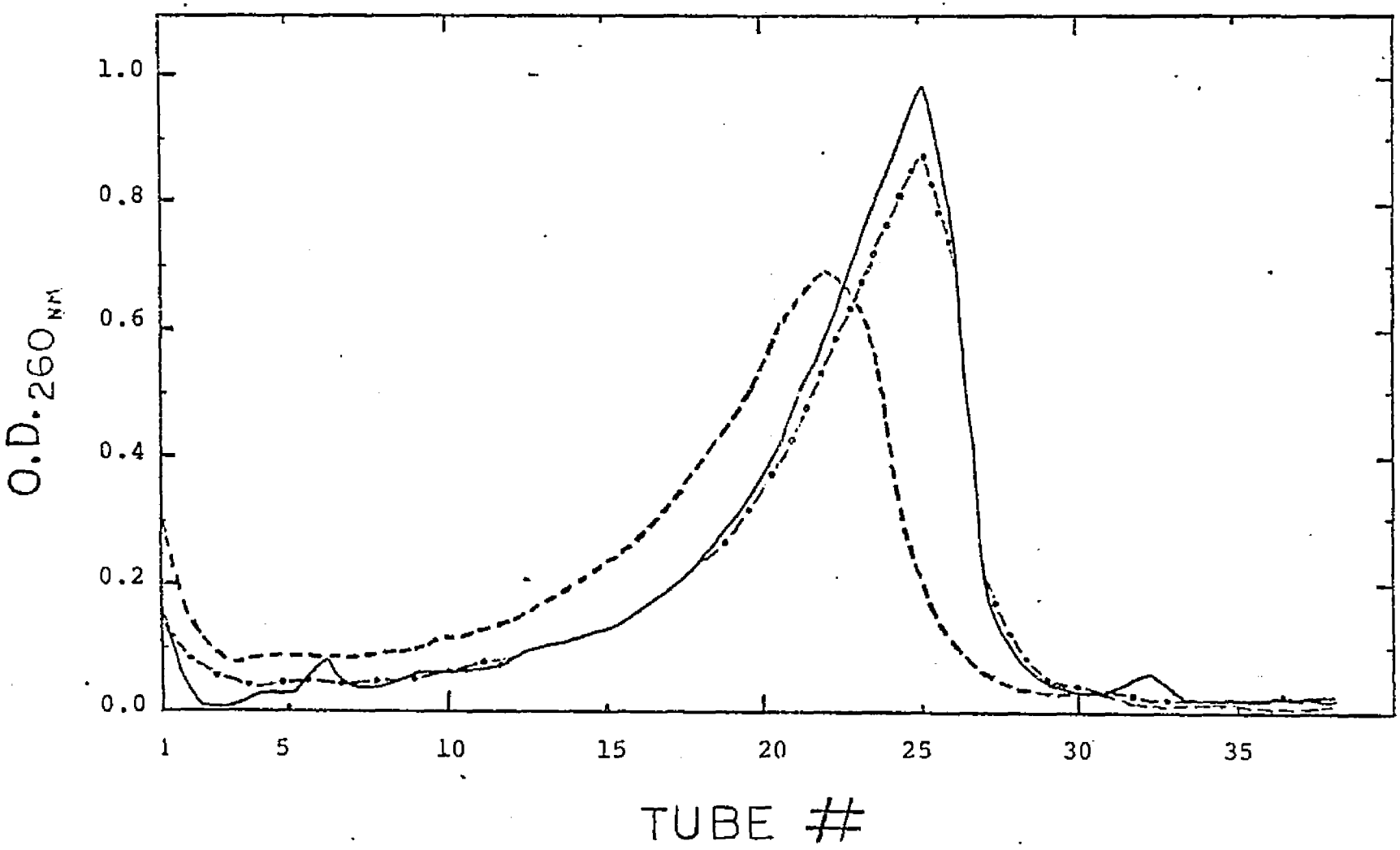

Fig.35. O.D.$_{260}$ versus Tube Number for Calf Thymus DNA samples in neutral sucrose gradients. Run conditions: 23.5 hrs., and 24,500 r.p.m. at 10°C. Control DNA (-•-), control + $Na_2S_2O_4$ (—·—), and DNA-mitomycin C (b.r.=.087, (---)).

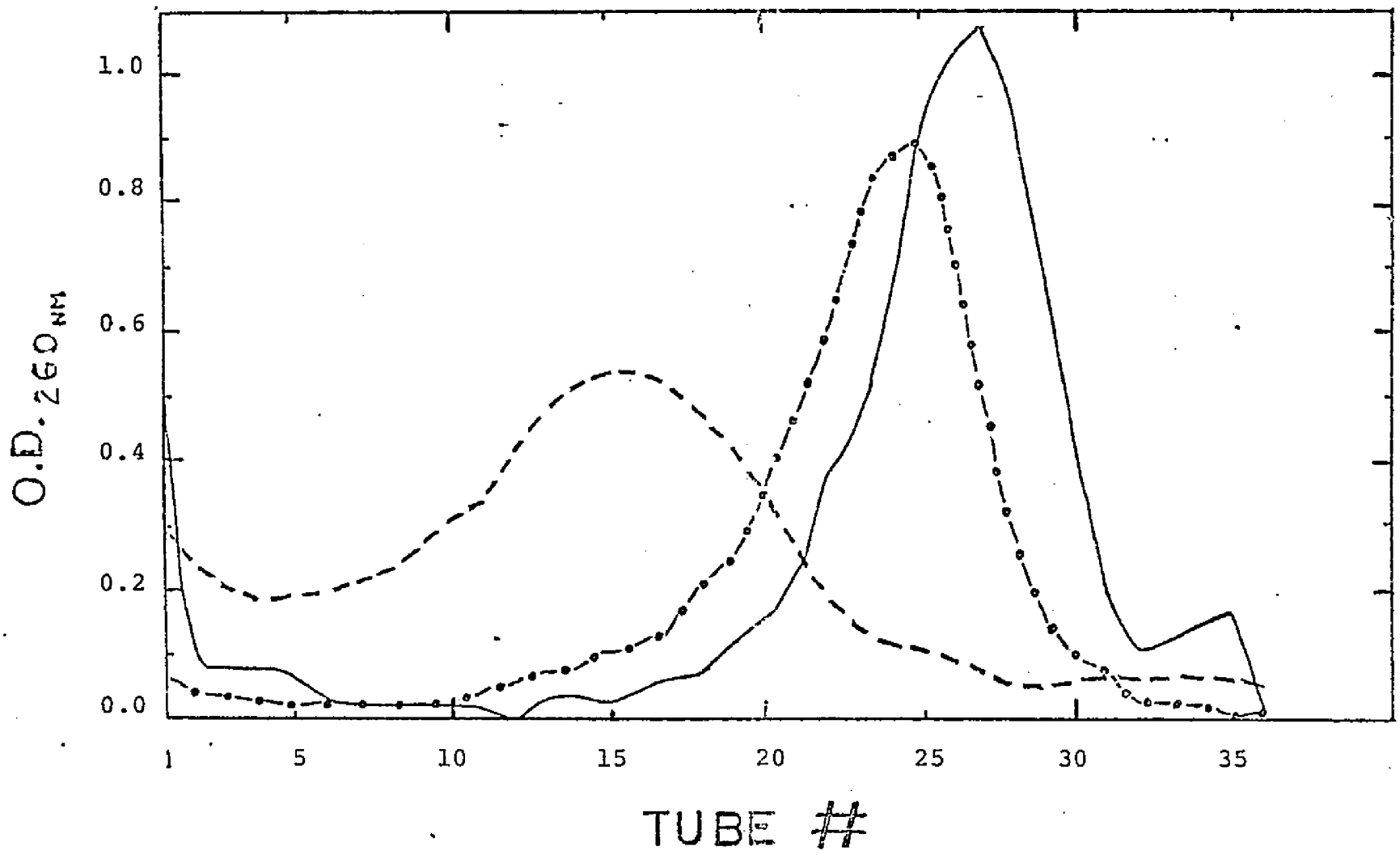

Fig.36 : O.D.$_{260}$ versus Tube Number for alkali denatured DNA in alkaline sucrose gradients (pH 12.0). Run conditions: 24,000 r.p.m. for 24 hrs. at 10°C. Control DNA (-•-), control + $Na_2S_2O_4$ (——), and DNA-mitomycin C (b.r.=.087, (- - -)).

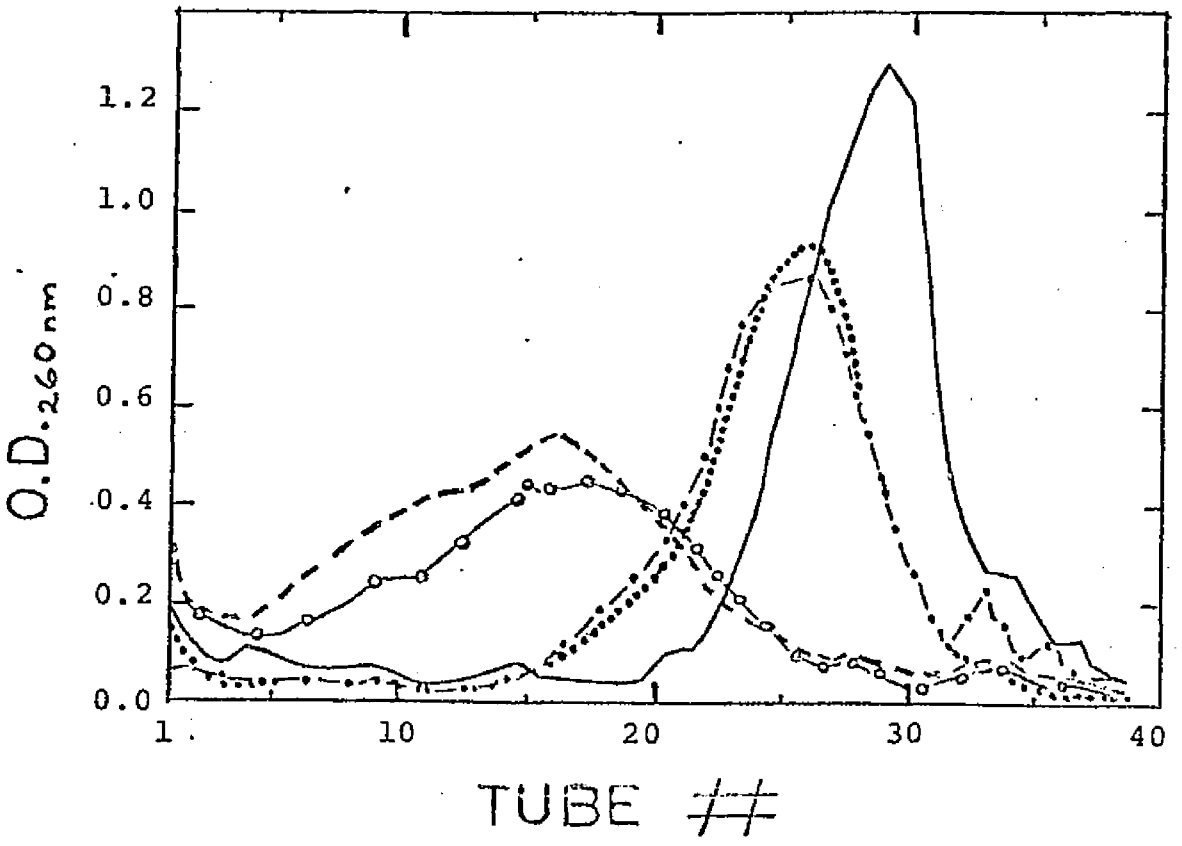

Fig. 37. O.D.$_{260}$ versus Tube Number for alkali denatured Calf Thymus DNA samples in alkaline sucrose gradients (pH 12.0). Run conditions: 24,000 r.p.m. for 22 hrs. at 10°C. Control DNA (—o—), control + $Na_2S_2O_4$ (——), DNA-mitomycin C (b.r.= .09, (– – –)), control + $Na_2S_2O_4$ + catalase + superoxide dismutase (••••), and DNA-mitomycin C (b.r.= .09) + catalase + superoxide dismutase (–o–o–).

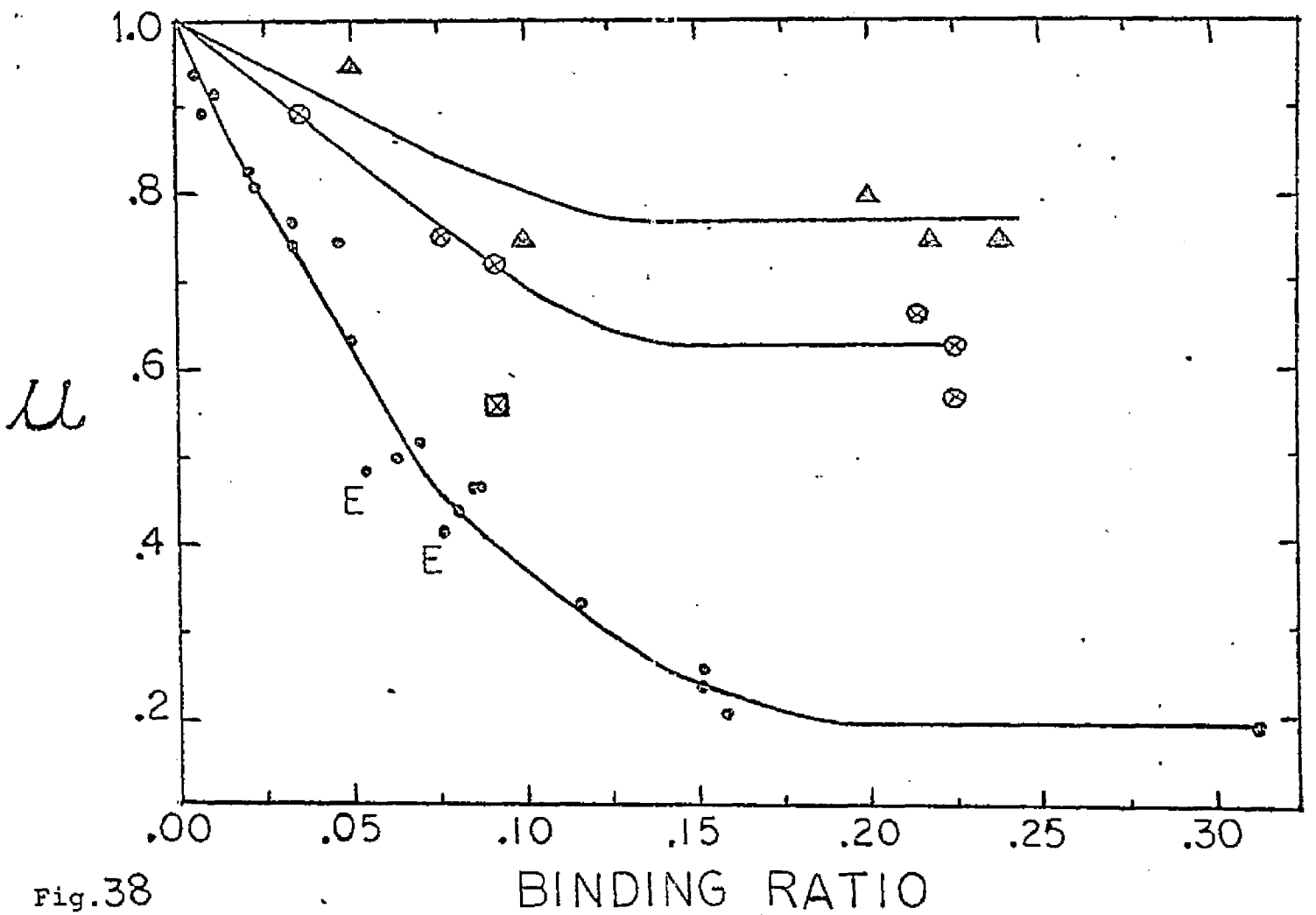

Fig.38

Legend: Electrophoretic Mobility (μ) vs. Binding Ratio for a series of DNA complexes in 3.5% polyacrylamide. Complexes are unsonic. calf thymus DNA-mitomycin C with DNA MW of~3.6 x10^6 (●), c. thymus DNA-MC with DNA MW of~10^6 (⊠), unsonic. E. Coli DNA-MC with DNA MW of~3.6x10^6 (E), unsonic. c. thymus DNA-ethidium (▲), and sonic c. thymus DNA-MC (⊗).

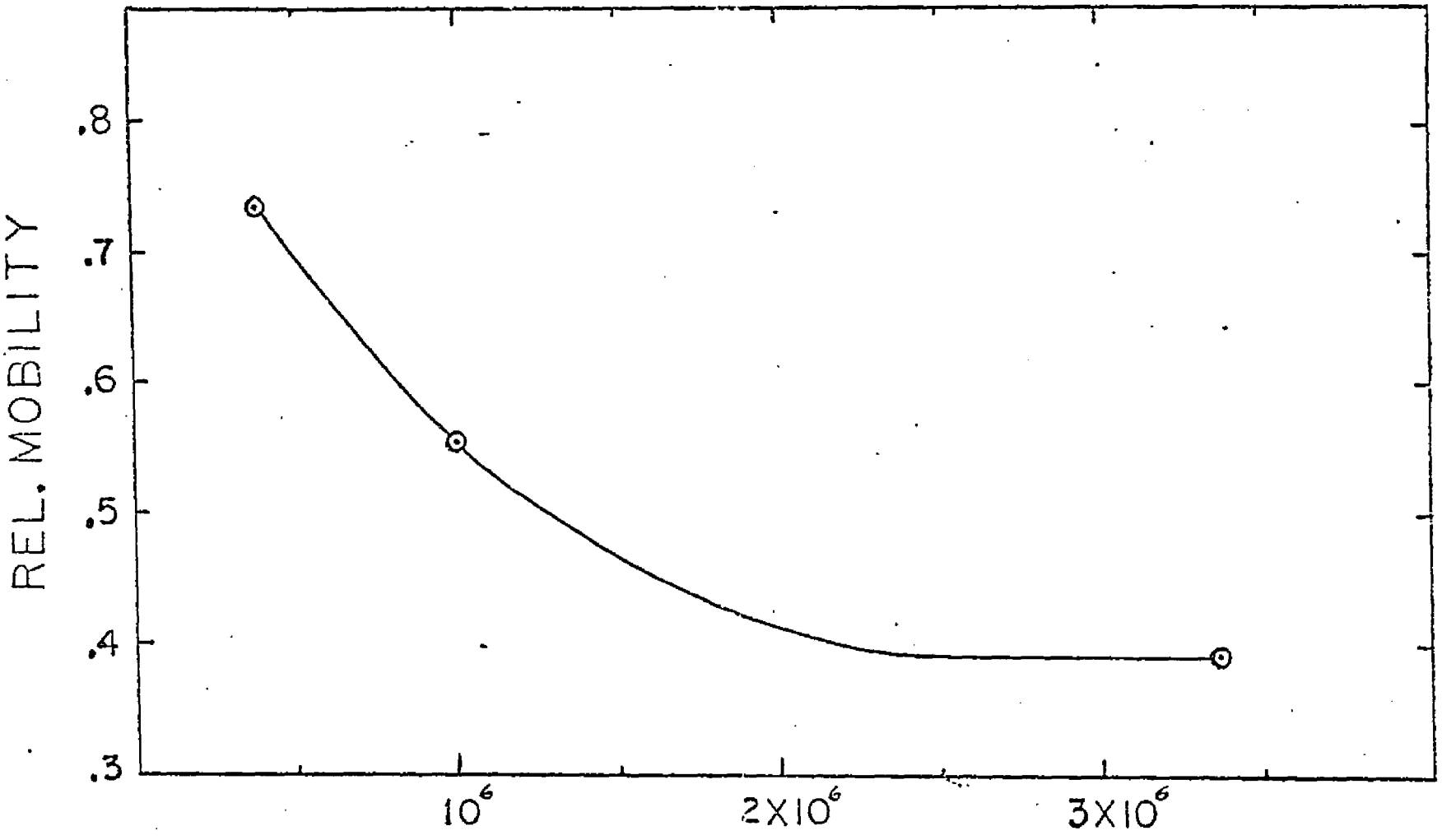

Fig.39

Legend: Relative Mobility vs. DNA Molecular Weight for a series of calf thymus DNA-mitomycin C complexes of binding ratio .09 in 3.5% polyacrylamide.

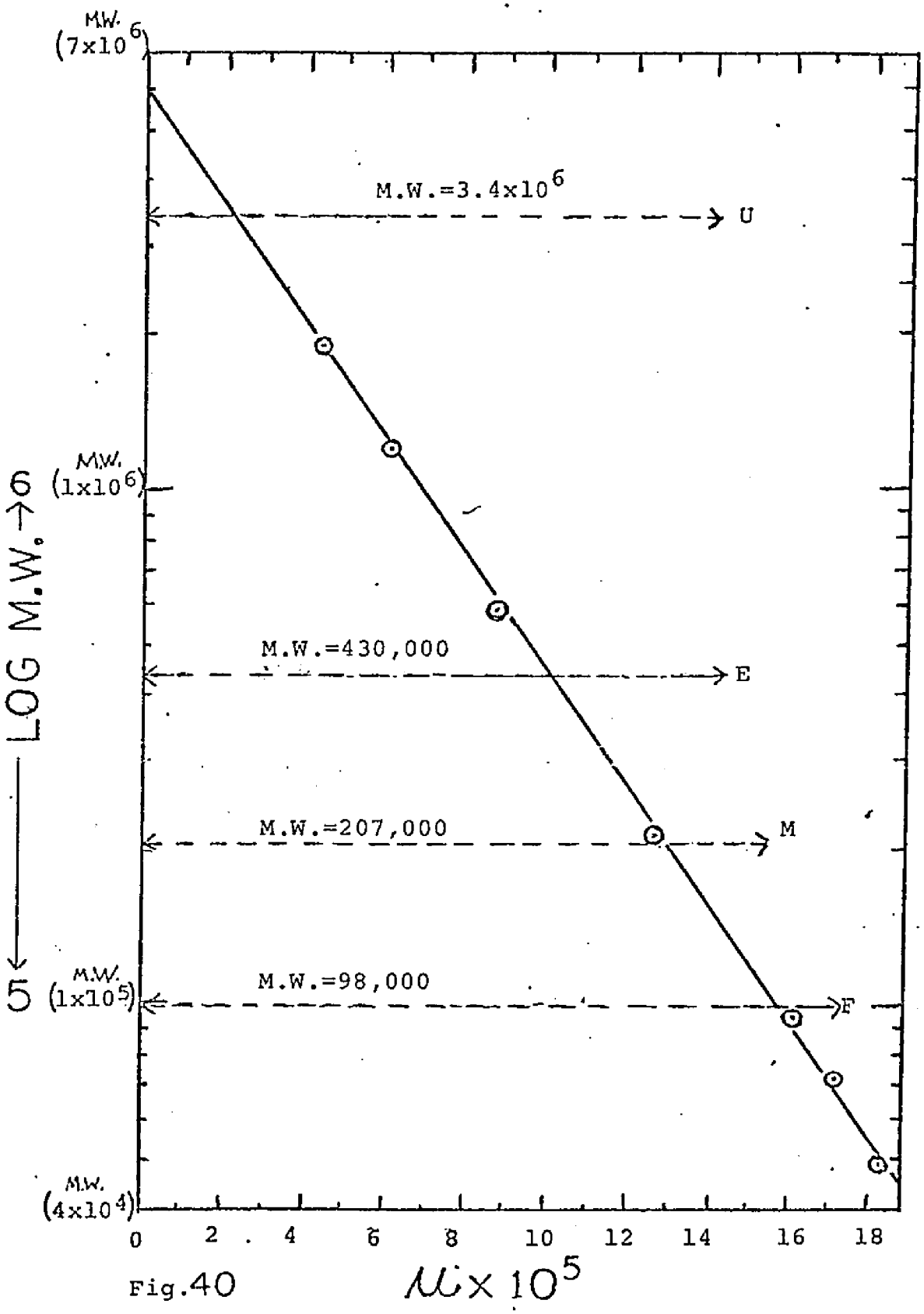

Fig.40

Log M.W. vs. Electrophoretic Mobility (μ)x10^5 for a f_1RFI DNA digest (⊙) in agarose. By extrapolation: U is unsonic. calf thymus DNA, and E, M, & F respectively are the end, middle, and front portions of a sonic. c. thymus DNA electrophoretic band.

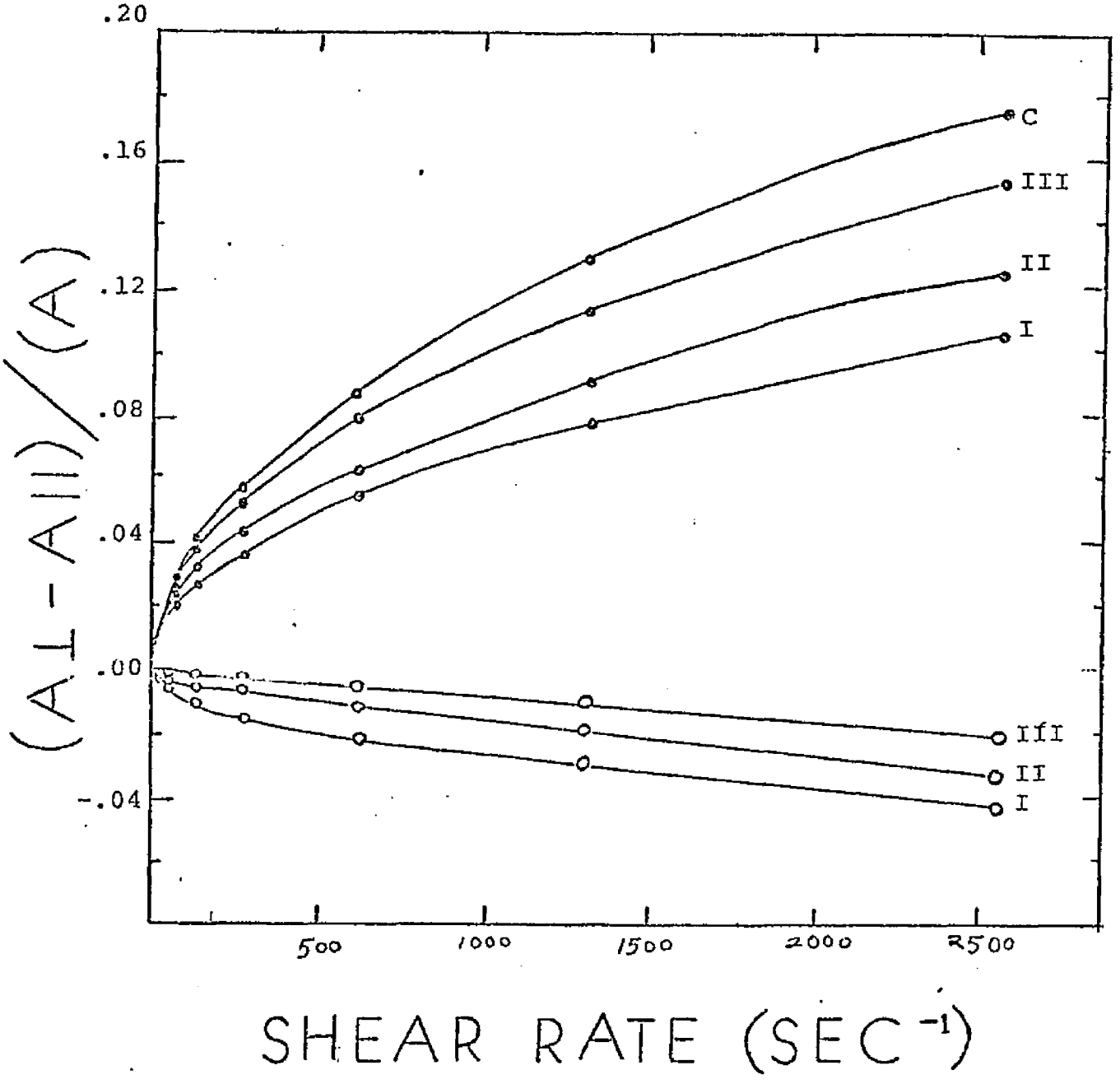

Fig.41 . Uncorrected Reduced Dichroism versus Shear Rate for a series of native unsonicated calf thymus DNA-mitomycin C complexes. C (control), I (complex, b.r. = .15), II (complex, b.r. = .09), III (complex, b.r. = .06). Reduced dichroism at 260 nm (o). Reduced dichroism at 310 nm (o).

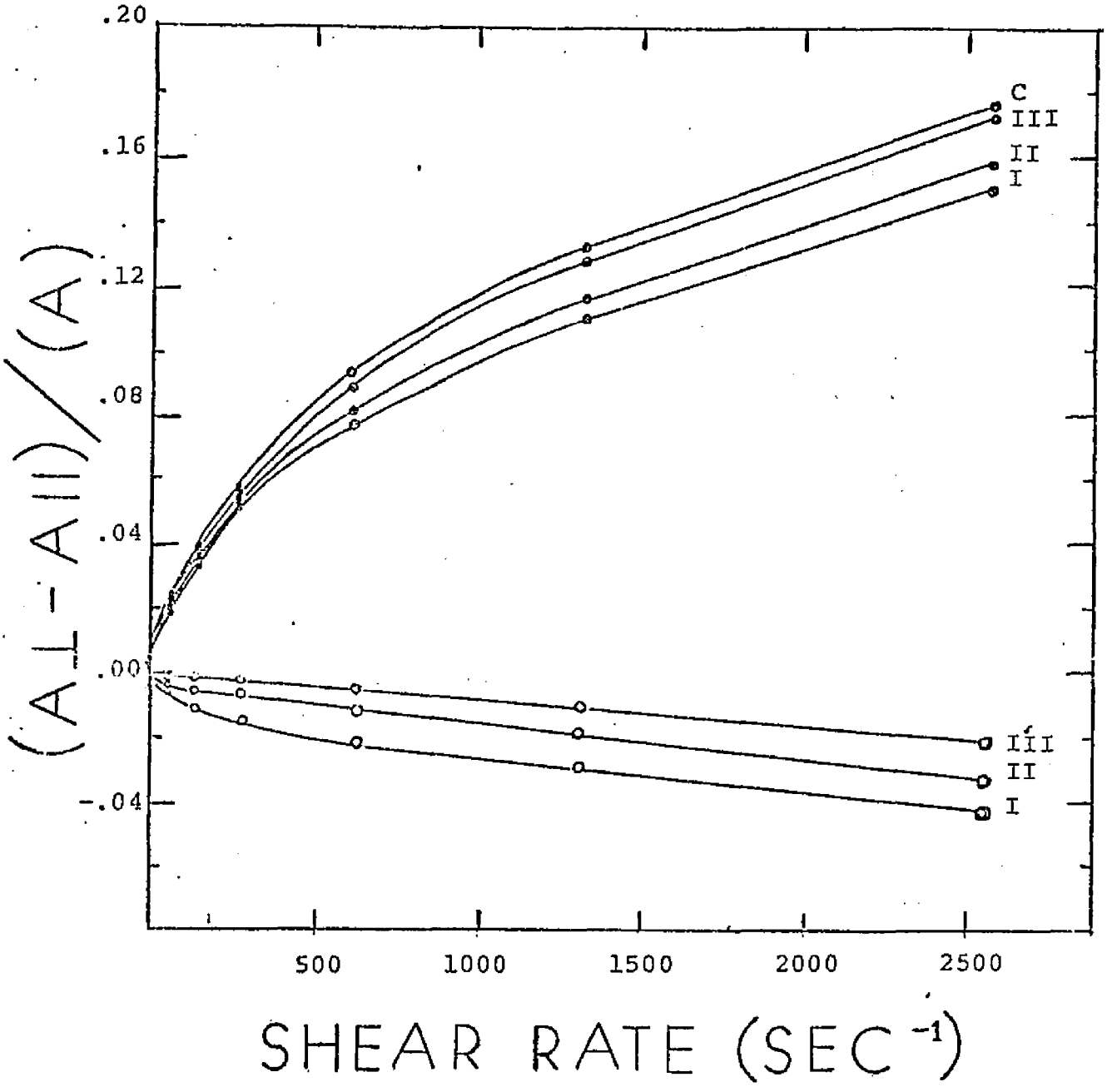

Fig.42. Reduced Dichroism versus Shear Rate for a series of native unsonicated calf thymus DNA-mitomycin C complexes. C (control), I (complex, b.r. = .15), II (complex, b.r. = .09), III (complex, b.r. = .06). Reduced dichroism at 260 nm (●). Reduced dichroism at 310 nm (○).

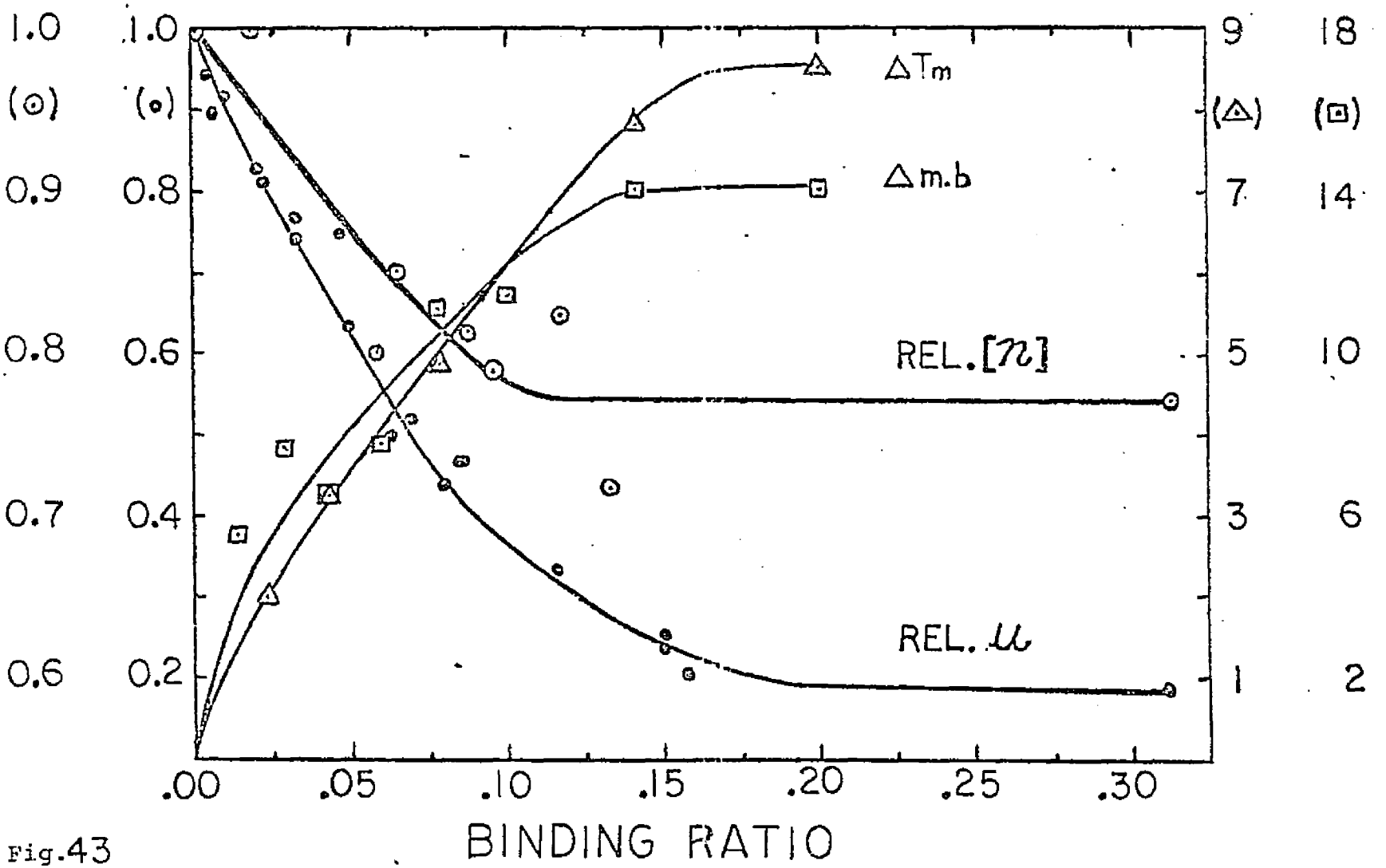

Fig.43

Legend: The Variance in Physico-Chemical Properties (Relative Intrinsic Viscosity $[\eta]$, Relative Electrophoretic Mobility (u), Δ Melting Temperature, and Δ Melting Breadth) with Binding Ratio for Unsonicated Calf Thymus DNA-Mitomycin C Complexes.

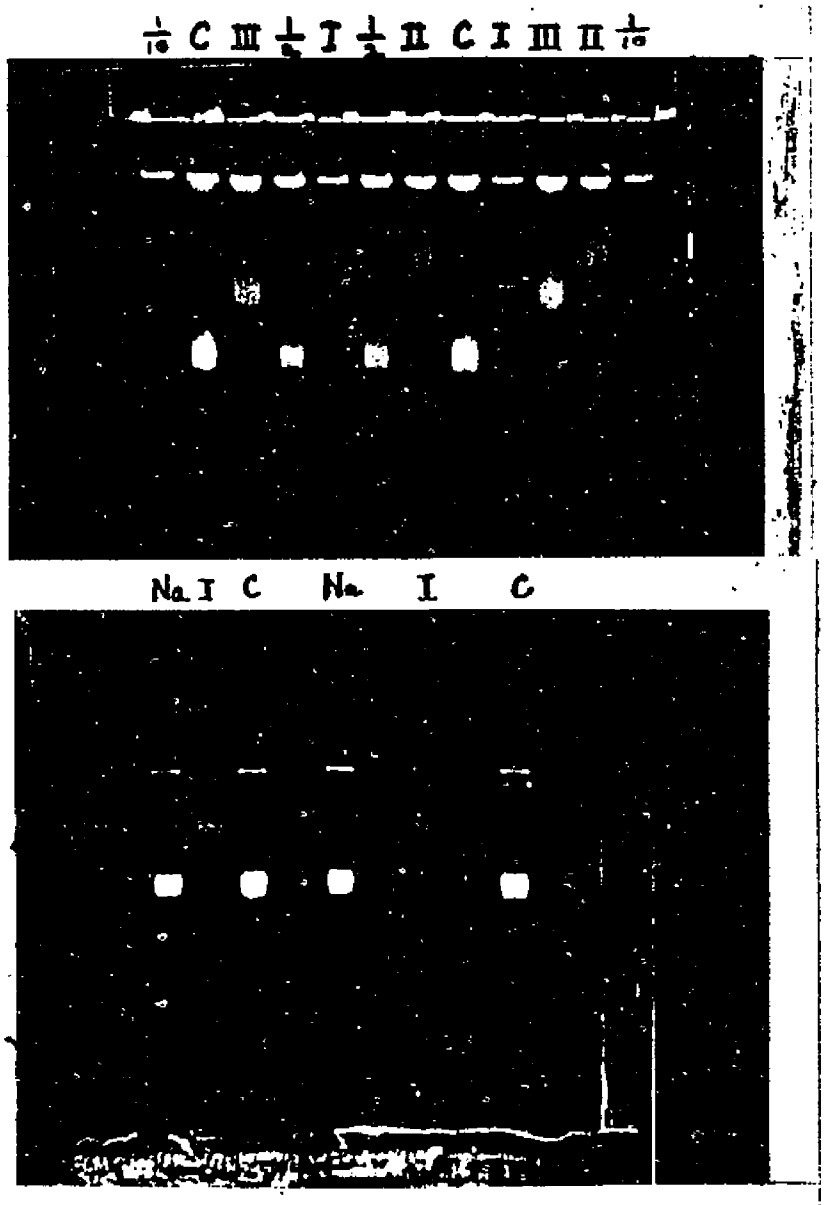

Plate A1 : 3.5% Polyacrylamide

Slot	Description
C	Control Native E.Coli DNA
I	Native E.Coli DNA-MC Complex (B.Ratio = 0.17)
II	Native E.Coli DNA-MC Complex (B.Ratio = 0.08)
III	Native E.Coli DNA-MC Complex (B.Ratio = 0.05)
1/2	A Two-Fold Diluted Control
1/10	A Ten-Fold Diluted Control

Plate A2 : 3.5% Polyacrylamide

Slot	Description
C	Native C.Thymus DNA Control
Na	Control Treated with $Na_2S_2O_4$ (13.5 umoles to 6 umoles of DNA)
I	Native C.Thymus DNA-MC Complex (B.Ratio Approx. 0.09)

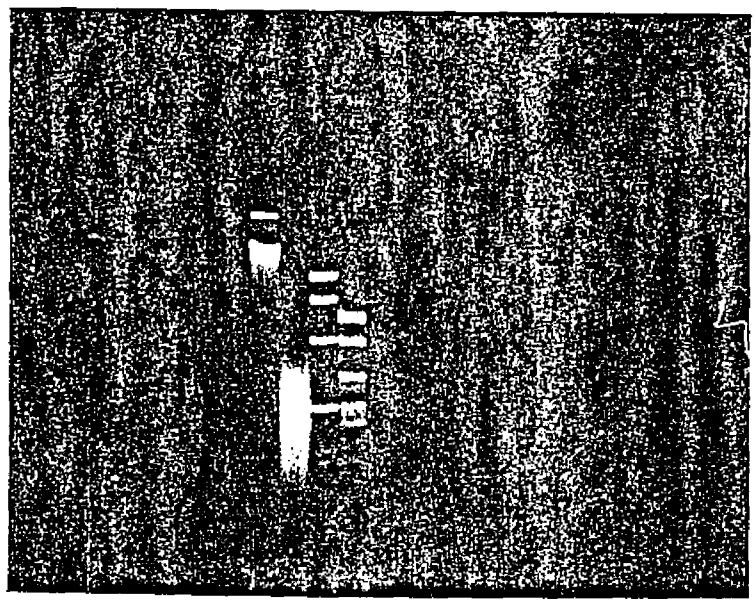

Plate H : - 1.8% Agarose Gel Electrophoresis of Several Nucleic Acid Samples.

Slot	Description
U	Unsonicated Native Calf Thymus DNA.
S	Sonicated Native Calf Thymus DNA.
R_2	f_1RF_1 Restrictioned Fragments (See Results and Methods).
R_1	Single Stranded DNA f_1 form Restrictioned (See Results and Methods).

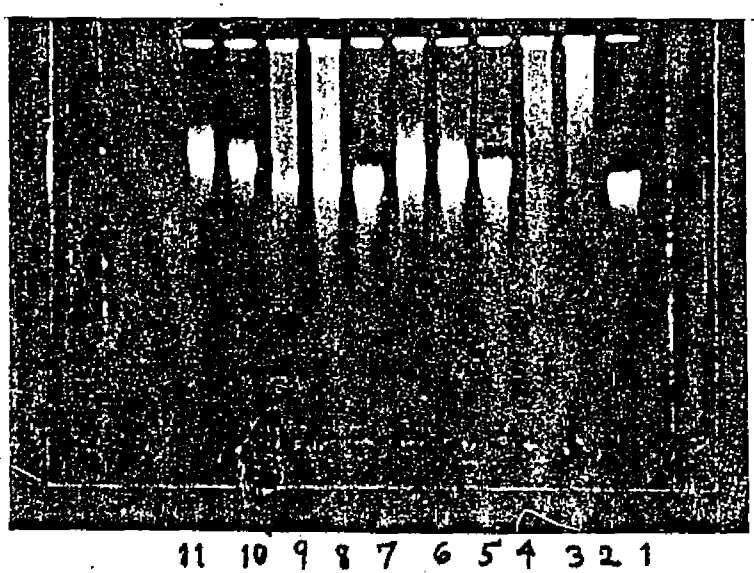

Plate B2 : 3.5% Polyacrylamide - Unsonicated C.Thymus DNA Crosslinked with Nitrous Acid. (HNO_2).

Slot	Description
1	Control DNA
2	Control DNA Alkali Denatured
3	Control DNA Thermally Denatured
4	HNO_2-Crosslinked(100%)-DNA (Sample 4)
5	Sample 4 Thermally Denatured
6	Sample 4 Alkali Denatured
7	HNO_2-Crosslinked(80%)-DNA (Sample 7)
8	Sample 7 Thermally Denatured
9	Sample 7 Alkali Denatured
10	DNA-MC Complex of B.Ratio(0.02)-Samp.10
11	Sample 10 Thermally Denatured

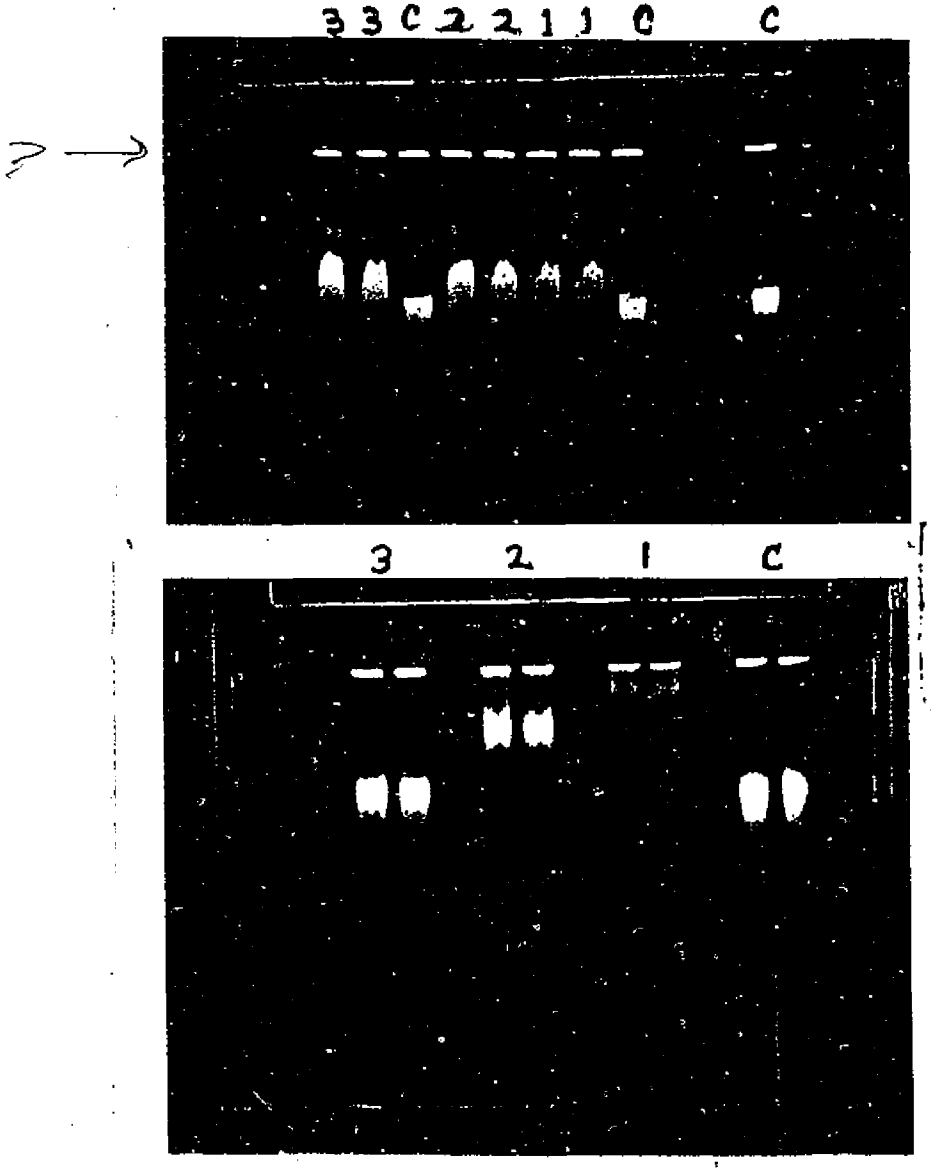

Plate C1 : 3.5% Polyacrylamide - Unsonicated C.Thymus DNA-Ethidium Complexes. (Native)

Slot		Description
C	-	Control Calf Thymus DNA
1	-	DNA-Ethidium Complex (B.Ratio 0.24)
2	-	DNA-Ethidium Complex (B.Ratio 0.21)
3	-	DNA-Ethidium Complex (B.Ratio 0.10)

Plate C2 : 3.5% Polyacrylamide - Unsonicated C.Thymus DNA-Mitomycin C Complexes. (Native)

Slot		Description
C	-	Control Calf Thymus DNA
1	-	DNA-MC Complex of B.Ratio 0.16
2	-	DNA-MC Complex of B.Ratio 0.05
3	-	DNA-MC Complex of B.Ratio 0.01

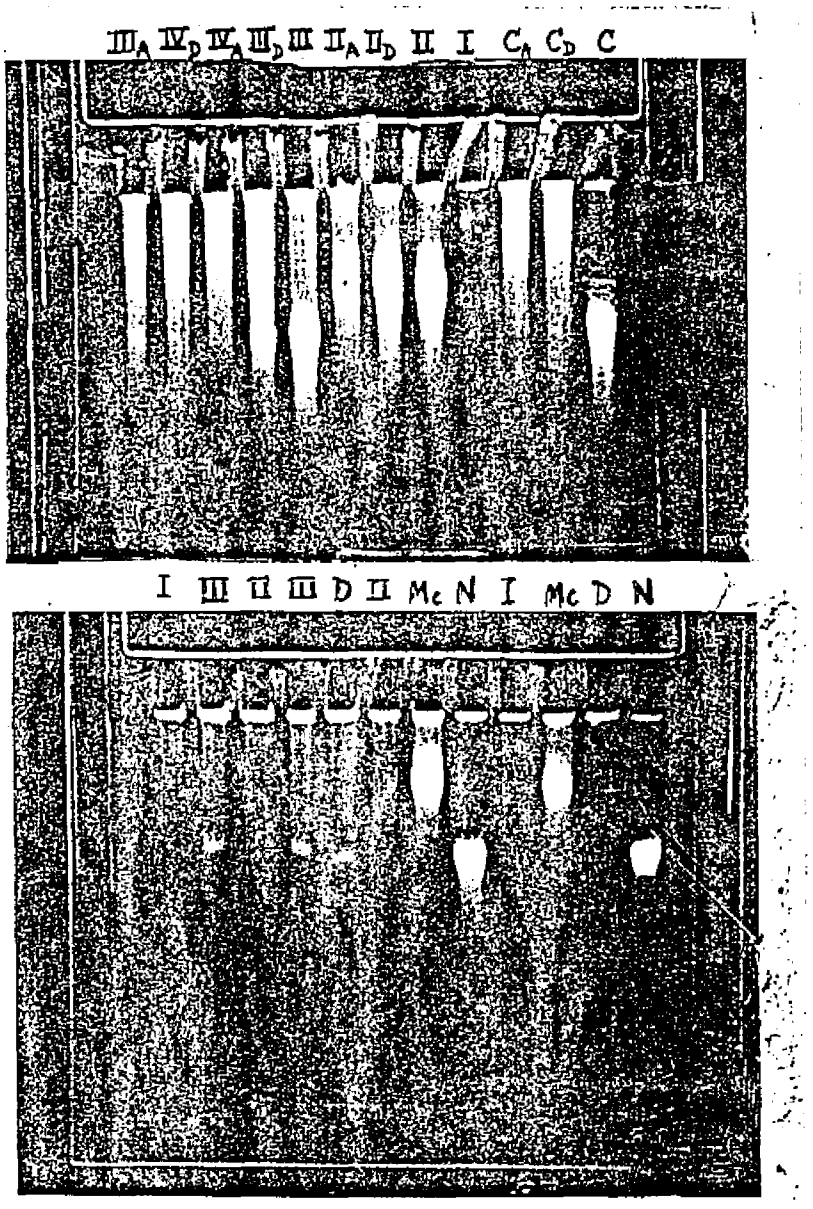

Plate E1 : 3.5% Polyacrylamide - Unsonicated Calf Thymus DNA-MC Complexes Subjected to Thermal and Alkali Denaturation.

Slot	Description
C	Control Native DNA
C_A	Control Alkali Denatured
C_D	Control Thermal Denatured
I	DNA-MC Complex (Native) (B.Ratio 0.26)
II	DNA-MC Complex (Native) (B.Ratio 0.05)
II_A	DNA-MC - (B.R.=0.05) Alkali Denatured
II_D	DNA-MC - (B.R.=0.05) Thermal Denatured
III	DNA-MC Complex (Native) (B.Ratio ~.005)
III_A	DNA-MC (B.R.~.005) Alkali Denatured
III_D	DNA-MC (B.R ~.005) Thermal Denatured
IV_A	DNA-MC (B.R <.005) Alkali Denatured
IV_D	DNA-MC (B.R.<.005) Thermal Denatured

Plate E2 : 3.5% Polyacrylamide - Unsonicated Calf Thymus Denatured DNA-MC Complexes. (Alkali Denatured)

Slot	Description
N	Native Control DNA
D	Denatured Control
I	Denat.DNA-MC Complex (B.Ratio 0.29)
II	Denat.DNA-MC Complex (B.Ratio 0.08)
III	Denat.DNA-MC Complex (B.Ratio 0.02)
Mc	Native DNA-MC Complex (B.Ratio 0.07)

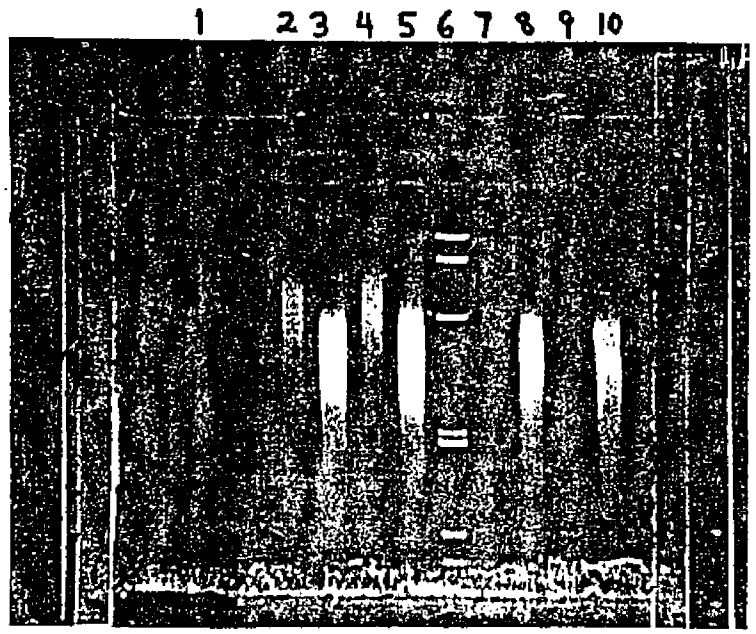

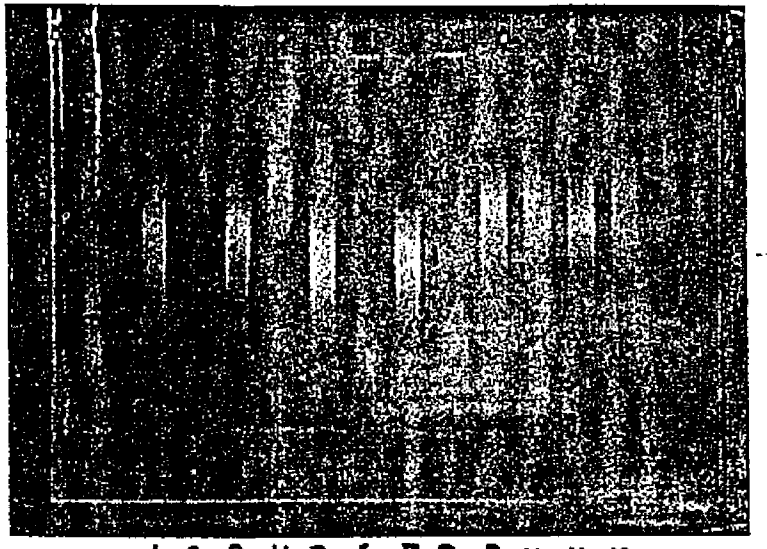

Plate F1 : Polycrylamide 3.5% - Sonicated Calf Thymus DNA-MC Complexes (Native).

Slot	Description
3&5	Native Calf Thymus DNA (Controls for Slots 2&4).
2&4	Sonic. DNA-MC Complex (B.Ratio 0.08).
8&10	Native Calf Thymus DNA (Controls for Slots 7&9).
7&9	Sonic. DNA-MC Complex (B.Ratio 0.23).
1	A repeat of slot 7&9 runs using 2X the Normal DNA Concentration.
6	f_1RF_1 Phage DNA Restrictioned by Endo R Hae III Enzyme.

Plate F2 : Polyacrylamide 3.5% - Sonicated Calf Thymus DNA-MC Complexes (Native).

Slot	Description
1&3	Unbound DNA Controls for Slots 2&4.
2&4	Sonic. DNA-MC Complex (B.Ratio 0.09).
5&7	Unbound DNA Controls for Slots 6&8.
6&8	Sonic DNA-MC Complex (B.Ratio 0.21).
9&11	Unbound DNA Controls for Slots 10&12.
10&12	Sonic. DNA-MC Complex (B.Ratio 0.04).

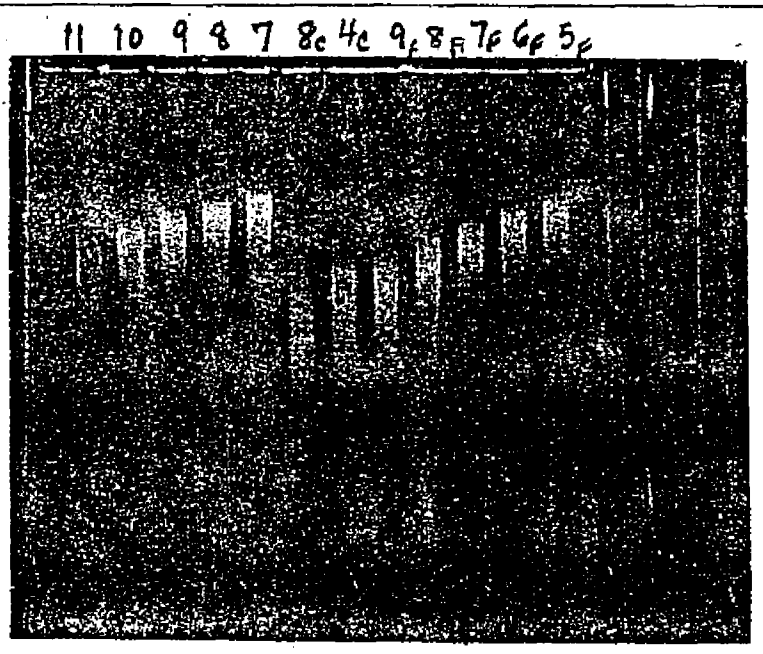

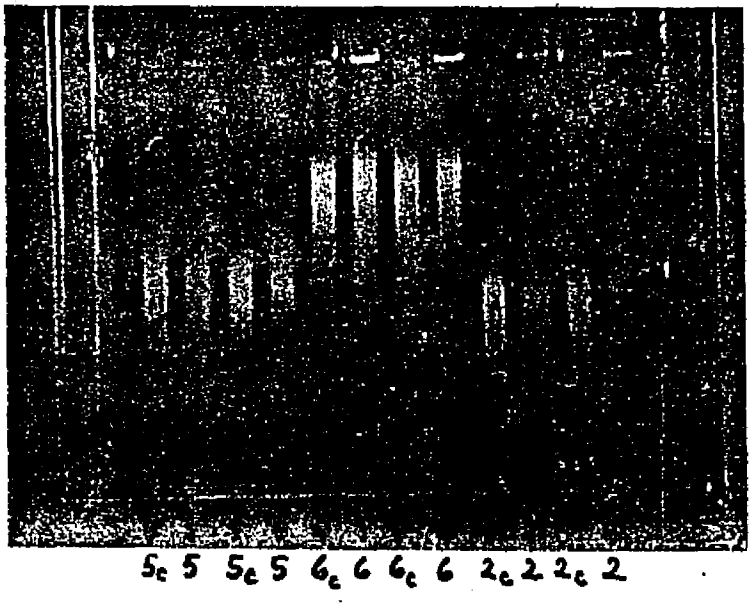

Plate G1 : Polyacrylamide (3.5%) - Sonicated DNA Fractioated by Sucrose Gradient Ultracentrifugation. Samples in Slots 11 to 7 (From left to Right) are DNAs in Increasing M.W. Fractionated One Test Tube Apart Via a Punctured Polyallomar Tube.

Samples in Slots 8_c to 5_f are similar Except this Set of Fractions was from a Duplicate Preparative Centrifugation.

Plate G2 : - Polyacrylamide (3.5%) - Sonicated Calf Thymus (Native) DNA-Compound A Complexes.

Slot	Description
5_c	Unbound Controls for Slots 5
5	Sonic. DNA-Compound A Complex of B.Ratio 0.09.
6_c	Unbound Controls for Slots 6
6	Sonic. DNA-Compound A Complex of B.Ratio 0.11.
2_c	Unbound Controls for Slots 2
2	Sonic. DNA-Compound A Complex of Binding Ratio 0.23

Legends for Plates 1-8

Plate 1: Unsonicated calf thymus DNA (control).

Plate 2: Unsonic. calf thymus DNA treated with $Na_2S_2O_4$.

Plate 3: (a&b) Unsonic. calf thymus DNA-MC complex, b.r. 0.1

Plate 4: Unsonic. calf thymus DNA + catalase + superoxide dismutase.

Plate 5: Unsonic. calf thymus DNA + $Na_2S_2O_4$ + catalase + superoxide dismutase.

Plate 6: Unsonic. calf thymus DNA-MC complex (b.r.- 0.1) + catalase + superoxide dismutase.

Plate 7: Sonicated calf thymus DNA (control)

Plate 8: Sonicated calf thymus DNA-MC complex, b.r. 0.1

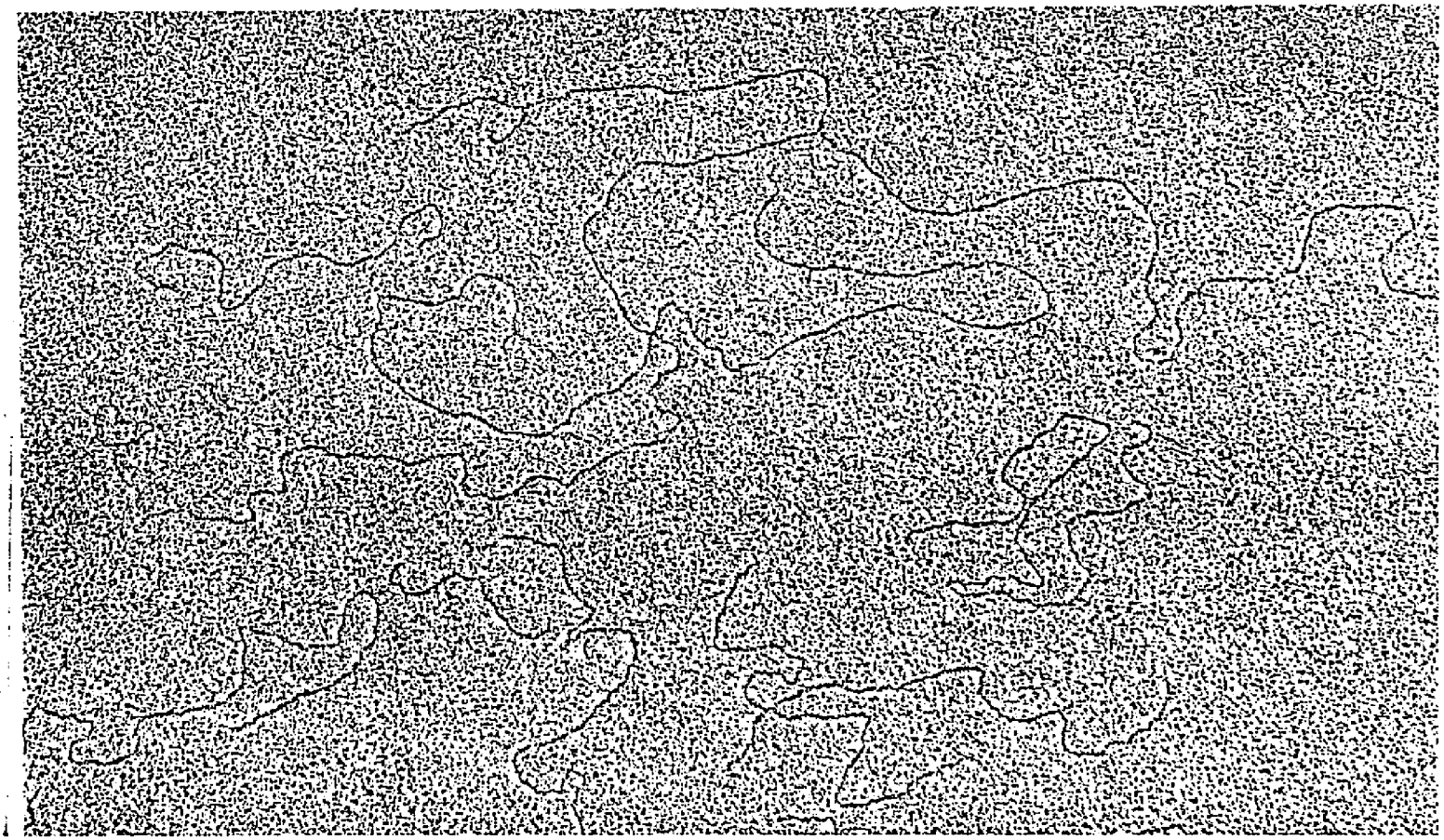

Plate 1 (Top) ↑

Plate 2 (Bottom) ↓

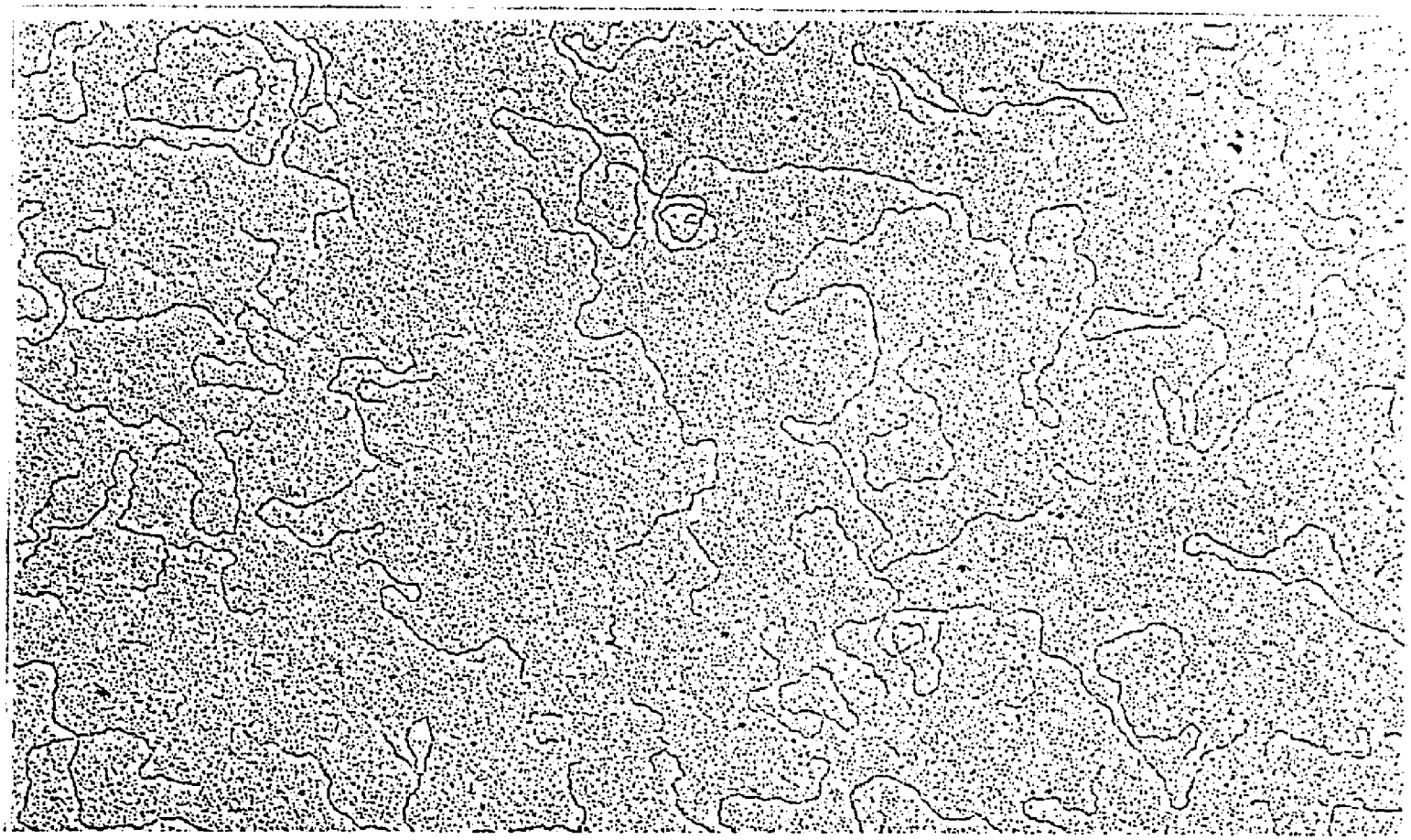

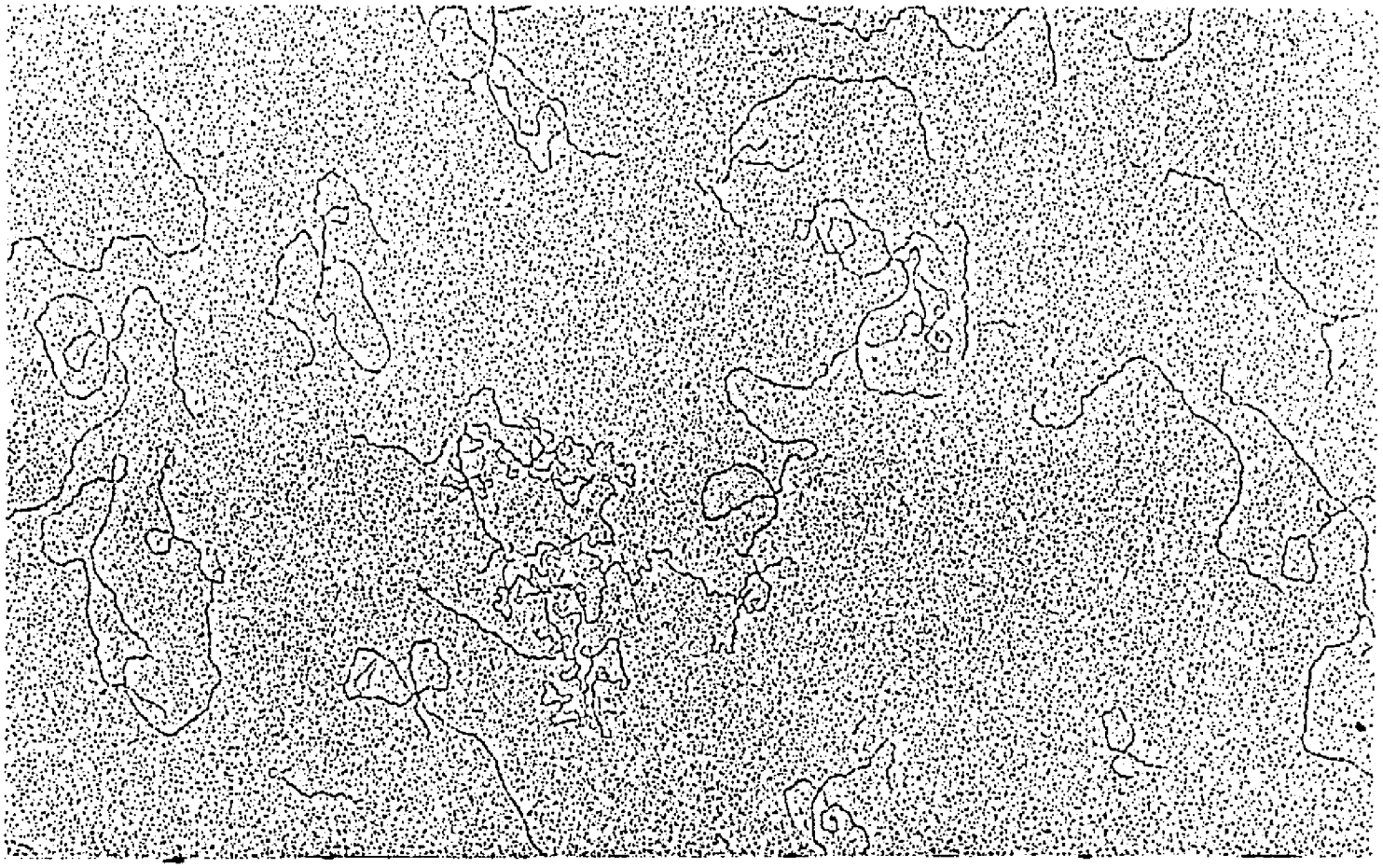

Plates 3a&b

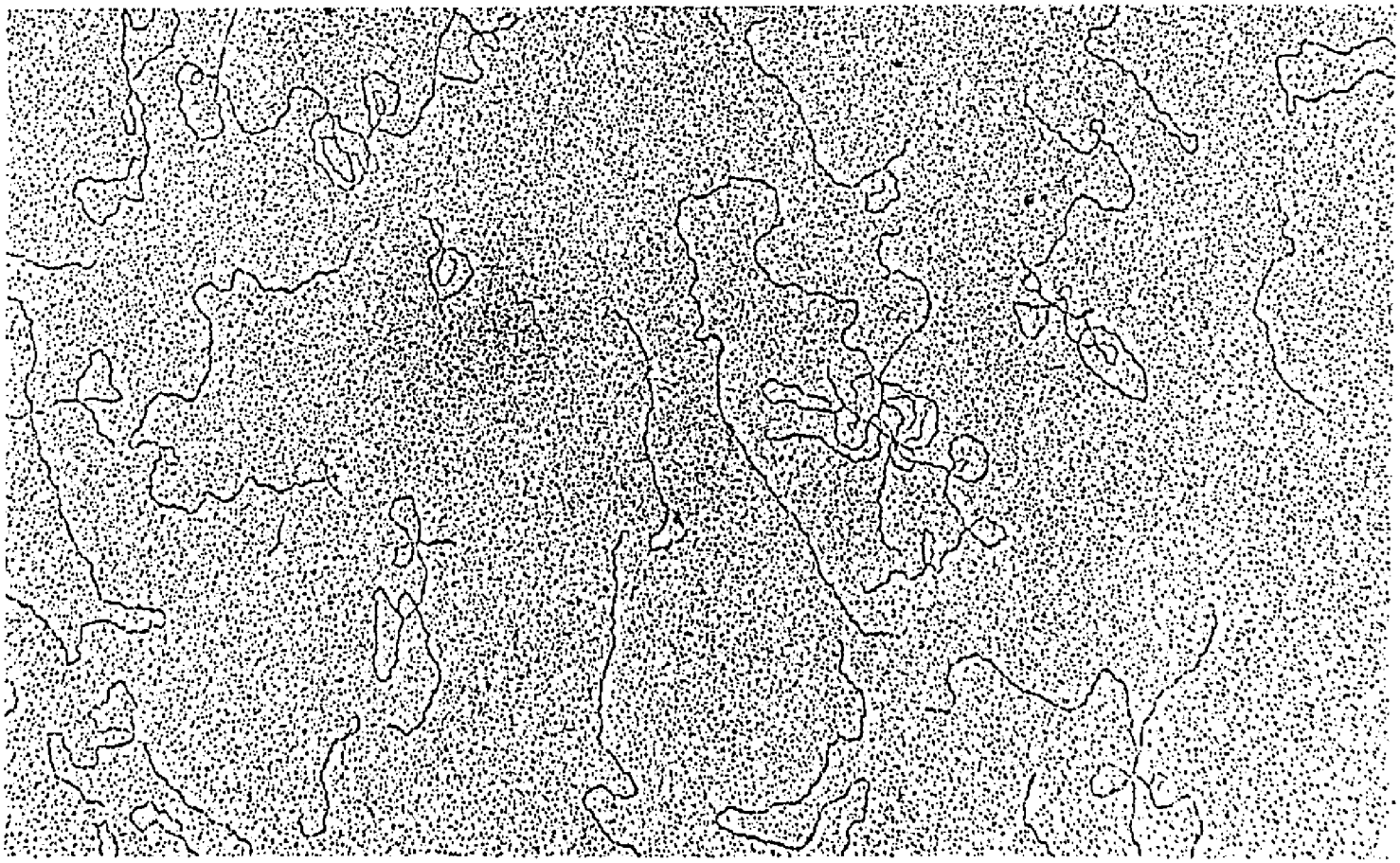

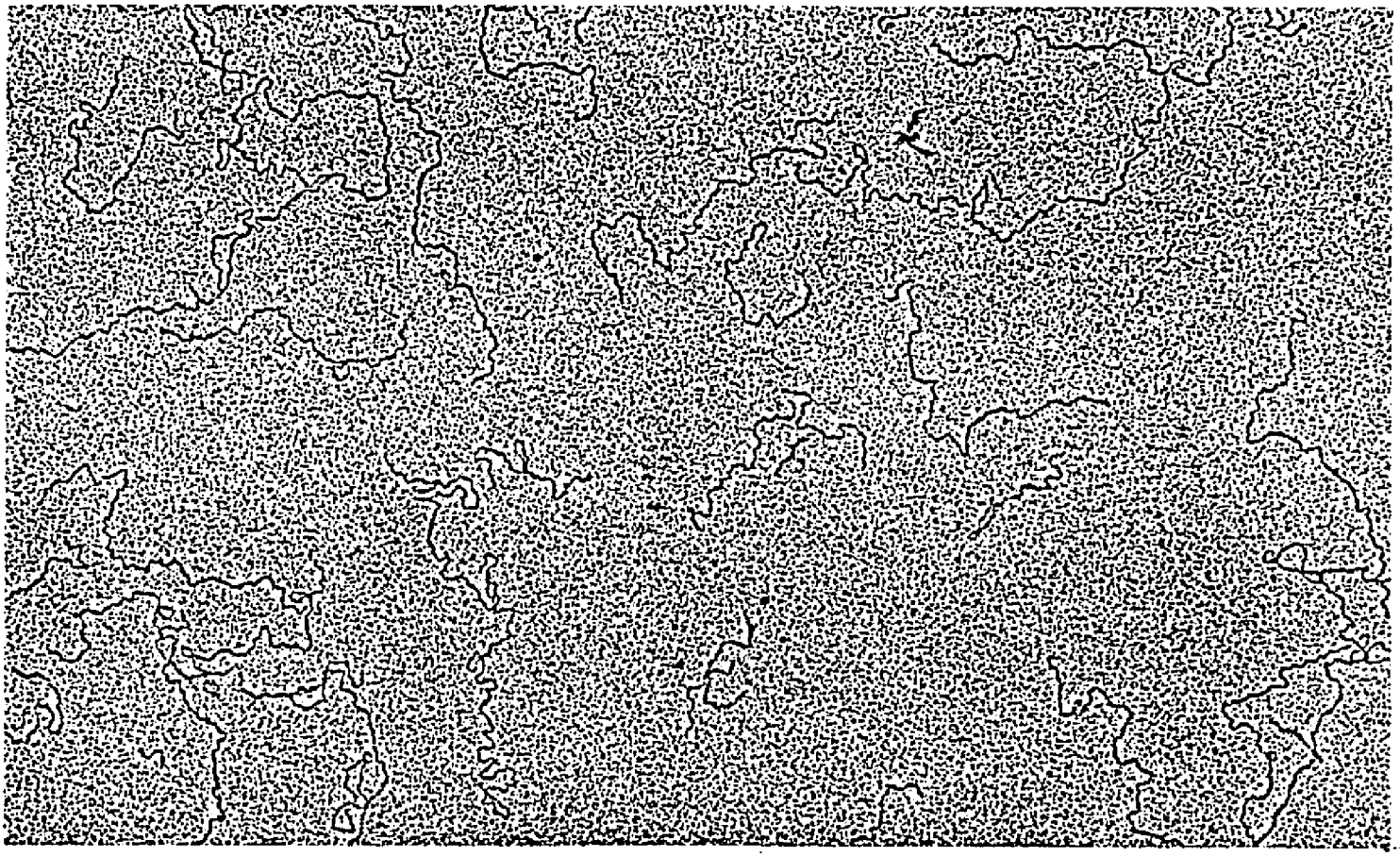

Plate 4 (Top) ↑

Plate 5 (Bottom) ↓

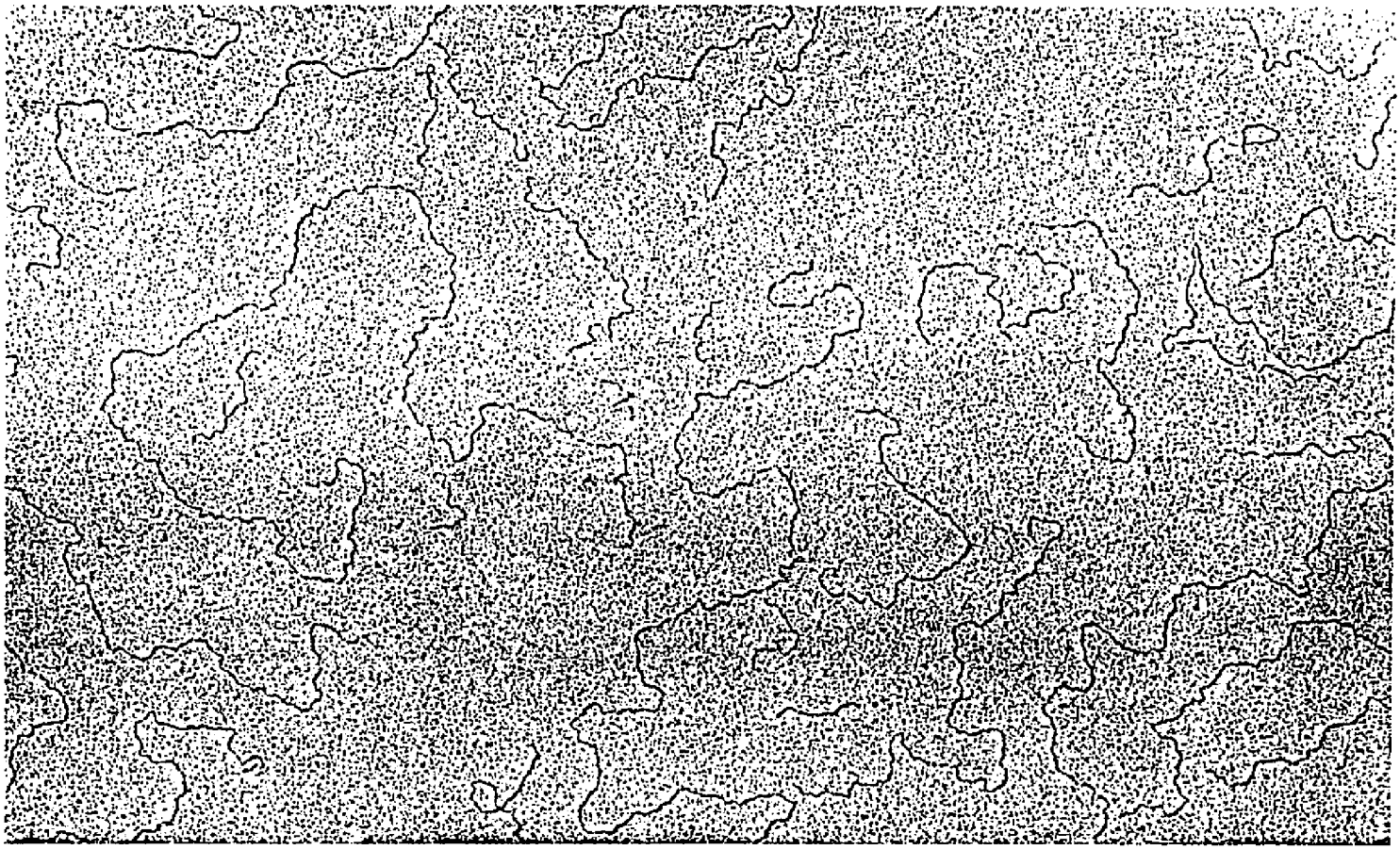

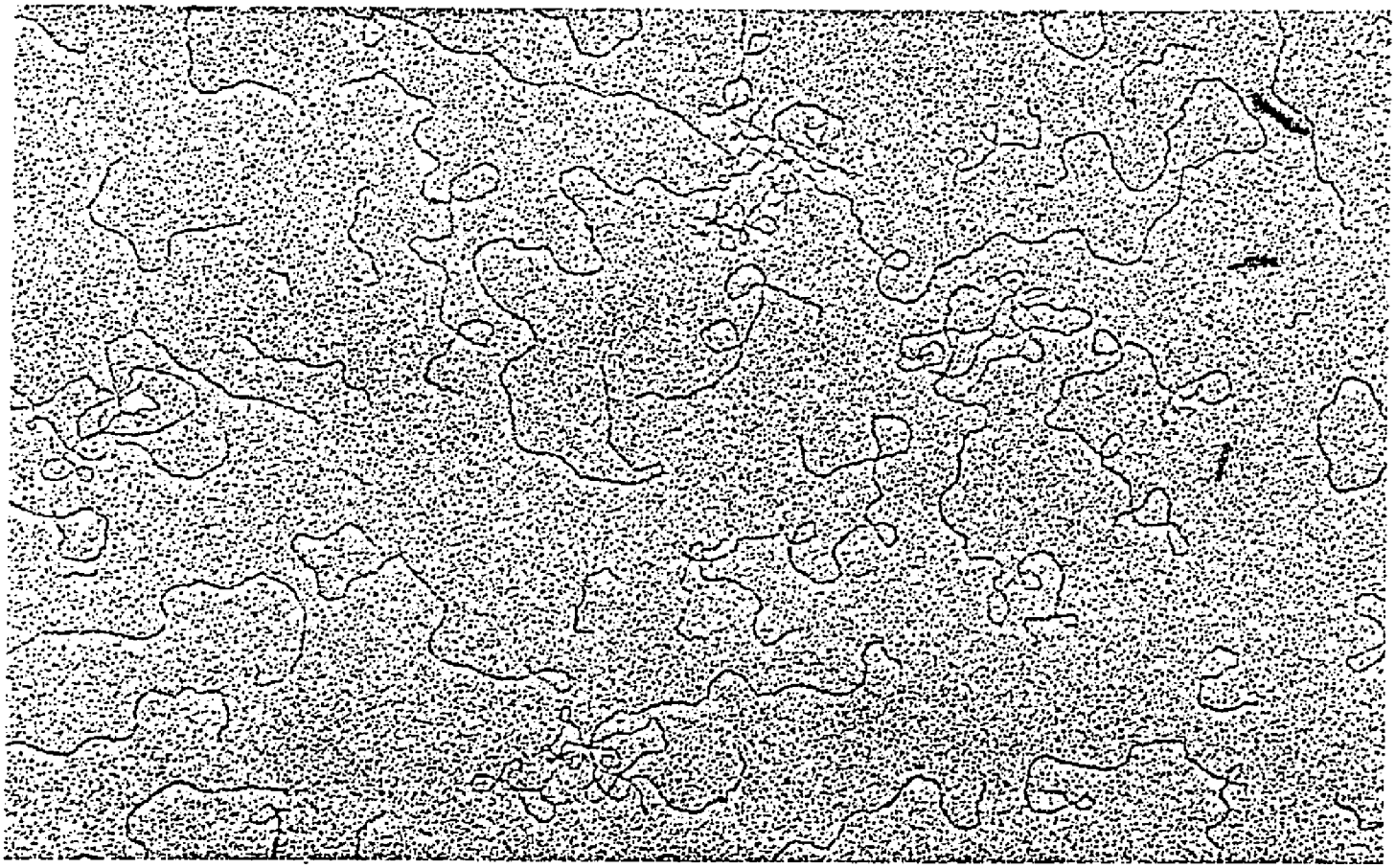

Plate 6

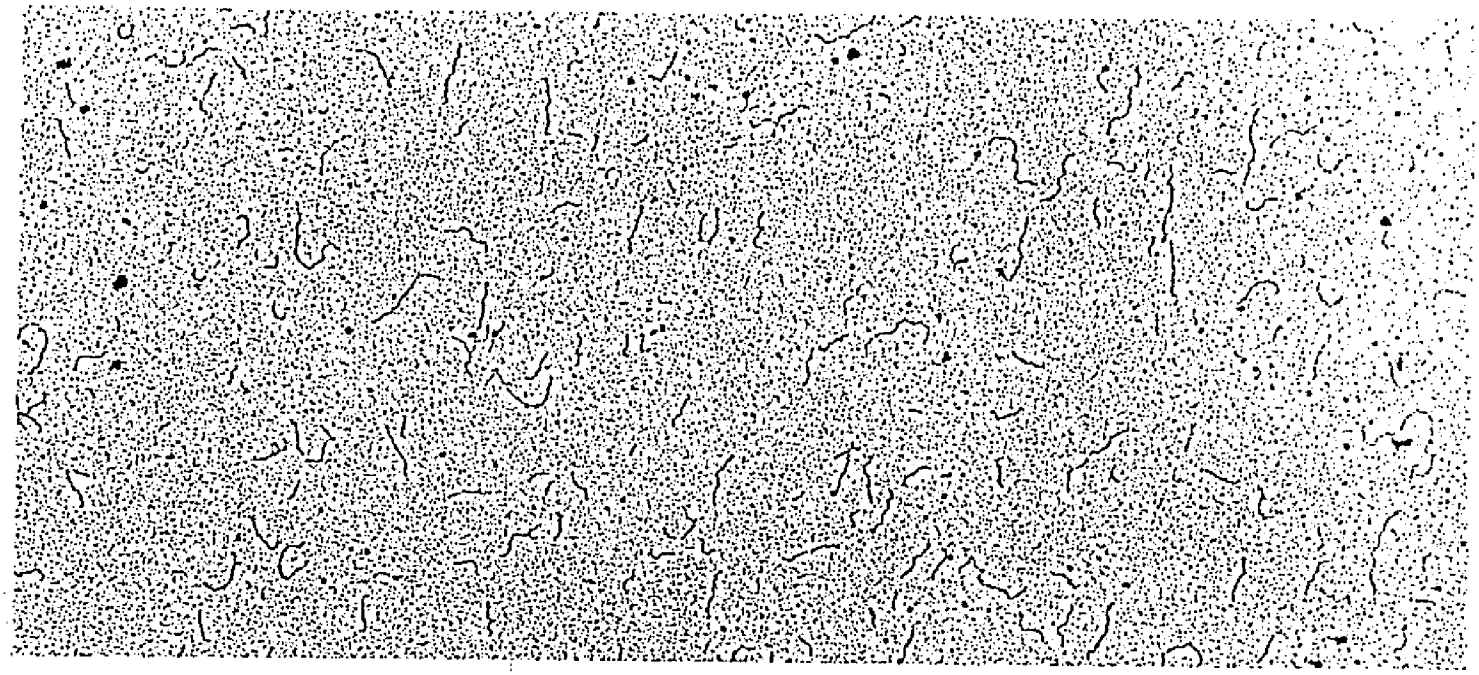

Plate 7

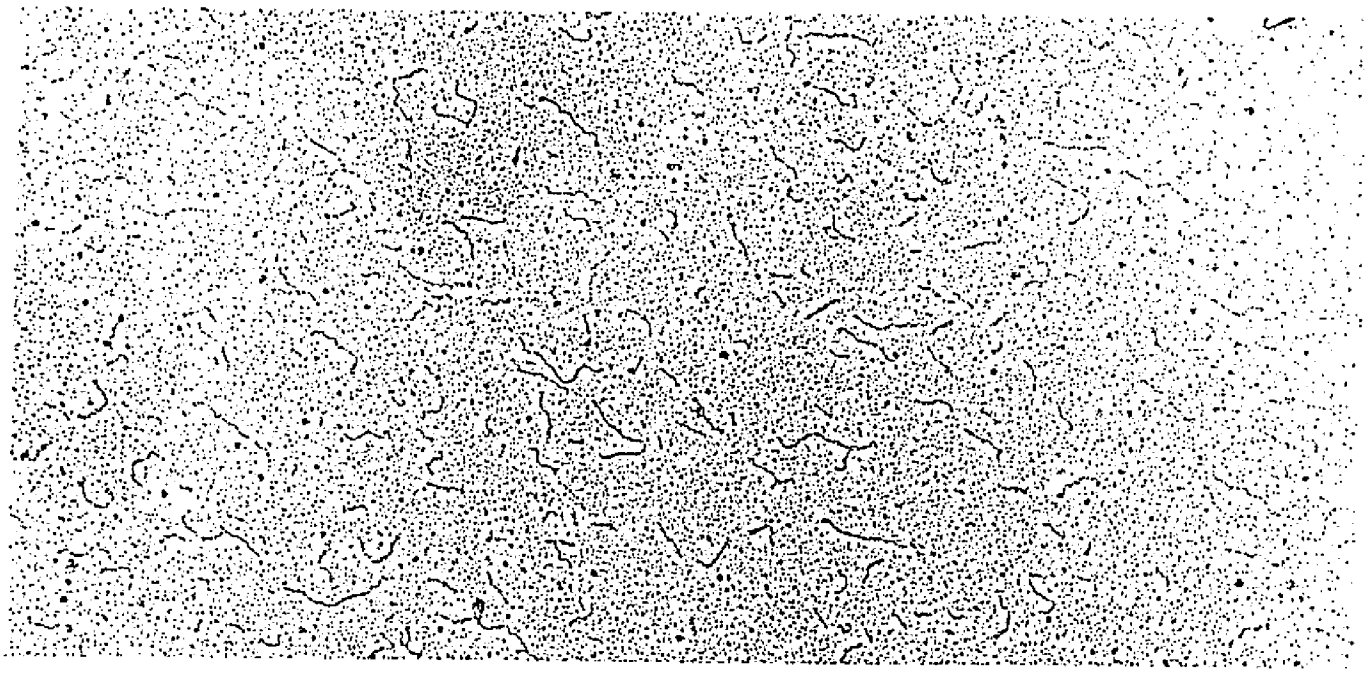

Plate 8

Table 1-A. Melting Characteristics of Sonicated Calf Thymus DNA-Mitomycin C Complexes in DSC Buffer

Sample	Binding Ratio	Tm °C	ΔTm °C	%Hyperchromicity	%Crosslinked	Melting** °C Breadth	ΔMelting °C Breadth
Control	-	68.5	-	32.9	0	18.0	-
Complex	0.20	75.8	7.3	30.7	43.1	31.0	13.0
Complex	0.10	75.2	6.7	33.1	37.4	28.5	10.5
Complex	0.06	72.5	4.0	34.3	33.9	23.0	5.0
Complex	0.04	71.0	2.5	36.7	35.5	29.0	11.0
Complex	0.02	68.5	0.0	35.6	21.9	21.0	3.0
Control*	-	69.0	-	33.0	0	11.5	-
Complex*	0.04	70.0	1.0	29.2	39.6	17.0	5.5
Complex*	0.12	70.5	1.5	31.0	43.1	18.5	7.0

* These samples of DNA and complexes were sonicated after their formation. See appendix 3.

** Melting breadth is the temperature difference between 10% and 90% hyperchromicity for a DNA sample (Dove and Davidson, 1962)

Table 1-B Melting Characteristics of Unsonicated Calf Thymus DNA-Mitomycin C Complexes in DSC Buffer

Sample	Binding Ratio	Tm °C	ΔTm °C	%Hyperchromicity	%Crosslinked	Melting °C Breadth	ΔMelting °C Breadth
Control	-	72.0	-	39.3	0	11.5	-
Complex	0.20	80.5	8.5	34.5	80.3	25.5	14.0
Complex	0.14	79.8	7.8	34.6	74.1	25.5	14.0
Complex	0.10	78.1	6.1	34.5	75.3	23.5	12.0
Complex	0.08	76.9	4.9	34.3	77.2	22.5	11.0
Complex	0.06	76.0	4.0	35.3	77.4	19.2	7.7
Complex	0.04	75.3	3.3	36.1	89.9	18.0	6.5
Complex	0.03	74.9	2.9	36.0	87.0	19.2	7.7
Complex	0.02	74.0	2.0	37.7	86.4	21.5	10.0
Complex	0.01	72.0	0.0	38.4	82.3	17.0	5.5

Table 2. Melting Characteristics of Unsonicated E.Coli DNA-Mitomycin C Complexes in DSC Buffer

Sample	Binding Ratio	Tm °C	ΔTm °C	%Hyperchrcm-icity	%Crosslinked	Melting °C Breadth	Δ Melting °C Breadth
Control	-	77.0	-	34.0	0	7.0	-
Complex	0.20	86.0	9.0	32.5	85.1	17.0	10.0
Complex	0.16	85.0	8.0	34.0	74.5	22.5	15.5
Complex	0.06	84.0	7.0	32.5	73.9	21.5	14.5
Complex	0.05	82.0	5.0	31.3	85.2	19.5	12.5
Complex	0.03	80.0	3.0	34.5	72.1	13.5	6.5
Complex	0.02	79.5	2.5	35.0	96.5	10.0	3.0
Complex	0.10	77.0	0.0	34.5	77.2	7.5	0.5

Table 3. Melting Characteristics of Unsonicated Calf Thymus DNA-Mitomycin C Complexes in 1:1 Methanol:DSC Buffer.

Sample	Binding Ratio	Tm °C	ΔTm °C	%Hyperchromicity	%Crosslinked	Melting °C Breadth	Δ Melting °C Breadth
Control	-	56.0 58.0	- -	46.0	0	13.0 (Av.)	-
Complex	$\leq$ 0.005	58.0	0.0	43.5	16.2	12.0	-1.0
Complex	$\leq$ 0.005	56.0	0.0	42.4	37.7	13.5	0.5
Complex	0.01	56.5	0.5	44.1	84.6	15.5	2.5
Complex	0.02	56.5	0.5	43.1	97.7*	17.0	4.0
Complex	0.05	57.5	1.5	46.3	96.7*	16.0	3.0
Complex	0.08	57.o	1.0	42.7	100.0*	18.5	5.5
Complex	0.15	58.0	2.0	40.0	100.0*	19.5	6.5

* %Crosslinked values represent corrected values taking into account absorption in the 260 nm region due to bound drug. See appendices 1&2 and fig.'s 11,16,17&18

Table 4. Observed and Corrected Melting Temperatures for a Series of Sonicated and Unsonicated Calf Thymus DNA-MC Complexes in DSC Buffer

Sonicated DNA Samples	Fraction Cross-linked $f_{c.l.}$	Fraction Non-Cross-linked $f_{n-c.l.}$	$T_m^{obs.}$	Unsonicated DNA Samples	$f_{c.l.}$ Fraction Cross-linked	Observed T_m of Unsonic. DNA	Corrected T_m ($T_m^{c.l.}$)
Control DNA	-	-	68.5°C	-	-	72.0°C	-
Complex b.r.= .20	.58	.42	75.8°C	Complex b.r.= .20	1	80.5°C	81.1°C
Complex b.r.= .10	.53	.47	75.2°C	Complex b.r.= .10	1	78.1°C	81.1°C
Complex b.r.= .06	.49	.51	72.5°C	Complex b.r.= .06	1	76.0°C	76.7°C
Complex b.r.= .04	.50	.50	71.0°C	Complex b.r.= .04	1	74.9°C	73.5°C

Table 6. Relative Intrinsic Viscosities [η] of Various DNA-Mitomycin C Complexes in DSC and EDTA ($9X10^{-4}M$)

Samples and Descriptions	Binding Ratio	Relative [η]: [η]Sample/[η] Control
Unsonicated Calf Thymus DNA-Mitomycin C Complex	0.02	1.00
"	0.07	0.85
"	0.09	0.81
"	0.10	0.79
"	0.32	0.77
Unsonicated E.Coli DNA-Mitomycin C Complex	0.08	0.92
"	0.18	0.45
Sonicated Calf Thymus DNA-Mitomycin C Complex	0.15	1.57
"	0.10	1.37
"	0.07	1.31
Sonicated Calf Thymus DNA-Compound A Complex	0.11	1.40
"	0.06	1.31
Unsonicated DNA + $Na_2S_2O_4$ * Calf Thymus	-	1.00
Unsonicated DNA (C.Thymus) + $Na_2S_2O_4$ + Catalase	-	0.98
Unsonicated Calf Thymus DNA-Mitomycin Complex **	0.10	0.88
Unsonicated C.Thymus DNA-MC Complex + Catalase **	0.10	0.85

*- Viscometric studies of unsonicated Calf Thymus DNA with or without $Na_2S_2O_4$ show no change (LaRusso et al., 1978).

**- All DNA-MC Complexes are formed in the presence of $Na_2S_2O_4$.

Table 7. Viscosity Measurements (in triplicate) and Precision for Samples of C.Thymus & Pneumococcal Native DNA.

Sample	Intrinsic Viscosity	Mean Value	Average Deviation	*Percentage Average Deviation (Precision)
Calf Thymus Unsonicated DNA (Sample-1)	46.9	44.0	±1.9	4.3%
"	42.7	"	"	"
"	42.5	"	"	"
Calf Thymus Unsonicated DNA (Sample-2)	46.6	44.5	±1.4	3.2%
"	44.6	"	"	"
"	42.4	"	"	"
Pneumococcal Unsonicated DNA	70.6	69.3	±0.9	1.3%
"	69.0	"	"	"
"	68.2	"	"	"

* - The method of Skoog and West (1965) is used to calculate the precision.

Table 8. Sedimentation Measurements and Characteristics for Native DNA-Mitomycin C Complexes.

Sample	Binding Ratio	Fig. #	Time Run	Av. Dist. Sedimented	M.W. (Daltons)	Sediment. Coeffic.**
Unsonicated Calf Thymus DNA	-	33	9.5 hrs.	1.20±.05 cm*	5.4X10^6 +	15.0 S ++
Unsonicated C.Thymus DNA-MC Complex	0.10	33	"	1.70±.05 cm	"	21.2 S
Unsonicated C.Thymus DNA-MC Complex	0.05	33	"	1.40±.05 cm	"	17.5 S
Triplicate Run of C. Thymus Unsonic. DNA	-	31	17.0	2.10±.05 cm	"	15.0 S
^{3}H-Labeled Pneumococcus Unsonic. DNA	-	31	17.0	2.60±.05 cm	10.0X10^6	18.6 S
Sonicated Calf Thymus DNA	-	32	93.7	5.90±.05 cm	3.8X10^5 i	7.6 S
Sonicated Calf Thymus DNA-MC Complex	0.11	32	93.7	6.10±.05 cm	"	7.9 S
Sonicated Calf Thymus DNA-MC Complex	0.05	32	93.7	6.00±.05 cm	"	7.7 S

*- Maximum %Average Deviation (Precision) found amongst samples was 3.5%. Precision for C.Thymus was 1.4%, but nevertheless ±.05 cm was used to express widest possible deviation.

**- See footnote 7. + M.W. calculated by Zimm-Crothers modification (Zimm and Crothers, 1965) of Mandelkorn-Flory Eq. and use of the Cox (1960) Eq. for M.W. corrections due to differences in salt conc. i- M.W. calculated by the Eigner and Doty (1965) Eq.

++ Obtained through extrapolation using plots displaying the variation of (S) and $[\eta]$ with counterion conc. (Eigner and Doty, 1965) and also using the equation shown in footnote 7.

Table 9. Actual and Expected Distances of Sedimentation for Native Calf Thymus DNA-Mitomycin C Complexes.

Sample	Binding Ratio	(A) Actual Dist. Sedimented	%* Change	(B) Expected Dist. Sed'mt.	(A - B) cm
Unsonic. C.Thymus DNA	-	1.20±.05 cm	0	1.20±.05 cm	0
Unsonic. C.Thymus DNA-MC	0.10	1.70±.05 cm	41.7	1.20±.05 cm	0.50±.05
Unsonic. C.Thymus DNA-MC	0.05	1.40±.05 cm	16.7	1.20±.05 cm	0.20±.05
Sonicated C.Thymus DNA	-	5.90±.05 cm	0	5.90±.05 cm	0
Sonicated C.Thymus DNA-MC	0.11	6.10±.05 cm	3.4	6.10±.05 cm	0
Sonicated C.Thymus DNA-MC	0.05	6.00±.05 cm	1.7	6.00±.05 cm	0

(A) - Data obtained from Table 8.

(B) - Expected distance sedimented, after correction for M.W. increase due to bound drug in DNA-MC complexes. The factors of 1.10 and 1.05 were used (respectively for binding ratios 0.10 and 0.05) for correction (by multiplying the M.W. of control by these values one obtains the expected dist. of sediment. when using the appropriate equation (see footnote 7)

(A - B)- Is the increase in distance sedimented, relative to control, not due to bound drug.

*- Is the percentage increase of the control distance sedimented by the complex:

D = Distance Sedimented

$$\%\text{Change}^{*} = \frac{\text{Complex}D - \text{Control}D}{\text{Control}D} \times 100$$

Table 10. The Electrophoretic Mobilities According to Binding Ratio for Calf Thymus DNA Complexes.

Samples and Description	Binding Ratio	Relative Electrophoretic Mobility ***
Unsonicated Native Calf Thymus DNA-MC Complex	0.01	0.92 ± .02
"	0.02	0.86 ± .02
"	0.05	0.47 ± .02
"	0.08	0.42 ± .02
"	0.15	0.26 ± .02
"	0.16	0.20 ± .02
"	0.31	0.18 ± .02
Unsonic. C.Thymus Native DNA-Ethidium Complex	0.04	0.90 ± .02
"	0.22	0.75 ± .02
**Sonicated Native Calf Thymus DNA-MC Complex	0.04	0.90 ± .02
"	0.08	0.75 ± .02
"	0.23	0.63 ± .02
Sonic. Calf Thymus Native DNA-Compound A Complex	0.04	1.00 ± .02
"	0.11	1.00 ± .02
"	0.23	0.98 ± .02
Unsonic. C.Thymus Native DNA treated with $Na_2S_2O_4$- Unsonicated Native C.Thymus DNA-MC Complex*	-	1.00 ± .02
	0.09	0.56 ± .02

*- Molecular weight of DNA in this complex was approximately, as assessed through electrophoretic determination of M.W., $1X10^6$ daltons.

**- Molecular weight of the sonic. DNA used here was $\sim 4X10^5$.

***- The electrophoretic mobility of complex divided by that of the control.

DISCUSSION

Part I: Thermal Stability, Viscosity, Rate of Sedimentation, and Flow Dichroism of DNA-MC Complexes.

Increased T_m of DNA-MC complexes is probably due to the crosslinks: Increased T_ms[3] of DNA-MC complexes compared to that of control DNA have been found previously (Tomasz et al., 1974) and were on theoretical grounds (Crothers and Zimm, 1965) alleged to arise from the crosslinks present in these complexes. No clear-cut experimental proof exists, however for this hypothesis. In order to test it, an attempt was made to find an experimental correlation between the degree of crosslinking and the observed T_m of DNA-MC complexes. No such correlation in general has been described previously, due to inherent difficulties associated with most crosslink systems. These difficulties are: (a) crosslinking agents (e.g. UV, bifunctional mustards, nitrous acid, low pH, etc.) usually induce additional "monofunctional" damage confusing the T_m effects of the crosslinks alone. (b) quantitative assay of crosslinks is feasible only at extremely low crosslinks/base pair ratios. The reason for this is the following: All known assays of crosslinked DNA are based on the extent of spontaneous renaturation of denatured DNA. (Geiduschek (1961) explains this renaturation as being due to a bifunctional covalent bonding (crosslinking) between the complementary chains of DNA. As a result of this, and despite secondary structure loss of the DNA due to thermal denaturation, the contiguous base pairs (those bases con-

nected and proximal to the bifunctional link (crosslink) are constrained to remain in a small volume zone. Once the conditions become thermodynamically favorable (cooling) for the reestablishment of ordered structure (reannealing of complementary DNA strands) those nucleotides which were confined in a limited volume element reassociate in the correct sequence and, by doing so, provide a nucleus from which a complete reannealing of the specifically paired double helix is possible (see tables 1,2,3, and figures 3 and 11).) In view of this it is important to note that the average number of crosslinks per DNA molecule (m) is usually calculated from the Poisson relationship:

$$m = \ln \frac{1}{P_o}$$

where P_o = 1 - (fraction of crosslinked DNA). The fraction of crosslinked DNA is experimentally determined by denaturing DNA and measuring the amount of the spontaneously renatured (i.e. crosslinked) fraction by various methods (Iyer and Szybalski, 1963). In this work the melting curve reversibility method was used (see methods, p.10). As an example of an application of this assay method, assume that the melting curve of a crosslinked DNA-MC complex shows 80% reversibility compared to 0% reversibility of control DNA. Thus the number of crosslinks per DNA molecule (m) is:

$$m = \ln \frac{1}{1 - 0.8} = 1.61$$

and the number of crosslinks per base pair (approx. M.W. of 654) of DNA (average M.W. = 10^6) is

$$\frac{1.61}{10^6/\ 654} = 1.61 \times 654 \times 10^{-6} = 0.001$$

or reciprocally, one crosslink per 1000 base pairs.

This example demonstrates that, even at this low level of crosslinkage, 80% of the DNA population is crosslinked. Once the entire DNA population is crosslinked (100%; minimum of one crosslink per each DNA molecule), an upper limit in the assaying of crosslinkage by these methods is reached; that is they will become insensitive to further increases in the number of crosslinks. It is also obvious that this limit is extended higher, on a crosslink/base pair basis, if the M.W. of the DNA is lower. This is easily understood from the following diagram:

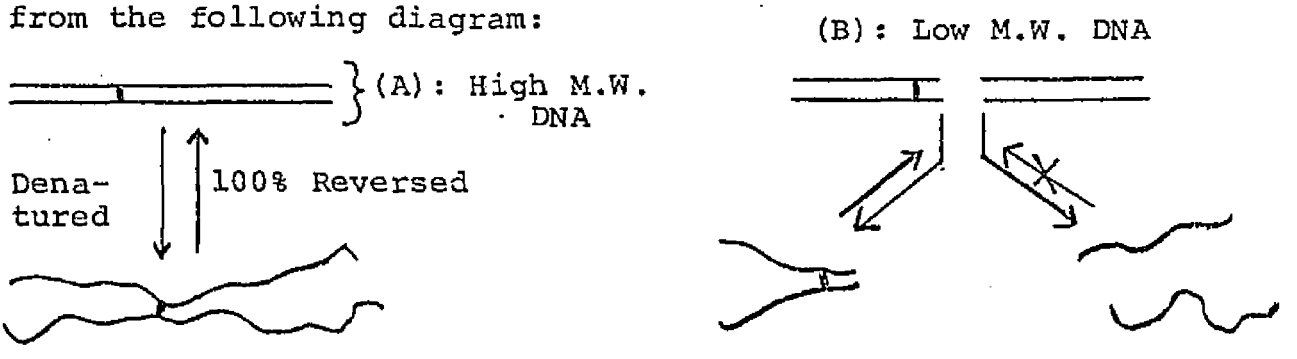

(A) and (B) are identical amounts of DNA containing one crosslink per that amount. Since the average M.W. of DNA in (A) is twice that in (B), one crosslink in (A) gives 100% crosslinked DNA, while one crosslink in (B) gives only 50% crosslinked DNA.

The difficulties described so far in the study of crosslinking (e.g. inherent difficulties described in (a) and (b) in the preceding pages) are also associated with the mitomycin-induced crosslinks. For example, the monofunctional "damage" (i.e. binding) is 10-20 fold more frequent than the crosslinks (see introduction). Nevertheless, by a new method of analysis, it was possible to distinguish the effects of the crosslinks alone, as follows: In order to test whether a correlation between T_m and crosslinks exist, T_ms of sonicated DNA-MC complexes were compared with T_ms of unsonicated DNA-MC complexes. The complexes to be compared had identical drug binding ratios. These results are shown in table 4. The measured T_m is obviously a composite of T_ms of the crosslinked and non-crosslinked molecules in the sonicated DNA case, and it is the T_m of the pure crosslinked molecules alone in the unsonicated DNA case (100% crosslinked). We argued that if the higher T_m of the latter is due to a greater degree of crosslinking, then correction of the T_m of the former sonicated complex for its non-crosslinked fraction should give the same higher T_m value for its crosslinked fraction as that of the latter unsonicated complex. The basic formula for this correction is

$$(f_{c.l.} \times T_m^{c.l.}) + (f_{n-c.l.} \times T_m^{control}) = T_m^{obs.}$$

and, consequently, $$\left(T_m^{c.l.}\right) = \frac{T_m^{obs.} - (f_{n-c.l.} \times T_m^{control})}{f_{c.l.}}$$

($T_m^{c.l.}$ is the hypothetical T_m of the crosslinked population, $T_m^{obs.}$ is the observed T_m, $T_m^{control}$ is the T_m of control sonicated DNA, $f_{c.l.}$ is the fraction of the total DNA crosslinked, and $f_{n-c.l.}$ is the fraction of total DNA non-crosslinked.) If we apply this, for example, to the complex of binding ratio 0.2 (table 4) we obtain

$$T_m^{c.l.} = \frac{75.8 - (0.42 \times 68.5)}{0.58} = 81.1^{\circ}C$$

This is indeed very close to the T_m of the corresponding unsonicated (100% crosslinked) complex ($T_m = 80.5^{\circ}C$). These $T_m^{c.l.}$ values were calculated for each of the sonicated complexes in table 4 and are shown in the column "corrected T_m". It is clear that the agreement between these and the observed T_m of the non-crosslinked complexes is excellent in most cases. These results suggest that the original assumption, namely that the crosslinks are the cause of the T_m increase is valid. This is said despite the fact that the formula for the correction (p.98) does not take into account the crosslinking density of a heterogeneous population of DNA molecules where the relationship between the fraction of molecules containing no crosslinks and the weight fraction of reversible DNA can become less direct (Geiduschek, 1964). Nevertheless, the original assumption that the crosslinks are responsible for the increase of T_m of DNA is maintained "since the number of sites in each molecule (DNA) available for crosslinking must be very large" (Geiduschek, 1964).

An additional and independent support for crosslinking as the cause of T_m comes from the thermal behavior of DNA complexes of the monofunctional MC derivative "compound A". Compound A binds to DNA but is unable to crosslink it (Tomasz et al., 1974). The finding that there is no increase of T_m of these complexes (figure 7 and 8) is consistent with the conclusion that the T_m increase is the consequence of the crosslinks.

The crosslinking of DNA by mitomycin C probably plays a major role in the broadening of the melting transition of the DNA-MC complexes: Paralleling the T_m increase for the DNA-MC complex is the finding, obtained here (see figures 6 and 7) and elsewhere (Cohen and Crothers, 1970), of a broadening in the transition of melting (transitional breadth). As the process of DNA melting is one , in general, of high cooperativity, where the entire chain, or large segments thereof, change directly from the helix to the random coil form (Van Holde 1971), then a broadening[4] in the transitional breadth can be related to a non-cooperativity in the strand separation process for DNA. Such broadening in the thermal transition, for instance, has been reported (Stewart, 1968) for samples of DNA bound with acridine orange (a known intercalator (Lerman, 1964)) and is explained as a result of the transfer of chromophores of acridine orange from denatured to native DNA during the melting process. Acridine molecules, in other words, during the heating of DNA, are released from early molecules, thus increasing the effective acridine concentration for the stabilization of the remaining molecules. This process eventually leads, therefore, due to the continual formation of complexes with higher thermal stability, to an increased transitional breadth. In contrast to this however, the binding of the mitomycin C chromophore to DNA has been shown to be covalent (Iyer and Szybalski, 1963) and stable to heat (Szybalski and Iyer, 1964a; Szybalski and Iyer, 1964b) and thus the increase in the transitional breadth of the DNA-MC complex cannot be explained by a mechanism which involves a release of drug alone. It appears, therefore, that the non-cooperativity in the DNA strand separation process for

the DNA-MC complex stems from some other factor.

In the attempt to determine the cause of this non-cooperativity in the melting of DNA-MC complexes, it is essential to briefly outline the accepted mechanism for DNA melting. It is understood that the duplex strands of high molecular weight DNA separate at internal points with the subsequent formation of alternating regions of helix and coil (Bloomfield, Crothers, and Tinoco, 1974). With the formation of these alternating internal points, a process of looping or ring-like formation comes into play allowing for a cooperative melting of the DNA (Crothers et al., 1965), (there is a free energy decrease when planar π electron systems are stacked rather than more dispersed as in looping, and since the transitional breadth is controlled by this free energy of base stacking, a cooperativity or sharpness (smaller transitional breadth) in the melting process occurs (Crothers et al., 1965). Low molecular weight DNA (several hundred thousand daltons M.W.; the size range of the sonicated DNA used in the thermal denaturation studies), on the other hand, melts by a mechanism involving strand separation from the ends of the molecule (Crothers et al., 1965). This mechanism which depends upon the increased importance of melting originating from the ends of the molecule does not include the cooperativity of internal strand separation, characteristic of high M.W. (unsonicated) DNA. This then results in an increased or broader transitional breadth for the shorter DNAs. The contrasts in the size of the transtional breadths

for sonicated vs. unsonicated DNAs, as well as their complexes, are shown in table 1(a & b).

In view of the foregoing discussion, involving mechanisms for strand separation, one may propose that since the efficiency of strand separation sharpens the transition of DNA, then it appears that the crosslinks, in their interference of strand separation, play a major role in the transitional broadening of DNA (Cohen and Crothers, 1970). A support for this reasoning is the fact that DNA-compound A complexes contain no crosslinks (Tomasz et al., 1974) and no broadening in melting transition, while DNA-MC complexes display both of these characteristics. (A further support for this is related also to the fact that the point (binding ratio 0.10-0.15) indicating the leveling off of the increases observed in the melting breadths of the DNA-MC complexes (figures 6 and 7) coincides with that point where the melting temperature increases similarly level off (fig.5). This concurrence suggests, strongly, a common element (crosslinking) as the cause for both the melting breadth and T_m increases.) The fact, furthermore, that similarities in the melting breadths (see appendix 5) and Δ melting breadths, for the sonicated and unsonicated DNA-MC complexes exist despite the fact that forms of DNA in these complexes exhibit differences in the mechanisms of melting, as indicated by wide differences in the magnitude of their melting breadths (for the control or unbound forms), demonstrates, it appears, that the general mechanisms of strand separation for short or long DNA

are being disrupted through a general crosslinking of the DNA duplex. It can then be said that the two different mechanisms (end melting or looping) of strand separation are "masked" through crosslinkage. In other words, although the mechanisms of strand separation for both high and low molecular weight DNAs are different, as expressed by differences in their melting breadths, the absolute difference, as a result of crosslinkage, between the melting breadths of any one complex, at any one specified binding ratio, and it's control, is independent, more or less, of the size (e.g. sonicated vs. unsonicated DNA, see table 1) of the DNA.

Differences in Some of the Melting Characteristics of DNA-MC Complexes in Aqueous vs. Aqueous-Organic Buffers.

The melting profiles of DNA-MC complexes in methanol-DSC buffer exhibit lowered ΔT_m and Δmelting breadths (Δm.b.) relative to those profiles obtained from DSC alone. It is interesting to note, however, that for the DNA-MC complexes, the ratios of $\Delta T_m/\Delta$m.b. in aqueous and organic buffers differ substantially (e.g. comparisons (see tables 1 and 3), for instance, of a complex of binding ratio 0.15 shows a $\Delta T_m/\Delta$m.b., in aqueous buffer, of $\simeq$.6 while this same ratio in methanol-DSC buffer is $\simeq$.3). From this difference, it appears that the rises in T_m and melting breadths for the DNA-MC complexes stem from different sources, an assertion that contradicts the view that the change in these two variables originates from the crosslinking

of DNA by mitomycin C. Supporting the view that these two variables are not necessarily concurrent is the fact that a number of compounds (e.g. ethidium bromide, netropsin, and methyl green) are known to increase the T_m of DNA significantly without increasing its breadth of transition (LePecq and Paoletti, 1967; Zimmer et al., 1971; Krey and Hahn, 1975). With regard to this independence of T_m increase, it can thus be said that these compounds are able to stabilize their respective complexes to melting (in respect that additional thermal energy is needed in the dissociation of the helix) without changing the cooperativity of DNA strand separation). It is important to note however, that the two solvent systems being compared here differ somewhat in the effects they have on DNA melting. For instance, since it is known that DNA in solutions of increasing methanol concentration display properties indicating secondary structural changes (e.g. decreases in viscosity and in the radius of gyration and increases in the sedimentation coefficients (Herskovits et al., 1961)) then it is understood that direct comparisons of the $\Delta T_m/\Delta$m.b. ratios for aqueous and organic systems cannot be made with any degree of certainty.

The Possibility of Intercalation and the Viscometry of DNA-Mitomycin Complexes

Although the previously described analysis of the melting behavior of DNA-MC complexes shows that the crosslinkage of DNA by mitomycin C is a very likely cause for the observed T_m increase, other modes of chromophore binding, known to increase the T_m of DNA, deserve brief consideration in this discussion. Compounds (e.g. ethidium bromide and various aromatic cations) known to intercalate the base pairs of DNA (LePecq and Paoletti, 1967; Gabbay et al., 1973) for instance, have been shown to increase its melting temperature by a significant degree; even as high as 25-30°C (Lerman, 1964; Gabbay et al., 1973; Zunino et al., 1977; LePecq and Paoletti, 1967). This increase is due to the ability of the intercalating chromophore to increase the amount of effective base pairing in denaturing DNA. As explained by Lerman (1964), the increase in T_m corresponds to the additional energy needed to dissociate the intercalating agent from the helix in addition to separating the strands. The fact that covalent interaction is usually lacking in the instances of compounds reported to bind to DNA through the intercalative mode does not, in itself, rule out mitomycin as a possible intercalating agent.

Viscosity measurement is another method used as probe for the nature of drug-DNA interactions. Variations in the viscosity

of DNA are due to changes in the length and flexibility characteristics of the DNA molecule (Lerman, 1961; Lerman, 1964) attributed to the various ways in which compounds may bind to the helix. With a lengthening and/or stiffening of the DNA helix, DNA solutions encounter a greater restriction to flow with the resulting effect of increased viscosity (Lerman, 1961). The non-intercalating antibiotics distamycin A and netropsin, at certain levels of binding, are known to increase DNA viscosity by binding along the DNA strands in a manner (e.g. probably on the outside of and perpendicular to the helical axis (Zimmer et al., 1971) which allows for a stiffening of the helix. On the other hand, compounds that intercalate between the base pairs of DNA (e.g. ethidium bromide and proflavin, (Lerman, 1961), increase the viscosity mainly by increasing the length of the DNA molecule (Drummond et al., 1966). This is made possible by an insertion (resulting in slight unwinding of the DNA double helix) of the intercalating agent's poly-, or heterocyclic aromatic ring structure between the DNA base pairs; a condition which then maintains adjacent base pairs to remain separated by a length about twice their normal distance apart (Lerman, 1961).

The flexibility of DNA diminishes as its molecular weight decreases and approaches the persistence length (a size parameter, $0.8\text{-}3.3\text{X}10^5$ daltons, characterizing the limit of flexibility of DNA) or rod-like state of DNA (Bloomfield, Crothers and Tinoco, 1974). In view of this circumstance, changes

in viscosity of short rod-like DNA are the result of changes in the length of the DNA molecule rather than in its flexibility (Gabbay et al., 1973). Therefore the viscosity increases observed for the sonicated DNA-MC and compound A complexes (figs.24, 25, and 28), using DNA of approximately 200,000 daltons M.W., are explained, it appears, by the lengthening of the DNA helix obtained upon its reaction with mitomycin C. This condition of lengthening is generally concluded to result from the intercalation of chromophores into the DNA helix, since this mode of binding is the more likely, and prevalent form of binding responsible for extending the DNA molecule in the helix axis direction (Gabbay et al., 1973; Kapicak and Gabbay, 1975). (The qualitative effect of a small molecule on the observed viscosity of a DNA solution is a test for substances that might be intercalators (Lerman, 1964).)

The extent of the viscosity increase for the DNA-MC complexes fits into the pattern (fig.30) of viscosity change displayed by a variety of complexes containing intercalated DNA[8]. Is MC therefore an intercalator? The β anomer of adriamycin has been shown (Zunino et al., 1977) not to intercalate DNA (atypical scatchard plots (Müller and Crothers, 1975) and sigmoidal binding curves (Blake and Peacocke, 1968) indicates a cooperative outside binding process for this anomer). Yet, sonicated DNA complexes containing this anomer display significant viscosity increases (Zunino et al., 1977) (see fig.30). This demonstrates that viscosity measurements alone, for the

determination of intercalation, are not sufficient, and that other experimental techniques [(e.g. sedimentation, flow dichroism, light and low angle X-ray scattering etc. (Bloomfield, Crothers, and Tinoco, 1974)], are necessary to conclusively show the presence of intercalation. In view of this, therefore, no definite conclusion can be made from the viscosity results as to whether MC or its analog (compound A) intercalates DNA. In recognizing, however, that the increments of viscosity increase for both MC and (A) complexes are similar (see figures 24,28 and 30) suggests strongly that it is the monofunctional binding, or some form of it, that is responsible for the observed viscosity increase (compound A is monofunctional in binding).

Rate of Sedimentation of Sonicated DNA

In order to probe further into the question of possible intercalation, another property of DNA-MC complexes was investigated; the sedimentation coefficient. Variations in the length and/or stiffness of DNA are known to lead to changes in its hydrodynamic volume (Lerman, 1961); a characteristic which in turn determines the coefficient of sedimentation for DNA (Bloomfield, Crothers, and Tinoco, 1974). However, for DNA samples that are rod-like (e.g. sonicated DNA) a possible increase in stiffness should have negligible effect on the sedimentation coefficient, and thus the hydrodynamic changes can be interpreted in terms of the dimensions of the rod. In regard to this it is important to note that since the minor axis (e.g.

width of helix, perpendicular to helical axis or length) of DNA is assumed not to change significantly (Cohen and Eisenberg, 1969), as in the case of acridine intercalation (Lerman, 1961), then variations in sedimentation for these rod-like molecules are assumed to derive directly from changes in its molecular length (major axis). For compounds that intercalate in DNA, an increase in the length of the helix occurs by a process of helical unwinding (Waring, 1970) made possible by the tendency of these chromophores to slip in between and stack with the DNA base pairs. As a result of this linear expansion of the helix, there is an increase in the hydrodynamic volume (or decrease in the density) of the molecule with the resulting effect of a decrease in its coefficient of sedimentation (see appendix 8). As our results show however, there is no significant change in the sedimentation coefficients for sonicated DNA-MC complexes compared to control DNA (other than that from the increased mass of DNA due to bound drug; see table 9). From this absence of change in the coefficients of sedimentation, one may immediately conclude that there is no intercalation present in the DNA-MC complexes. One notes, however, that the magnitude of the decreases in the sedimentation coefficients for DNA vary according to the intercalator used (Bloomfield, Crothers, and Tinoco, 1974)[6] and that when these decreases are expressed as the fraction of the control sedimentation coefficient, they can range, for binding ratios of 0.10, for example, from 0.88 (proflavin; Waring, 1970) to 0.97 (actinomycin; Müller and Crothers, 1968).

0.88 and 0.97 represent, respectively, a 12% and 3% difference in the coefficients of sedimentation, or a 12% and 3% difference in the distance sedimented. In consideration of this and the fact that these sedimentation experiments contain an inherent maximum average deviation of approximately 3.5% (see results), no one can then exclude the possibility, with absolute certainty, on the basis of these results, that intercalation is taking place in DNA-MC complexes.

Flow Dichroism of DNA-MC Complexes

As yet another test of intercalation, flow dichroism of drug-DNA complexes has been used successfully by various investigators. The DNA helix, when oriented by flow in a shear gradient perpendicular to polarized light, will absorb light maximally since the electronic transtion moments in the bases are perpendicular to the helix axis (i.e. they lie in the plane of the base ring (Van Holde, 1971)), parallel to the electric vector of light. Any factors that affect this orientation, such as those that cause base tilting, will decrease the reduced dichroism of the DNA helix (Lerman, 1963), since DNA will absorb minimally when its axis is parallel to the polarized light (Bloomfield, Crothers, and Tinoco, 1974). In the case of intercalation where the planes of the intercalating chromophores are shown to be parallel to the base plates (Lerman, 1963), the mag-

nitude of the flow dichroism and the sign are similar for both the DNA bases (as observed at 260 nm) and dye chromophores (as observed at a wavelength unique to the bound dye) in these complexes (Bloomfield, Crothers and Tinoco, 1974).

The flow dichroism results (fig.42) display an increase of reduced dichroism with increasing shear rate. This increase can be best characterized as an initial rapid rise followed by a leveling off of the dichroism at higher shear rates. A linear dependence of flow dichroism for DNA has been observed at low shear rates (Lee and Davidson, 1968) and is the expected pattern according to theory (Blocmfield, Crothers and Tinoco, 1974). However, at higher shear rates, the dichroism becomes saturated (Collins and Davidson, 1969) and levels off, a characteristic indicating that the DNA is becoming deformed and oriented, with respect to flow, to a maximum extent. Our results (fig.42) conform to these patterns. The term deformation refers to the stretching of the DNA helix which has been observed at higher shear stresses (Lee and Davidson, 1968). It is known that the stretching of DNA fibers, presumably through the introduction of a tilt to the base pairs, reduces the dichroism of the double-helix (Lerman, 1963).

The dichroic curves for the complexes (fig.42) either approach closely (curves I and II), or assume the magnitude of the reduced dichroism for control DNA. (The discrepancies in the magnitudes of these curves may stem from experimental deviations. However, it is noted (fig.42) that the order of decrease follows the pattern of increasing binding ratio. Therefore, the

likelihood, especially in curves I and II, of some form of DNA deformation, at very low levels, may be occurring.

In contrast to the positive reduced dichroic spectra found at 260 nm for DNA, the reduced dichroism curves for bound mitomycin C at 310 nm (fig.42) display negative values which decrease (become more negative) with increasing drug binding ratio.Since intercalated drugs would show positive flow dichroism (Lerman, 1963) these results strongly indicate that mitomycin C is not intercalated in DNA. The small negative value observed indicates that the bound drug shows some preference for polarized light parallel to the DNA axis (equation (2), p.16). If the magnitude of this negative flow dichroism were equivalent to the positive flow dichroism of DNA alone, one could say that the drug chromophore is fixed in an orientation parallel to the helix axis (i.e. perpendicular to the bases). Such a case was described by Krey and Hahn (1970). (In their studies with distamycin A-DNA complexes, the flow dichroism for both the DNA bases and drug chromophores in the complex have equal magnitudes but are of opposite signs. Due to the negative flow dichroism of the chromophores, the allignment of the bound drug is thus believed to be parallel to the helix axis of the DNA molecule.) If the orientation of the mitomycin C chromophore were not complete, however, a fraction of the full magnitude of dichroic change would result as seen in figure 42. It seems, thus, that only a percentage of the bound mitomycin C chromophores are oriented in the DNA complex, and

that this orientation, as evidenced by the slight negative reduced dichroism, is perpendicular to the DNA base plates. The percentage orientation (or fraction of chromophores orientated in this manner) for complexes I, II, and III are approximately 25%, 20% and 15% respectively. (The percentage orientation of drug at 310 nm was calculated by dividing the increment of absolute reduced dichroism (.175) for control DNA (at 260 nm) into the increments displayed for each complex (at 310 nm); see fig.42 .) The variance in these values, which indicate an increased orientation with increasing binding ratio, suggests the possibility of a specific type of binding process which becomes more prevalent at higher binding ratios. One such possible binding process that should be considered is one of electrostatic nature, since this form of binding appears to predominate at binding ratios greater than 0.10 (Lipman et al., 1978).

In conclusion: The results of the flow dichroism measurements show that MC does not intercalate DNA.

DISCUSSION

Part II: Size Dependent Changes of DNA Properties of DNA-MC Complexes.

Sedimentation and Viscosity of Unsonicated DNA Complexes

The decrease in viscosity displayed by the unsonicated DNA-MC complexes (figures 25 and 29) is in obvious contrast to the increases of viscosity shown by sonicated DNA complexes. This indicates a size (DNA molecular weight) dependent effect on the hydrodynamic properties of DNA-MC complexes. The following hypothesis to explain these effects was at first considered: It is conceivable that the decreased viscosity of the unsonicated DNA-MC complexes is due to DNA strand breaks (double or main chain breakage). If strand breaks, such as those occurring by an overlap of single strand breaks on opposing DNA strands of a helix (Povirk et al., 1977) are relatively rare, they will effect the physical properties of long (unsonicated) DNA more so than those of short (sonicated) DNA. Such a phenomenon of molecular weight dependence in the scissioning of DNA was reported by LaRusso et al. (1978) for DNAs treated with $Na_2S_2O_4$, a reducing agent shown previously to produce single strand breaks in DNA (Cone et al., 1976). Single strand breaks induced by $Na_2S_2O_4$ in two different DNA samples caused a detectable decrease of the sedimentation coefficient only in the higher molecular weight DNA. Through the use of catalase or superoxide dismutase, one

is able to prevent such DNA strand breakage (Morgan et al., 1976), as has been shown in the case of DNA-MC complexes prepared in vitro (Lown et al., 1976). DNA strand breaks which were shown to occur in such complexes, due to the generation of superoxide radicals and hydrogen peroxides during the process of reductive activation of mitomycin C, were prevented when catalase was present. In our experiments, however, catalase had no effect on the viscosity decrease as shown in table 6. It is thus concluded that double strand breaks are not a likely cause of the size-dependent viscosity decrease of the DNA-MC complexes. (Single strand breaks do not effect the hydrodynamic properties of DNA in neutral solution; Parish, 1972; see also appendix 7.) The fact also that no decrease of the sedimentation coefficient of these complexes is detectable in neutral sucrose (another method for determining double strand breaks (Povirk et al., 1977); see figures 33 and 35) serves as additional evidence against the presence of main chain breaks in these complexes.

The size dependent effect found in the hydrodynamic properties of the DNA-MC complexes is similar to the case of DNA-actinomycin D complexes (Müller and Crothers, 1968). Müller and Crothers find, with the increasing binding ratio of drug, an increase in the viscosity of DNA-actinomycin complexes made from the sonicated form of DNA; a result expected for a compound (actinomycin D) that intercalates the DNA helix. However, for DNA-actinomycin complexes formed from the larger molecules of DNA, the opposite effect, a decrease in DNA viscosity occurs. Müller and Crothers (1968) explain this decrease as

one being due to a coiling or bending of the DNA helix, a condition possible for larger worm-like coiled DNA, but not for rod-like forms which approach the persistence length of DNA (see pages 106-107). This is facilitated by the tendency of actinomycin chromophores to increase the capacity of helical DNA to turn back on itself (a process often termed "intramolecular interaction" (Müller and Crothers, 1968) or "intramolecular crosslinking" (Alexander and Lett, 1960)). This interaction appears to originate from the affinity of the peptide rings of an actinomycin molecule bound at one point in DNA, for another part of the helix, as evidenced by the absence of viscosity decreases for DNAs bound with actinomycin D analogs lacking these peptide rings (Muller and Crothers, 1968). A diagram can illustrate these suggestions:

Bound Actinomycin Chromophore (AM)[1]

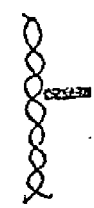

Sonicated DNA-AM Complex (Cannot bend unto itself)

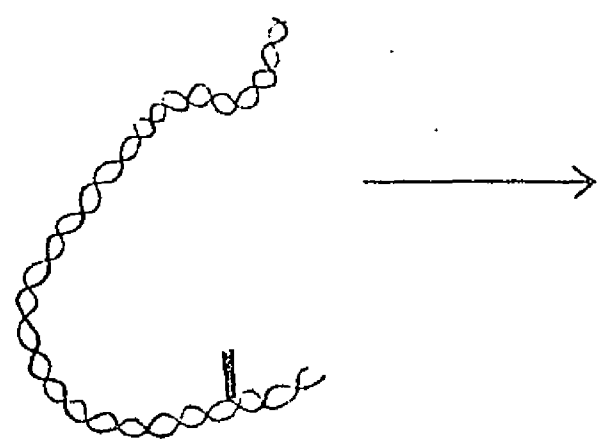

High M.W. DNA-AM Complex (Flexible)

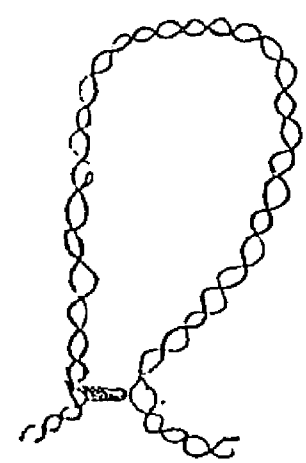

"Intramolecularly Crosslinked" DNA (Lowered Viscosity)

This explanation was consistent with another observed size-dependent change of DNA-AM complexes: Upon AM binding the sedimentation coefficient of high molecular weight DNA was increased, while that of sonicated DNA was not (Waring, 1970; Müller and Crothers, 1968; Rauen et al., 1969). The authors attribute the increased rate of sedimentation of high M.W. DNA as an additional proof for intramolecular looping or crosslinking of DNA. In the comparison of the sedimentation coefficients for a series of polyoma DNAs which vary in configuration (linear, nicked, and closed circular), one sees an increase in the coefficients of sedimentation (14S, 16S, and 20S respectively (Vinograd et al., 1965)) for those DNA configurations which exhibit an increasing compacting of DNA structure. In this series, linear DNA (14S) is the most expanded structure (largest radius of gyration), while the closed circular DNA form (20S), containing a twisted or supercoiled configuration, has the most compacted structure (smallest radius of gyration) (Bloomfield, Crothers, and Tinoco, 1974). The increase in the rate of sedimentation for these forms of compacted or coiled DNA is attributed to a lowering of the hydrodynamic frictional coefficient for DNA (Bloomfield et al., 1974; Zimmer et al., 1967). The frictional coefficient is a parameter related to the frictional resistence of the solvent which is a sensitive function of the DNA molecular radius. Assuming then a minimal change in the DNA partial specific volume (Bloomfield et al., 1974), a decrease in the frictional coefficient will result in an increased coefficient of sedimentation for DNA (see appendix 8).

In order to test further whether DNA-MC complexes represent a similar case to the DNA-AM complexes, sedimentation studies were also undertaken. Again, a striking parallel to the size-dependent effect of actinomycin was found: The results of the sedimentation of the unsonicated complexes, in contrast to the sonicated complexes, clearly indicate an increase, with increasing binding ratio, in the coefficients of sedimentation for complexed DNA. The increased coefficients for these complexes cannot be explained by the increased mass of DNA due to bound drug, since an increase from this source (see table 9) can only account for a fraction of the total observed change in these coefficients. The presence of DNA aggregates, however, whose formation may be facilitated in some manner by the binding of mitomycin C to DNA, could be considered to account for this effect since such forms of DNA exhibit rates of sedimentation that are higher (Parish, 1972). (DNA aggregation, facilitated through intermolecular crosslinking, has been shown to occur in DNA complexes formed from distamycin A (Zimmer et al., 1971), N-acetoxy-N-2-acetylaminofluorene (Chiang-Tung et al., 1974), and various polyfunctional alkylating agents (Alexander and Lett, 1960; Doskocil et al., 1963), and has been detected as rapidly sedimenting gels (Lett et al., 1962; Alexander and Lett, 1960; Doskocil et al., 1963).) The fact, however, that nucleic acid aggregates are recognized by their very high coefficients of sedimentation, relative to controls, and by pronounced bands sedimenting ahead of sample (unaggregated forms) demonstrates the unlikelyhood, in view of the sedimentation patterns for the DNA-MC complexes (figures 33 and 35),

that aggregation is taking place.

An experiment in which a mixture of unsonicated unlabeled and sonicated labeled DNA was complexed with MC and subsequently submitted to sedimentation indicated no "hybrid" material: no label was attached to any faster sedimenting fraction (figure 34). This rules out aggregation of DNA-MC complex molecules in any stable manner.

In view of the aforesaid, and the fact that the parallel between the size dependent effects of AM and MC on DNA hydrodynamic properties (viscosity and sedimentation rates) is indeed striking, the following conclusion is drawn: MC causes a conformational change of high M.W. DNA, analogous to that caused by AM; namely a change from a linear form to an intramolecularly crosslinked, looped structure. Since MC is a bifunctional agent it is conceivable that the same functional groups are involved in loop formation as in the interstrand crosslinks. Considering the small size of MC, however, this would require extremely close range interactions between the two duplex segments. An alternative cause of the links could be intramolecular non-covalent self aggregation of heavily substituted segments of the DNA-MC complex[9] (see diagram below).

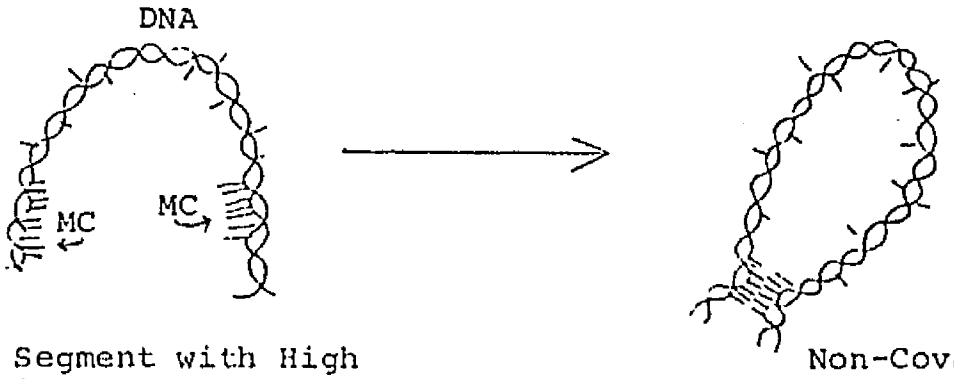

DNA Segment with High Binding Ratio of MC

Non-Covalent Self-Aggregated Structure of DNA

Electrophoresis of DNA-MC Complexes

The large contrast in the magnitudes of the relative mobilities for the sonicated and unsonicated complexes (fig. 38) is suggestive of a pattern similar to the one indicating a molecular weight dependence in the hydrodynamic properties (e.g. viscosity and sedimentation) of these complexes. Although one may readily conclude, in view of this parallel, a molecular weight dependent effect on the electrophoresis of DNA complexes, other factors (e.g. molecular charge (Olivera et al., 1964; Harley et al., 1973), shape (Strauss and Rees. 1959) etc.) other than size (Danna et al., 1973) must be first considered in explaining these mobility differences.

The reduction in the electrophoretic mobility displayed by unsonicated DNA-ethidium complexes (fig.38) represents a decrease in mobility due essentially to the partial neutralization of DNA charge by bound positively charged ethidium chromophores (Lippard et al., 1976). (Charge neutralization will decrease the average charge density of the macromolecule. Since the charge density is the essential characteristic responsible for macromolecular movement in electrical fields, its reduction will result in a decrease of macromolecular electrophoretic mobility (Van Holde, 1971).) In figure 38 a close agreement is seen in the electrophoretic mobility-binding ratio relationships (curves) for the sonicated DNA-MC and DNA-ethidium complexes. This suggests that charge neutralization is responsible for the reduction of mobility of the sonicated DNA-MC complexes. This view is supported by the fact that bound MC is a positive

ion (Mercado and Tomasz, 1977). The fact that some discrepancy is seen in the mobility curves for these two complexes (unsonicated ethidium-DNA and sonicated DNA-MC complexes; see fig.38) does not invalidate this assertion for several reasons: Since linear duplex DNAs of molecular weights greater than $4X10^5$- $1X10^6$ daltons are believed to migrate "end on" in polyacrylamide gels (Dingman et al., 1972; Maniatis et al., 1975), while smaller DNAs do not, then slight differences seen in these curves could result from differences in the modes of migration for these two DNA forms (e.g. sonicated vs. unsonicated). Secondly, the possibility that the binding of mitomycin C chromophores to DNA phosphate oxygens may result in an overall effect of producing 2 positive charges (see appendix 6) may account for the greater reduction in mobility (due to increased neutralization of DNA charge) for these complexes relative to the ethidium DNA complexes (see fig.38). Thirdly, the broadening displayed in the electrophoretic migrating bands for the ethidium-DNA complexes (plate C_1) may indicate a loss of bound ethidium cations for the complex which would explain, at least partly, the lower reduction in mobility (especially at higher binding ratios; note the leveling off in fig.38) relative to the sonicated DNA complexes. (Although ethidium-DNA complexes have been shown to be fairly stable (Aktipis and Kindelis, 1973) the use of cation exchange (Lerman, 1961) has successfully separated bound ethidium from DNA. In light of this, the 9 hr. electrophoretic runs at 90 volts may be slowly separating the drug from the

complex and thus causing a broadening in its zone of migration.)

When the curve displayed by the unsonicated DNA-MC complexes is compared with the others (fig.38) it is clear that the charge neutralization, alone, cannot explain the great reduction in electrophoretic mobility of these complexes. In the consideration of other possible factors, the presence of aggregation in DNA samples is known to cause a reduction in the electrophoretic mobility of DNA. With the formation of aggregates there is an effective increase in DNA molecular volume paralleling a lowering of the electrophoretic mobility (Chrambach and Rodbard, 1971; Parish, 1972). However a widening in the electrophoretic bands also occurs for such samples containing aggregates, as demonstrated for actinomycin D-complexes made from T_4 DNA (Dingman et al., 1972), since, due to the formation of dimers, trimers or larger aggregate forms in the aggregation process, there is a tendency for a broadening in the sample migration zone in gels due to differential rates of aggregate mobility (Dingman et al., 1972). In view of the fact that no such widening occurs (zone broadening) for the DNA-MC complexes, even at the higher binding ratios, makes the presence of such DNA forms rather unlikely. In addition, previous described experiments (viscometric and sedimentation, pages 24 & 118) involving the unsonicated DNA-MC complexes also eliminate the possibility of aggregation.

The absence of zone broadening in the electrophoretic

bands for the unsonicated DNA-MC complexes indicates also the absence of double strand breakage in these complexes, since with such forms of DNA degradation there would appear a smear effect, or an increased banding (zone broadening), due to the fragmentation of DNA into units of various molecular weights via the double strand scissioning process (Lloyd et al., 1978). Such increased banding has been reported to occur for bleomycin treated PM2 DNA samples. The newly formed bands, as displayed in these electrophoretic patterns, represent DNA fragments of lower molecular weight which migrate ahead of the main band (Povirk et al., 1977).

In an effort to test the possibility that single strand cleavage of DNA, which was reported to occur in DNA-MC reactions (Lown et al., 1976), may somehow lead to the observed decrease in electrophoretic mobility, a DNA control treated with a standard quantity of $Na_2S_2O_4$ shown to produce single strand breakage (see sedimentation results; page 28-29) was run against the untreated control. The negative results, which indicate no mobility change (see plate A_2), thus eliminate single strand breaks as the cause of the mobility reduction for the unsonicated complexes.

In the attempt to explain further the reduction in mobility for the DNA-MC complexes, it is pertinent to discuss the electrophoresis of denatured DNA samples. The rather heterogeneous electrophoretic patterns of low mobility displayed by these denatured calf thymus DNA samples (plate E1) demonstrates a conformation dependent effect of counterion fixa-

tion on the mobility of DNA. The denaturation of DNA is known (Constantino et al., 1964) to induce a large decrease of charge density on the polyanion which is attributed to the extended conformations of the chains in the disordered region of DNA. The decrease in the charge density is ascribed to a marked increase in the average distance between ionized phosphate groups in the disordered molecule (e.g. there are 7A° between phosphate groups in denatured DNA, as opposed to a 3.4A° distance in native DNA (Bloomfield, Crothers and Tinoco, 1974). Concurrent with this increased extension of the polymer chains is the increase in the activity coefficient for the counterion, sodium (Na^+), which, by virtue of its subsequent increased screening of polyanionic charge, results in a lowering of charge density and in a reduction of electrophoretic mobility for samples of denatured DNA (Lyons and Kotin, 1965).

With respect to charge density and its effect on the electrophoretic mobility of macromolecules, it is pertinent to note that moving boundary electrophoresis (as performed with the Tiselius Klett apparatus) of native and heat denatured calf thymus DNA in aqueous solution (Constantino et al., 1964), gives values (respectively) of 1.00 and 0.73 for the relative electrophoretic mobilities of these samples. The fact, however, that a visual inspection of the relative electrophoretic band positions for similar samples of native and denatured calf thymus DNAs (see plates E_1 and C_2) in polyacrylamide gels shows a significantly larger difference in relative mobilities suggests that some factor other than a decrease in charge density

alone is leading to a reduction in mobility of denatured DNA.

In attempting to identify factors other than charge density that lead to reduced mobility of denatured DNA it is important to briefly discuss the fact that separations of polynucleotides according to size and conformations have been achieved through the use of gel electrophoretic techniques (Peacocke and Dingman, 1968; Fisher and Dingman, 1971; Bishop et al., 1967). In the molecular weight range for polynucleotides greater than $3.4X10^5$ daltons, it has been demonstrated that single stranded polynucleotides may be distinguished from their double stranded counterparts by virtue of their different rates of mobility in polyacrylamide (Dingman et al., 1972) and agarose (Fisher and Dingman, 1971) gels. The explanation for this difference in the rates of mobility for these two different forms of DNA (or RNA) is related to the fact that double stranded polynucleotides migrate "end on" in gels, thus presenting the gel with a profile of small cross sectional area. As the voltage gradient is increased (e.g. from 2 to 10 volts/cm gel) the shear stress on these macromolecules increases and the double strand polynucleotides would be the forms more capable, relative to single strand species, of orientating in a manner which would minimize the frictional resistance to their motion and thus maximize their rate of migration through the gel (Dingman and Kakefuda, 1972; Fisher et al., 1971). Single stranded species (including those such as denatured DNA) on the other hand are assumed

to present the gel with rather globular profiles, the cross-sectional areas of which are not significantly altered by various orientations of the polynucleotide structure. As a result, the rates of migration of single stranded polynucleotides, under these conditions, are low compared to those displayed by duplex structures. Such "end on" movement of duplexed polynucleotides in gels infers, partly, a "sieve-like" function for these gels which is responsible for the impediment or retardation of the movement of macromolecular structures according to their size and shape. In regard to this, it is noted that by varying the quantity of crosslinker, N-N'-methylbisacrylamide, in gels (Chrambach and Rodbard, 1971) or by increasing the total concentration of polyacrylamide (Dingman et al., 1972) or agarose (Johnson et al., 1977) in gels, variations in the separation of a number of DNA conformational isomers have been achieved. For example, by increasing the polyacrylamide concentration in gels to 3.0% or more (Dingman et al., 1972), optimal separations, in the order of decreasing electrophoretic mobility, respectively, for linear, nicked circular, and closed circular duplexes of SV40 DNA have been obtained. As this order of separation parallels also the order of increasing sedimentation coefficients (e.g. 14.5, 15.9, and 22.2 S, respectively for the linear, nicked, and closed circular SV40 DNA (Dingman et al., 1972)), and thus the order of increased compacting of structure, for these forms of SV40 DNA, demonstrates the ability of the polyacrylamide's "sieve-like" matrix to selectively retard the electrophoretic migration of these DNAs whose structures contain greater degrees of coiling.

In view of the foregoing discussion, it appears that the large reduction of electrophoretic mobility displayed by the unsonicated DNA-MC complexes is due largely to a conformational change in the structure of the complexed DNA relative to control DNA. Figure 39 shows a decrease in mobility with increasing DNA molecular weight for a series of DNA-MC complexes of equivalent binding ratio. This relationship demonstrates the increased likelyhood of structural bending or coiling of DNA with increasing molecular weight of DNA; a condition that would explain, in analogy with the electrophoresis of the SV40 DNA conformational isomers, the decreased electrophoretic movement of the larger DNA-MC complexes in polyacrylamide gels. It is noted further that this decrease in movement of the unsonicated DNA-MC complexes levels off at a binding ratio of 0.10 to 0.15 (figure 38). The fact that this binding ratio is identical to that range where decreases in the viscosity of unsonicated DNA-MC complexes similarly level off, is consistent with the assertion (but does not prove it) that the intramolecular crosslinks discussed previously (p. 119) are the common origin of these effects. Caution is advised, however, in this interpretation, in view of the fact that aberrent behavior of some double stranded nucleic acids in polyacrylamide gels have been previously reported (Mertz and Berg, 1974; Maniatis et al., 1975; Schuerch and Joklik, 1973).

The view that the crosslinks are the cause of the conformational change in DNA was finally explored by electron microscopy. Again, DNA size-dependent effects were evident as follows:

Electron Microscopy of DNA-MC Complexes

(A) Unsonicated DNA Complexes. Comparisons of plates 1,2 and 3(a&b) clearly indicate an increase in the coiling of DNA in unsonicated DNA-MC complexes relative to the control

DNAs. Although some similarity does exist in the characteristics of contour for a number of the molecules shown in plates 1,2, and 3a and 3b, a general inspection of these plates indicates a distribution towards considerable coiling for the DNA-MC complexes. The contention that such coiling of DNA structure is due to the binding of mitomycin C requires, it appears, that all such molecules exhibit this characteristic change. However, significant distributions have been observed by measurements of the end to end distance (a function of the molecular conformation or shape) for full length homogeneous T3 DNA molecules (Lang et al., 1967). Such variations stem, in part, from differences in coiling from one molecule to the next (Flory, 1953). In addition to this, the procedures of adsorption of DNA from solution onto the monolayers of surface denatured cytochrome C protein (as in the Kleinschmidt procedure; Kleinschmidt and Zahn, 1959), and the subsequent consecutive procedures of film transfer onto electron microscopic specimen grids, etc., may also lead to variations in the patterns seen in terms of DNA contour. The distribution of such effects, however, will indicate, on the average, the degree of contour (or average contour) for measured samples (Lang et al., 1967). The fact remains that there is more coiled structure in the MC complex than in the control DNA and that these patterns appear to be indicating, at least on an average basis, real changes in the conformation of DNA.

Comparisons of plates 4,5, and 6 similarly demonstrate an increase in the coiling of MC bound DNA relative to its unbound. Plates 4 and 5 (control DNAs treated with the enzymes

catalase and superoxide dismutase, with and without sodium dithionite, on the other hand, display non-coiling patterns that are relatively the same, but which do exhibit some moderate jaggedness in contour. Similar patterns have been obtained in electron microscopy studies involving λ DNA (Inman, 1967) and have been explained in terms of the interaction of DNA with the relatively highly concentrated salt (.1M NaCl) present in the preparative hypophase solutions used in these experiments. (The "smoothing out" (Inman, 1967) of this jagged contour when H_2O is used, instead of .1M salt, indicates a salt effect on the linear extension of these DNA molecules (Lang, 1967). Since the concentration of salt (.01M Tris (Davis and Hyman, 1971)) used in the preparative hypophase for the calf thymus DNA samples here is relatively dilute when compared to .1M salt concentration (determined as the cause of this contour change) some other factor, it appears, is responsible for this effect in the calf thymus DNA samples seen here. A possible cause of this effect could be linked to the presence of excess proteins present in these samples. By virtue of ion pair formation between DNA phosphates and the basic amino acids of protein, a partial screening of phosphate charge occurs, the repulsion of which is responsible for the opposite or elongation effect (Lang et al., 1967). As the presence of excess cytochrome C appears to be unlikely (due to the reproducibility of the spreading techniques), it is possible that residual, but sufficient quantities of catalase and/or superoxide dismutase escaping the deproteinizing procedure are present and causing this effect. However, in view of the fact

that the DNA in plate 6 (which is treated similarly as the DNAs in plates 4 and 5) lacks this jaggedness, makes such reasoning only conjectural.)

The slight coiling in DNA structure indicated in plate 2 (DNA + $Na_2S_2O_4$) appears to be absent in plate 5 (DNA + $Na_2S_2O_4$ + catalase + superoxide dismutase). This may imply that single strand breaks are the cause of this coiling. The fact, however, that the coiling displayed in plate 3 (DNA-MC complex) is maintained in the presence of single strand scission inhibiting enzymes (plate 6) rules out that the conformational change is caused by single strand breaks in DNA-MC complexes. These results clearly indicate that the conformational change as shown in plates 3 and 6 is caused by the presence of mitomycin C.

(B) Sonicated DNA Complexes. A striking support for the aforementioned conclusion are the findings from the electron microscopic examination of the sonicated DNA samples. The absence of any difference in the shape or contour of the DNA strands for the sonicated DNA-MC complex (plate 8) and its control (plate 7) demonstrates that the coiling patterns displayed by the unsonicated DNA-MC complexes are the result of the ability of long (unsonicated) DNA to bend extensively upon itself as a consequence of MC binding. The contrast, therefore, found in the

comparisons of the electron microscopy results for the sonicated and unsonicated DNA-MC complexes, with respect to the assessment of conformational change in the latter, parallels the findings of the hydrodynamic and electrophoretic measurements.

SUMMARY AND CONCLUSION

The viscometric and sedimentative studies of DNA-MC complexes demonstrate a size dependent change in the hydrodynamic properties of these complexes; a change which is explained by the ability of large (unsonicated) DNA to coil or bend upon itself. The resulting decrease in the radius of gyration for unsonicated DNA, acquired upon its complexing with mitomycin C, is in contrast to the results displayed by the sonicated complexes, which show no such effect, demonstrating, thus, the inflexible nature of rod-like DNA.

The size dependent changes displayed in the electrophoresis of DNA-MC complexes parallels the findings of the hydrodynamic experiments. In consideration of this, and the fact that both electrophoretic and hydrodynamic measurements are known to complement each other, in regard to the discerning of conformational differences in DNA (e.g. linear, nicked and supercoiled forms of SV40 DNA (Dingman et al., 1972)), it appears that the contrasts seen in the electrophoretic patterns of these DNA-MC complexes is consistent with and may be indicating conformational differences in DNA similar to those assessed bythe hydrodynamic measurements. This conclusion is further supported by direct electron microscopic observations of the DNA-MC complexes which show an increased coiling of DNA relative to control DNA.

What is the molecular mechanism whereby MC holds DNA in looped forms? The crosslinking of DNA, it has been shown, is

the most likely cause for the increase in the melting temperatures and transitional breadths observed in the DNA-MC complexes. It is important to note that while maximum renaturability of DNA, tantamount to 100% crosslinkage, occurs between a binding ratio of .01 and .02 (see fig.22), the leveling off of the increases in the T_m and melting breadths occurs in the binding ratio range of .10 to .15. In view of this, and understanding that only one crosslink per DNA molecule is sufficient to permit full renaturation of such molecules (Iyer and Szybalski, 1963), it appears likely that the binding ratio (.10-.15) represents a saturation point for possible crosslinking sites in calf thymus DNA. As this range of binding is also the leveling off point for the decreases in the viscosity and electrophoretic mobilities of unsonicated DNA-MC complexes suggests strongly that the same covalent bifunctional binding of MC to DNA is responsible for the observed conformational changes. An alternative possibility is non-covalent aggregation of two segments of the same DNA molecule.

Another set of findings in this work resulted from the analysis of size-independent changes of DNA properties. It was shown that the crosslinks not only cause reversible denaturation in DNA but also cause an increase in the temperature required for DNA strand separation. It was also deduced that the steric arrangement of DNA-bound mitomycin C is not the intercalation type between the base pairs of DNA.

The ability of mitomycin C to crosslink DNA is considered an important factor in its antitumor activity (Dermer and Ham,

1969) and, as discussed previously, has also been reported to be a direct cause of bacterial cell death (Iyer and Szybalski, 1963). In regard to such phenomena caused by mitomycin C it is important to indicate that although the presently discovered ability of MC to freeze DNA in a looped structure is demonstrated only in vitro and at relatively high binding ratios of the DNA-MC complex, it may occur in the cell as well. This may especially be the case when one considers that cellular DNA, in general, is already folded into non-covalent structures and therefore, unlike in solution, the kinetic barrier for the bifunctional action of MC is not present. If this indeed proves to be the case, the phenomenon is very likely to cause biological consequences.

Footnotes

1 Abbreviations: MC, mitomycin C; AM, actinomycin D; N-Aco-AFF, N-acetoxy-N-2-acetylaminofluorene; SSC, saline sodium citrate (1.5 M sodium chloride and .2 M citric acid, pH 7.4); DSC, dilute sodium citrate (.015 M sodium chloride and .002 M citric acid, pH 7.4).

2 UV spectra of mitomycin C bound to DNA displays a 310 nm/260 nm absorption ratio of approximately 1.34 (Lipman and Tomasz).

3 The melting or transition temperature is defined as that temperature at which the measured parameter has changed halfway from the value characteristic of a helix to that of a coil (Bloomfield, Crothers and Tinoco, 1974).

4 It is pointed out that a heterogeneous population of DNA molecules will have different temperatures of strand separation due to fluctuations in size and individual G-C content (Bloomfield, Crothers and Tinoco, 1974). This heterogeniety in thermal stability with respect to strand separation will lead to an "average" total transiton (transitional breadth) that may be several degrees wide (Hamaguchi and Geiduschek, 1962).

5 Lett, Parkins and Alexander (1962) have shown that a transalkylation mechanism is probably involved, where purine alkylation follows esterification of the phosphates. The slow drop in molecular weight of DNA is a consequence of the purine alkylation where the quatern-

ized purine is readily split out from the DNA leaving an apúrinic acid residue which is known to be unstable and to hydrolyze resulting in chain scission.

6 Variations in the coefficients of sedimentation are explained partly, as in the case for actinomycin D versus proflavine, by the greater mass of actinomycin, which tends to make the sedimentation coefficient increase (Bloomfield, Crothers, and Tinoco, 1974).

7 For sucrose gradients the relationships of sedimentation coefficient (S), time (t), distance sedimented (D), and the molecular weight (M) of DNA are as follows (From Burgi and Hershey (1963)):

$$\left(\frac{t_1}{t_2}\right) = \left(\frac{D_1}{D_2}\right) = \left(\frac{S_1}{S_2}\right) = \left(\frac{M_1}{M_2}\right)^{0.35}$$

8 It should be noted here that the variance displayed in figure 30 in the ability to increase the viscosity of DNA, has been explained (Gabbay et al., 1973) in terms of differential steric interaction between DNA binding chromophores and base pairs which may lead to differences in helical length. This is related to the positions and number of substituents on the intercalating chromophores, which effects its "aromatic ring thick-

ness", a characteristic leading to variations in helical length and viscosity.

9 This intramolecular aggregation is to be distinguished from aggregation between separate molecules of DNA, which has been shown not to occur (see page 119). .

APPENDIX

Appendix (1): These corrections are in addition to the basic correction (see page 11) which corrects for the 260 nm absorption contribution by bound MC to the total 260 nm of the DNA-MC complex. The purpose of this additional correction is two-fold: (1) To account for, at higher temperatures, the additional 260 nm contribution to the total 260 nm absorption of the complex due to a presumed 260 nm hyperchromic rise for bound drug which may complement its 310 nm hyperchromic rise (see appendix 4), (2) To account for the observed irreversible 310 nm hyperchromicity, in terms of this assumed 260 nm absorption increase, after a heated complex is cooled.

Since at room temperature, $A_{260}:A_{310}$ of bound MC is 1.34[2] we can then calculate the hyperchromic increase of A_{260} due to DNA alone from the observed increase for the DNA-MC complex minus the calculated increase for bound MC as follows: The A_{260} of DNA alone at any temperature (t) is obtained from the following formula : $A_{260}(DNA)_t = A_{260}(observed)_t - 1.34(A_{c310})_t$**

from which the % hyperchromicity obtained upon heating to (t) can be calculated in the usual manner.

** (A_{c310}) is obtained as follows: The total 310 nm absorption (A_{310}) times the increment of 310 nm hyperchromic increase ((I), which varies with temperature; see fig.12) at a specified temp.(t) minus (A_{310}) gives corrected 310 nm (A_{c310}): $(A_{310})(I) - (A_{310}) = (A_{c310})$

Appendix (2): Corrected 260 nm Melting Profiles

In figure 18 are displayed two melting profiles for a DNA-MC complex (binding ratio = .11) in aqueous buffer. Melting profile 1 is a standard melting curve constructed as outlined in methods. Profile II represents profile I corrected for the estimated 260 nm absorption increase associated with the 310 nm hyperchromicity for bound drug. Increments of 310 nm hyperchromicity (I) used for the correction, at the various temperatures associated with the DNA melting curve, were obtained from figure 12. The corrected melting profile II, although showing a reduction in hyperchromicity and a slight decrease in melting breadth, exhibits no change in the T_m relative to the uncorrected profile. The retention of the T_m at 260 nm of the original DNA-MC complex (profile I, fig.18) by the corrected profile II demonstrates, thus, that the 310 nm hyperchromicity has no effect on the calculated T_m at 260 nm. Furthermore, a more complete renaturation, due to crosslinking, is evident upon this correction (see also fig.11 and table 3 for similarly corrected renaturation values of DNA-MC complexes in methanol-DSC buffer.). Corrections for 310 nm hyperchromicities are also shown in figures 16 and 17. Here the increments for the 310 nm hyperchromicity (similar to those in fig. 12) were obtained directly from the 310 nm profiles of these complexes.

Appendix (3): Melting Profiles of DNA-MC Complexes Sonicated Following their Formation

The melting profiles of two calf thymus DNA-MC complexes of binding ratios .12 and .04, respectively, are displayed in figures 20 and 21. These samples were sonicated following their formation. Although they exhibit the expected levels of cross-linkage (see table 1A), they do not display the increases in T_m and melting breadth expected of DNA-MC complexes formed from DNA sonicated prior to its complexing with mitomycin C.

These experiments were attempted to equate two conditions for DNA-MC complexes: That complexes formed from DNA, sonicated prior to its reaction with mitomycin C, were equivalent to complexes obtained from DNA-MC sonicated after its formation. Comparisons, as shown in table 1A, of T_ms and melting breadths vary for these two conditions, and may be the result of an inherent difference in the relative conformations of DNA used for sonication. (In the first condition, uncomplexed DNA is used, while in the second condition, DNA complexed with MC, which has been shown to be more coiled than uncomplexed DNA (see discussion), is used. This difference may thus lead to a variation in the sonication of relatively linear versus coiled DNA, which may account for the variation in melting properties.)

Appendix (4):

"Thermal Denaturation Profiles" at 310 nm

Figures 12*, 13*, 14*, and 15*, respectively represent the thermal denaturation profiles for sonicated DNA-MC, denatured DNA-MC, polyvinyl sulfate (PVS-MC) and DNA-compound A complexes at 310 nm (see also table 5)*. All complexes show a gradual "hyperchromic" increase or shift at 310 nm. Upon cooling only a slight "renaturation" occurs. Unsonicated calf thymus DNA-MC complexes similarly show increases of 310 nm absorption after heating (table 4). It is shown (see table 5) that no mitomycin C is released from this complex after heating upon extended dialysis. Approximately 50% of compound A, however, is released from heated complexes as shown by dialysis(see table 5). A comparative display of the 260 nm and 310 nm melting profiles (see table 5) for two unsonicated calf thymus DNA-MC complexes is shown in figures 16 and 17. These profiles show that the T_ms and melting breadths of DNA (260 nm) differ considerably from the "T_ms" and "melting breadths" for the bound drugs (310 nm) (see table 5). These findings are similar to those of Fuchs and Daune (1971) with respect to their cooperative melting curves at 305 nm (for bound drug) of N-acetoxy-2-acetylaminoflourene-DNA (N-Aco-AFF)[1] complexes.

The 310 nm hyperchromic shifts for bound drug (MC and compound A) differ from the 260 nm melting profiles for DNA in

* pages 148-150

several characteristics. First, at binding ratios where significant reversible denaturation is displayed by DNA (figures 16 and 17), 310 nm "thermal profiles" show only a slight to moderate reversibility in denaturation. Secondly, the "Tms", as measured by the midpoints of the 310 nm hyperchromic shifts (figures 16 and 17) are higher relative to the Tms of the 260 nm melting profiles for the same complexes. Thirdly the transitions of the 310 nm hyperchromic shifts are more gradual and wider relative to the transitional breadths displayed by DNA at 260 nm.

The irreversibility seen in hyperchromic shifts at 310 nm for the bound mitomycins are similar in many respects to the 305 nm hyperchromic shifts reported (Fuchs and Daune, 1971) for DNA bound N-acetoxy-2actyl amino flourene (a carcinogen) residues, and is interpreted (Fuchs and Daune, 1971) as an irreversible change in the position of some of the bound chromophores with respect to the DNA helix. Fuchs and Daune (1971) explain the 305 nm hyperchromic rise observed for DNA-N-Aco-AFF complexes as one due to a spectrophotometric detectable change, induced through heating, in the position of the N-Aco-AFF chromophore from it's original position of insertion in the internal field of the double helix. It is the non-resonant coupling, as Fuchs and Daune (1972) further explain of specific electron transitions of the carcinogen chromophore with all other transitions of the DNA bases that is responsible for the hypochromicity

of the drug (a condition before heating). Through the introduction of heating there is then a loss of stacking of fixed carcinogen with upper and lower corresponding base pairs which allows for a decrease in this non-resonant coupling and thus for a rise at 305 nm (Fuchs and Daune, 1972). The fact that Chiang, Miller and Wetmur (1974) conclude however, through electric dichroic studies of similar DNA-N-Aco-AFF complexes, that the carcinogen chromophore is more probably bound along the DNA helix winding angle of $60 \pm 4^{\circ}$ to the helical axis (as opposed to the stacking of this carcinogen with upper and lower corresponding base pairs) demonstrates the possible uncertainty that can be involved in the attempt to identify the position of the bound chromophore, relative to the helix, that is responsible, once the complex is heated, for the hyperchromicity. It is pertinent to note that the extended dialysis of heated complexes (see table 5) display essentially no loss of mitomycin C (Lipman et al., 1978). It has also been shown (Tomasz et al., 1974) that, except for the expected absorption increase (310 nm hyperchromic shift for bound chromophores), there is no difference in the U.V. spectra between bound and unbound reduced MC chromophores before and after heating; a finding supporting the absence of heat induced chemical change of bound chromophores. Absence of change in the silica gel and sephadex G-25 column (fig.23) chromatographies of heated and unheated compound A samples further supports the assertion that heating is not chemically changing the structures of the mitomycins.

The higher midpoints of "melting" observed for the 310 nm hyperchromic shifts, relative to the Tms at 260 nm for DNA-MC complexes (figures 16 and 17), have similarly been obtained at 305 nm by Fuchs and Daune (1971) for the N-Aco-AFF-DNA complexes and is explained by an increase in "Tm" being due to a preferential binding of the carcinogen to DNA regions of high G-C content where the melting temperature for DNA is higher than in other regions of the DNA molecule. The fact that mitomycin C similarly binds to G-C rich regions of the DNA molecule (Tomasz et al., 1974; Lipsett and Weissbach, 1965) may be the reason for the observed 310 nm "Tm" increase, but it is noted that the difference (7-12°C) (see table 5) between "Tms" at 310 nm and Tms at 260 nm displayed by DNA-MC complexes are higher than those (1-4°C difference range for all binding ratios) reported by Fuchs and Daune (1971) for N-Aco-AFF-DNA complexes. In view of this it seems quite likely that factors other than preferential binding to G-C regions are responsible for the differences observed for 260 nm and 310 nm "melting".

The broader widths of transition (as distinquished by their smaller slopes) found at 310 nm for DNA-MC complexes relative to those at 260 nm, indicate some independence in the events of DNA denaturation and chromophore "melting". It is interesting to note, in support of this independence in melting, that a similar "melting" of mitomycin C (or compound-A) chromophores occurs in polyanionic structures lacking significant helical content (e.g. denatured DNA, PVS etc.; see

table 5). It is appropriate here to introduce the fact that the intercalation of chromophores into the hydrophobic environment between DNA base pairs would decrease the ability of these chromophores to absorb light energy (Krey and Hahn, 1975). In considering this and the fact that a hyperchromic shift for intercalating chromophores would more or less overlap, or immediately succeed, the separation of DNA strands (Aktipis et al., 1975) supports the view that a general or classical mode of intercalative binding of the MC chromophores into the hydrophobic regions of DNA is not occurring. The fact, also, that the other polyanionic complexes described are essentially "non-intercalatable", due to the lack of significant helical content in their structures, further supports this view. It is also important to note here that since we are apparantly dealing with an irreversible change in the position of a substancial quantity of MC chromophores, we can eliminate any possibility of monofunctional binding as the cause for the T_m increase of DNA. The reasoning is that the T_ms for the 1st and 2nd meltings in the double melting profiles are equivalent despite the presumed positional change of the MC chromophores.

In regard to the determination of the possible modes of binding to DNA exhibited by MC, which may be responsible for the 310 nm hyperchromic shifts, two major forms of known mitomycin C binding (e.g. monofunctional and bifunctional (Iyer and Szybalski, 1963)) come into light. Understanding, as previously explained, that the 310 nm hyperchromic shifts

probably represent an irreversible change in the position of many of the bound MC chromophores relative to the DNA helix supports the view that it is a positional change in the monofunctional rather than bifunctional (crosslinking) bound MC chromophores which leads to the 310 nm shift. This is because MC molecules bound bifunctionally (to two DNA strands) via a minimum of two bonds are more likely to be restricted from molecular movement than those MC chromophores bound monofunctionally (e.g. possible pivoting, introduced via thermal agitation, of a molecule about a single bond is more likely). A support for this is the fact the DNA-A complexes (see table 5) which contain only monofunctionally bound chromophores (Tomasz et al., 1974) similarly display 310 nm hyperchromic shifts. Furthermore, since it is known that the MC chromophores responsible for the crosslinks in DNA comprise only a fraction of the total mitomycin C bound (e.g. 1/5 to 1/10 of total bound chromophores exist as crosslinks (Szybalski and Iyer, 1964a&b), then most likely, it is the repositioning of a significant quantity of monofunctionally binding chromophores that is leading to the 310 nm hyperchromic shift. The fact, also, that "310 nm hyperchromicities", comparable to those shown by native DNA complexes, are displayed by complexes (e.g. PVS and denatured DNA, see table 5) unlikely to contain crosslinks is an additional support for this assertion.

The heating of various complexes, containing MC, as shown in table 5, demonstrates that the 310 nm hyperchromic

shifts are essentially independent of the conformation of the polyanion. As Lipman, Weaver, and Tomasz (1978) have shown, the binding of compound A to various polyanions, and the binding of MC to PVS or to DNA (above binding ratios of 0.1) is essentially electrostatic in nature. The fact, therefore, that significant 310 nm hyperchromic shifts occur with complexes exhibiting considerable electrostatic interaction between bound chromophores and polyanions (e.g. PVS-MC, sonicated DNA-compound A, etc.) and with complexes (e.g. DNA-MC complexes at binding ratios 0.04 and 0.08, see table 5) not displaying, significantly, such interaction demonstrates the possibility that it is a general form of binding (e.g. to the phosphates of the DNA helix), independent of the nature of the bond (e.g. covalent vs. electrostatic) involved, which is responsible for the 310 nm hyperchromic shifts.

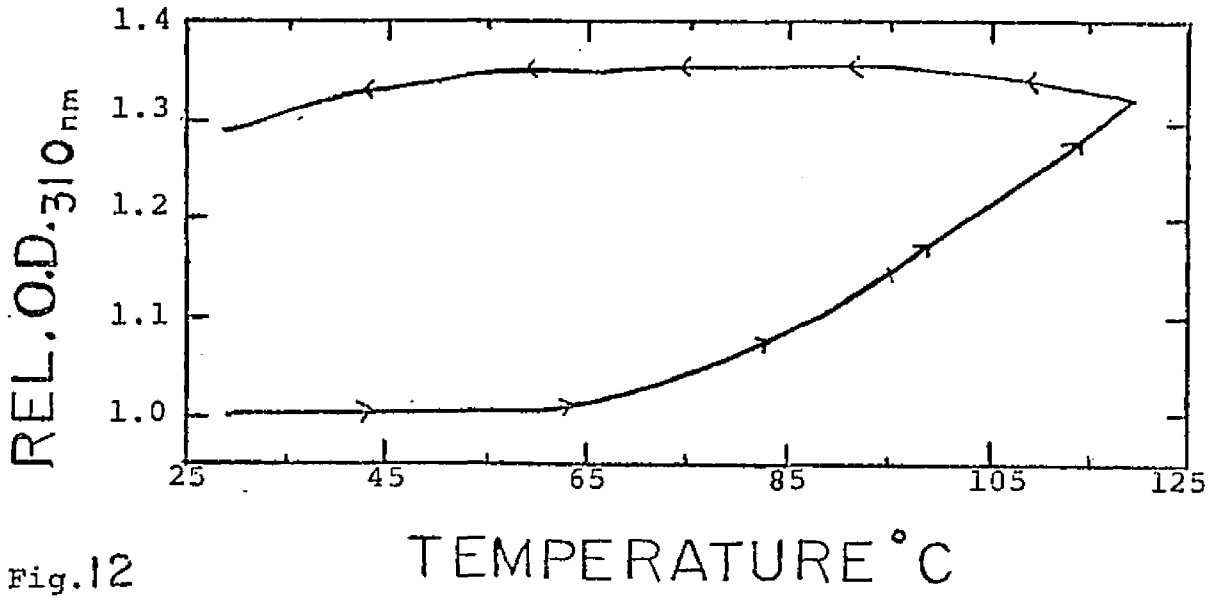

Fig.12

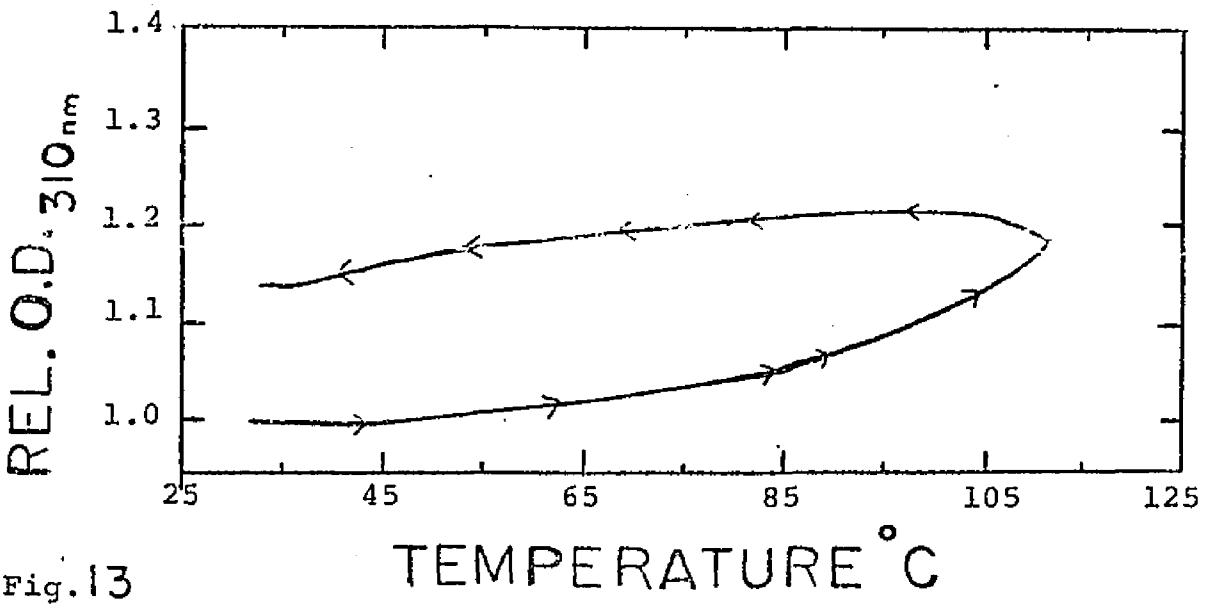

Fig.13

Legend: Fig.12 . Relative $O.D._{310}$ vs. Temp. for sonicated E.Coli DNA-mitomycin C complex of binding ratio .25 in DSC.

Fig.13 . Relative $O.D._{310}$ vs. Temp. for denatured E.Coli DNA complexed with mitomycin C (b.r.=.14) in DSC.

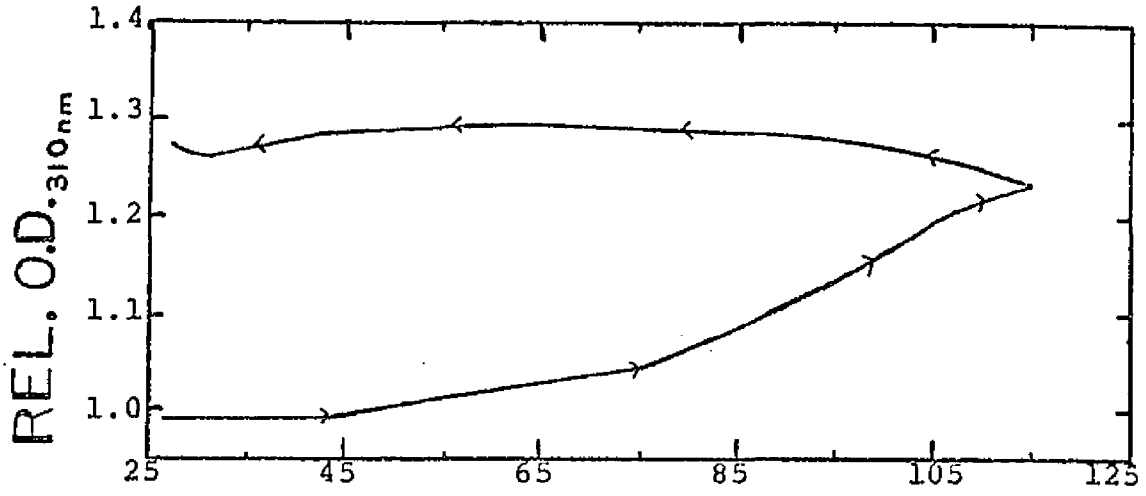

Fig.14

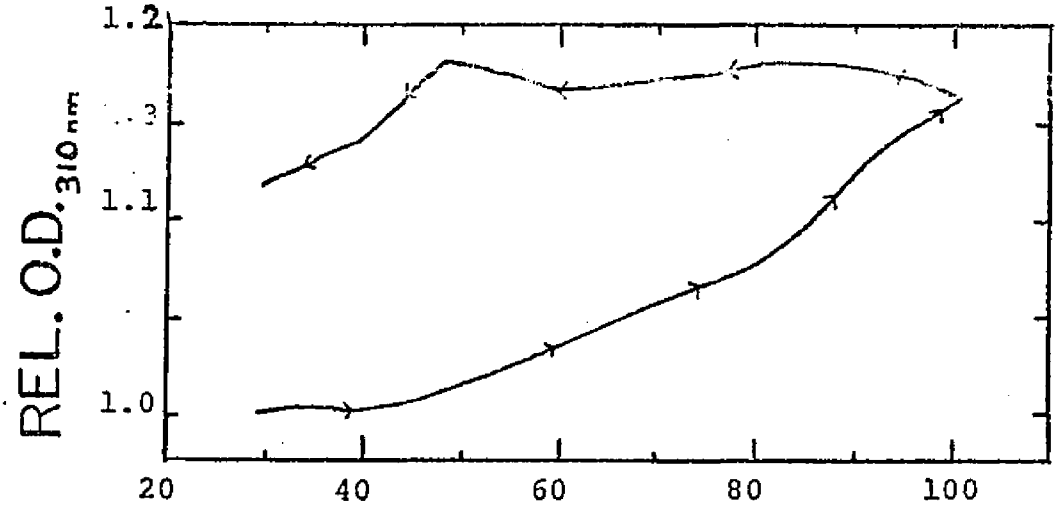

Fig.15

Legend: Fig.14 . Relative $O.D._{310}$ vs. Temp. for a polyvinylsulfate-mitomycin C complex in DSC.

Fig.15 . Relative $O.D._{310}$ vs. Temp. for a sonicated calf thymus DNA-compound A complex of binding ratio .14 in DSC. Binding ratio of complex after heating was approx. .07.

Table 5. Relative Absorbance Increase at 310 nm for various Mitomycin C and Compound A Complexes.

Complex	Binding Ratio	Relative[ii] OD(310 nm) increase	Maximum Hyperchromic Rise	"310[i] Tm"	"310[i] m.b."
PVS-MC Complex*	0.12	1.22	1.27	-	-
Denatured DNA-MC Complex*	0.14	1.14	1.21	-	-
Sonic. E.Coli DNA-MC Complex*	0.25	1.29	1.36	-	-
Calf Thymus DNA-MC Complex***	0.12	1.35	-	-	-
Calf Thymus DNA-MC Complex	0.04	1.18	-	-	-
Calf Thymus DNA-MC Complex	0.15	1.07	1.13	85 °C	38 °C
Calf Thymus DNA-MC Complex	0.08	1.08	1.14	80 °C	45 °C
Sonic. C.Thymus DNA-Compound A	0.14 ~(0.07)**	1.12	1.16	-	-
Compound A alone[iii]	-	~1.03	1.06	-	-
Auto-oxidized Compound A alone	-	~1.03	1.05	-	-
Mitomycin C alone	-	1.00	1.00	-	-

(i)- 310 nm "Tm"&"m.b.(Melt. Breadth)" were measured for the 2 complexes noted. (ii)- At room temp. after the cooling or renaturation of complex. (iii)- Done in Methanol-DSC

(*)- In DSC and heated to 120 °C. (**)- Binding Ratio after heating and dialysis. B.Ratio of this complex before heating was 0.14. After heating it was 0.07 (upon dialyzing). This represents a loss of 54% of drug through heating (.14-.065/.14 X 100 = 54%). Since 54% of drug is lossed, then hyperchromic. values for (A) complexes were multiplied by .54 and then subtracted from complex value.

(***)(Mitomycin C is not lossed from complex by heating as shown by dialysis. (DNA-MC before and after heat. has b.r. =.12)

Appendix (5) : The differences in melting breadths (see table 1) for sonicated versus unsonicated calf thymus DNA (in DSC) complexes can be explained (when taking into consideration the lower degree of consistency in melting breadth measurements as compared to those obtained in methanol-DSC solvent (see table 3) by the presence of noncrosslinked DNA in the sonicated samples. For example, when comparing the melting breadths for DNA-MC complexes of .10 binding ratios for sonicated and unsonicated forms, we find:

* Unsonicated complex - assuming full 100% crosslinkage has a real melting breadth (m.b.) Of 23.5°C (T_m=78.1°C).
* Sonicated complex sample - has, assuming a 50% crosslinkage (see results), an observed m.b. of 28.5°C.
* Control sonicated DNA (T_m=68.5°C) has a melting breadth of 18°C and represents 50% of the sonicated sample in terms of total molecules.

(1) Assuming that crosslinks are the reason for change in melting breadth, (2) knowing that the melting breadth in degrees centigrade is bisected by the Tm (see melting profiles) and (3) assuming that the m.b. of the sonicated sample is a combination of 50% control sonicated and, effectively, 50% of the unsonicated complex, then we can array the relation-

ships in this manner: (From the relationship below we find an estimated m.b. of 30.3°C, a value much closer ** to 28.5°C (m.b. of sonic.complex) than to 23.5°C (m.b. of unsonic.complex)

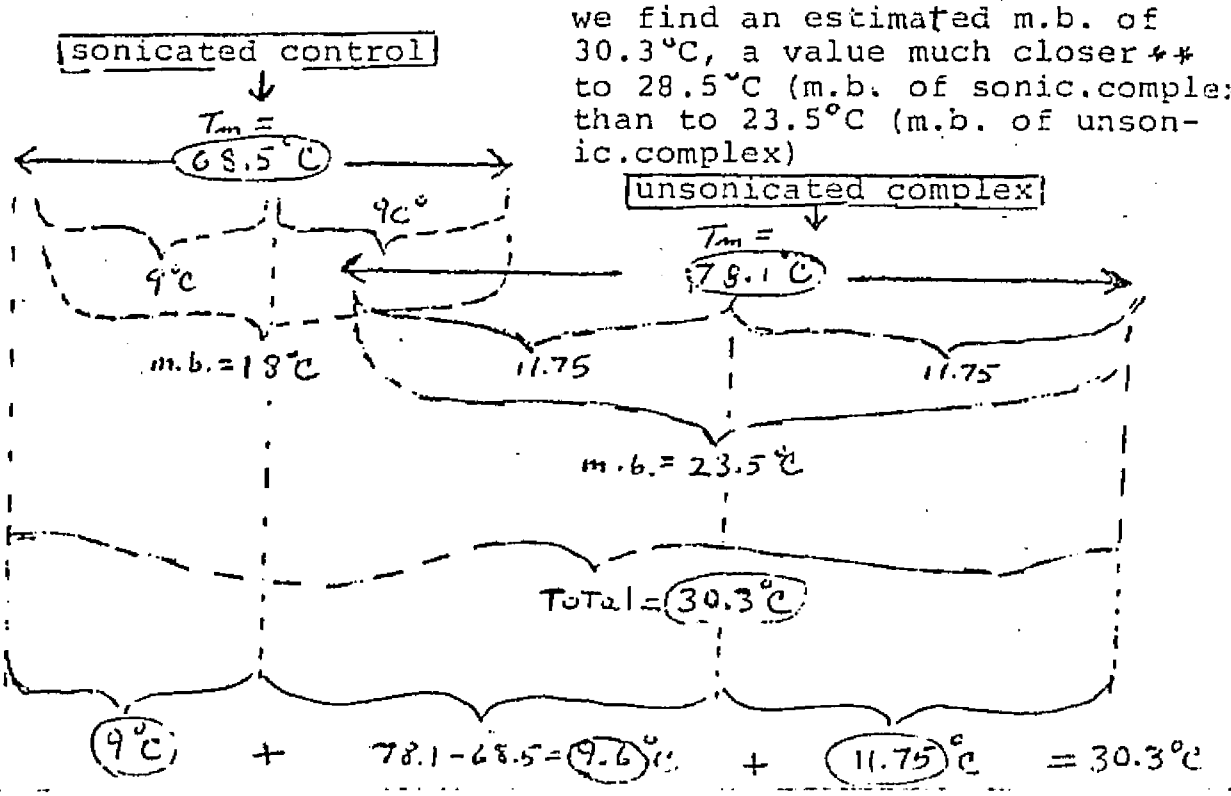

** Supports the assumption that crosslinks lead to increases in m.b.

Appendix (6) : An accepted reaction (Alexander and Lett, 1960) for alkylating agents containing the aziridine ring is: (1)

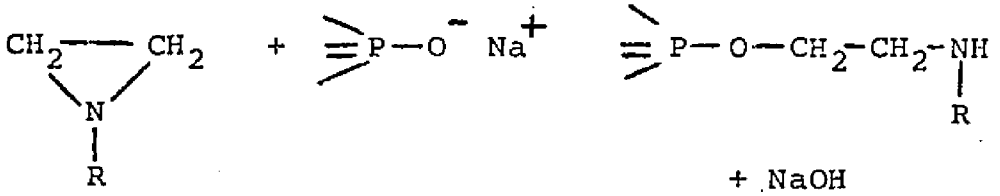

Ethyleneimine

Neutralization of one charge through esterification.

(2) In the case of Mitomycin C, a possible situation is:

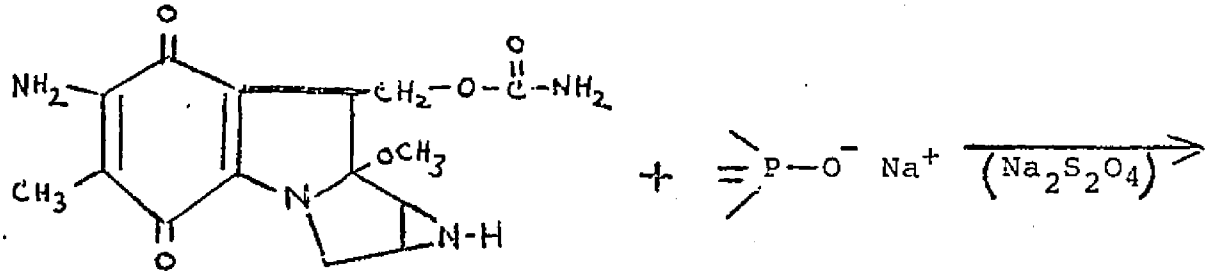

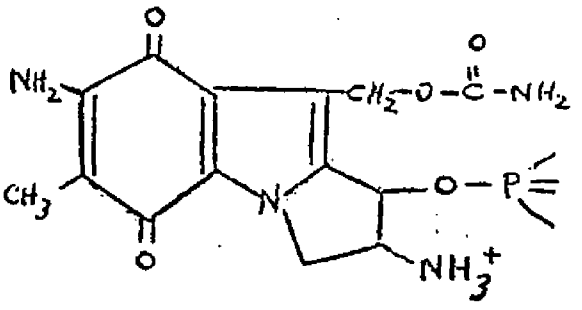

Neutralization of charge through esterification + the addition of positive charge

Appendix (7): Single strand breaks do not effect the flexibility of DNA in neutral buffer as has been determined by viscosity and sedimentation measurements of nicked (containing single strand breaks) and unnicked DNA (Hayes and Zimm, 1970). The explanation is that the nick or single strand discontinuity does not result in a "universal joint" in the molecule since the stacking interactions of the DNA bases overcomes any weakness introduced by the break (Parish, 1972).

In reference to $Na_2S_2O_4$; single strand breaks have been reported to be caused in many instances by other reducing agents including dithiothreitol, NADH, ascorbate (Bode, 1967), sodium bisulfite (Hayatsn and Miller, 1972) and cysteine (Rosenkranz and Rosenkranz, 1971). Since an oxygen dependence of the in vitro degradation of DNA has been shown in these cases, it can be said, similarly, that free radicals obtained from the oxidation of sodium dithionite may be responsible for the degradative effect seen in DNA.

Appendix (8): The rate of sedimentation of a macromolecule depends on the buoyancy of the particle as written by Cohen and Eisenberg (1969). The sedimentation coefficient (S) is:

(1) $$S = \frac{M_n}{f N} \cdot \left(\frac{\partial \rho}{\partial C_n}\right)_u = \frac{(1 - \bar{v}\rho) M_n}{f N}$$

$$S = \frac{M(1-\bar{v}\rho)}{Nf}$$

M_n = molecular weight of Nucleic Acid

f = particle frictional coefficient

N = Avogadro's number

$\left(\frac{\partial \rho}{\partial C_n}\right)_u$ = density increment due to nucleic acid at constant chem. potential of solutes

$\bar{v}$ = partial specific vol. of nucleic acid

ρ = density of solvent

Now for an ellipsoid of revolution (Müller and Crothers, 1968),

(2) $$\frac{f_r}{f_0} \simeq \left(\frac{L_r}{L_0}\right)^{.803}$$

f_r = frictional coefficient of a DNA-drug complex of binding ratio r

L_r = length of DNA-drug complex with binding ratio r

Subscript 0 denotes control DNA

it is clear that the frictional coefficient of DNA increases as its length increases and therefore, in regard to equation (1), the sedimentation coefficient would decrease.

Appendix (9): Bands are apparantly some form of DNA for the following reasons: First, all DNA has been previously deproteinated and further deproteinization (see methods) with subsequent Lowry protein determination insures the essential absence of protein. Secondly, these immobile bands stain with ethidium bromide and their flourescent intensity, as qualitatively seen, is reduced in parallel to the reduction of flourescent intensity of their appropriate mobile bands upon the binding of mitomycin C. Thirdly, unsonicated calf thymus DNA displays such immobile bands, but when sonicated, doe's not (compare figures (plates) C_2 and F_2). Therefore it appears that this band, if DNA, is being sonicated with the rest of the DNA into shorter fragments in the sonicated DNA samples. Furthermore, these bands do not interfere with the electrophoretic mobility of the moving band for the following reasons: First, the relative mobilities of various complexes, on any given gel, do not change in electrophoretic runs of various times (an interference in the mobility of the mobile band by the immobile band would probably produce different relative mobilities for the mobile band, according to time of the run, for a complex of any given binding ratio). Secondly, experiments varying the quantity of DNA (plate A_1) applied to the gel did not effect the relative mobility. Thirdly, the immobile bands of the DNA-MC complex with the highest binding ratio are not any larger than the immobile bands of control samples.

It is concluded that the large DNA fragments appear to be present for the following reasons: The calf thymus DNA was

prepared (personal communication; Worthington) using the method described by Zamenhof (1957). This method utilizes repetitive techniques of freezing, thawing, centrifugation and tissue grinder homogenizing which shears or breaks down the DNA to lower molecular weights. Viscosity measurements of calf thymus DNA (Zamenhof, 1957) prepared by this procedure give molecular weights of $5\text{-}6X10^6$ daltons, values which agree well with the viscometric determination of molecular weight in this lab. Calf thymus DNA prepared by means of a detergent method of DNA isolation (Kay et al., 1957) avoids mechanical shear breakage of DNA to any substancial level. As a result, the molecular weights of this DNA are in the area of $43\text{-}51X10^6$ daltons. From this information one may conclude that the immobile bands, as seen in the electrophoretic slab gels, are probably very large DNA fragments representing a small fraction of the total DNA.

Appendix (10): Lown et al.(1976) detected single strand breaks in DNA-MC complexes by an extremely sensitive assay: Unwinding of supercoiled PM2 DNA by the single strand breaks. These breaks were interpreted as being caused by superoxide formation. The autoxidation (reoxidation) of hydroquinones such as mitomycin C and streptonigrin may proceed via a semiquinone and the superoxide radical ($\cdot O_2^-$) which provides an explanation for the breakdown of DNA (Misra and Fridovich, 1972). Through the use of catalase or superoxide dismutase, or by the use of a combination of these enzymes, one is able to retard the induction of strand cleavage of DNA (Lown et al., 1976). (Although the hydroxyl radical ($\cdot OH$) has been shown to be the agent responsible for DNA strand cleavage itself (Morgan et al., 1976), the enzymes catalase and superoxide dismutase inhibit the formation of this radical by enzymatically inactivating, through chemical modification, key componants (i.e. ($\cdot O_2^-$) into H_2O_2, and H_2O_2 into H_2O and O_2) involved in a mechanism (Morgan et al., 1976) responsible for the production of this free radical.)

I used the more conventional assay, namely sedimentation in alkaline sucrose density gradients of calf thymus DNA to detect single strand breaks in DNA-MC complexes. (DNA containing single strand breaks such as those caused by streptonigrin (Cone et al., 1976) will, in alkali, sediment more slowly than control DNA due to its relatively shorter (lower M.W.) strands (Suzuki et al., 1969).) The results are negative (see figures 36 and 37) indicating that the breaks, if any, are undetectably rare in this system.

References

Aktipis, S., and Kindelis, A. (1973), Biochemistry 12, 1213.

Aktipis, S., Martz, W.W., and Kindelis, A. (1975), Biochemistry 14:2, 326.

Alberts, B.M., and Doty, P. (1968), J. Mol. Biol. 32, 379.

Alexander, P., and Lett, J.T. (1960), Biochemical Pharmacology 4, 34.

Ames, N.B., and Dubin, D.T. (1960), J. Biol. Chem. 235:3 769.

Beer, M. (1968), in Methods in Enzymology Vol. 12B, Grossman, L., and Moldave, K., Eds., Academic Press, N.Y.,p. 377.

Bishop, D.H.L., Claybrook, J.R., and Spiegelmen, S. (1967), J. Mol. Biol. 26, 373.

Blake, A., and Peacocke, A.R. (1968), Biopolymers 6, 1225.

Bloomfield, V.A., Crothers, D.M., and Tinoco, I., Jr. (1974), Physical Chemistry of Nucleic Acids, Harper and Row, Publishers, New York.

Bode, H.R., and Morowitz, H.J. (1967), J. Mol. Biol. 23, 191.

Brakke, M.K. and Pelt, N.V. (1970), Anal. Biochem. 38, 56.

Burgi, E., and Hershey, A.D. (1963), Biophys. J. 3, 309.

Chiang Tung, C., Miller, S.J., and Wetmur, J.G. (1974), Biochemistry 13:10, 2142.

Chrambach, A., and Rodbard, D. (1971), Science 172, 440.

Cohen, G., and Eisenberg, H. (1969), Biopolymers 8, 45.

Cohen, R.J., and Crothers, D.M. (1970), Biochemistry, 9:12, 2533.

Collins, P., and Davidson, N. (1969), Biopolymers 7, 335.

Cone, R., Hason, S.K., Lown, J.W., and Morgan, A.R. (1976), Can. J. Biochem. 54, 219.

Constantino, L., Liquori, A.M., and Vitagliano, V. (1964), Biopolymers 2, 1.

Cox, R.A. (1960), Journal of Polymer Science 47, 441.

Crothers, D.M., Kallenbach, N., and Zimm, B.H. (1965), J. Mol. Biol. 11, 802.

Crothers, D.M., and Zimm, B.H. (1965), J. Mol. Biol. 12, 525.

Danna, K.J., Sack, G.H., and Nathans, D. (1973), J. Mol. Biol. 78, 363.

Davidson, P.F. (1959), Proc. Natl. Acad. Sci. U.S.A. 45, 1560.

Davis, R.W., and Hyman, R.W. (1971), J. Mol. Biol. 62, 287.

Dermer, O.C., and Ham, G.E. (1969), in Ethylene and Other Aziridines, Academic Press, p. 425.

Dewachter, R., and Fiers, W. (1971), in Methods in Enzymology Vol. 21, Grossman, L., and Moldave, K., Eds., Academic Press, N.Y., p. 167

Dingman, W,C., Fisher, M.P., and Kakefuda, J. (1972), Biochemistry 11:7, 1242.

Doskočil, J., and Sormová, Z. (1963), Biochim. Biophys. Acta. 68, 313.

Doty, P., McGill, B.B., and Rice, S. (1958), Proc. Natl. Acad. Sci. U.S.A. 44, 432.

Douthart, R.J., and Bloomfield, V.A. (1968), Biopolymers 6, 1297.

Dove, W., and Davidson, N. (1962) J. Mol. Biol. 5, 467.

Drummond, D.S., Pritchard, N.J., Simpson, V.F.W., Gildemeister, P., and Peacocke, A.R. (1966), Biopolymers 4, 971.

Eigner, J., Schildkraut, C., and Doty, P. (1962), Biochim. Biophys. Acta. 55, 13.

Eigner, J., and Doty, P. (1965), J. Mol. Biol. 12, 549.

Eisenberg, H. (1969), Biopolymers 8, 1545.

Fisher, M.P., and Dingman, C.W. (1971), Biochemistry 10:10, 1895.

Flory, P.J. (1953), in Principles of Polymer Chemistry, chap. 10, Cornell Univ. Press, Ithica, N.Y.

Fuchs, R., and Daune, M. (1971), FEBS Letters 14:4, 206.

Fuchs, R., and Daune, M. (1972), Biochemistry 11:14, 2659.

Gabbay, E.J., Adawadkar, P.D., and Wilson, W.D. (1976a), Biochemistry 15:1, 146.

Gabbay, E.J., Grier, D., Fingerle, R.E., Reimer, R., Levy, R., Pierce, S.W., and Wilson, W.D. (1976b), Biochemistry 15:10, 2062.

Gabbay, E.J., Scofield, R.E., and Baxter, C.S. (1973), J. Am. Chem. Soc. 95:23, 7850.

Geiduschek, E.P. (1961), Proc. Natl. Acad. Sci. 47, 950.

Geiduschek, E.P. (1962), J. Mol. Biol. 4, 469.

Geiduschek, E.P. (1964), J. Mol. Biol. 8, 377.

Godfrey, J.E. (1976), Biophysical Chemistry 5, 285.

Haidle, C.W. (1971), Mol. Pharmacol. 7, 645.

Hamaguchi, K., and Geiduschek, E.P. (1962), J. Am. Chem. Soc. 84, 1329.

Harley, E.H., White, J.S., and Rees, K.R. (1973), Biochim. Biophys. Acta. 299, 253.

Hata, T. et al. (1956), J. Antibiotics, Japan, A, 9, 141.

Hayatson, H. and Miller, R.C. (1972), Biochem. Biophys. Res., Comm. 46, 120.

Hayes, S.B., and Zimm, B.H. (1970), J. Mol. Biol. 48, 297.

Herskovits, T.T., Singer, S.J., and Geiduschek, E.P. (1961), Arch. Biochem. Biophys. 94, 99.

Horiuchi, K. (1975), J. Mol. Biol. 95, 147.

Hotchkiss, R.D. (1957), Methods in Enzymology 3, 692.

Inman, R.B. (1967), J. Mol. Biol. 25, 209.

Iyer, V.N., and Szybalski, W. (1963), Proc. Natl. Acad. Sci. U.S.A. 50, 355.

Iyer, V.N., and Szybalski, W. (1964), Science 145, 55.

Johnson, P.H., and Grossman, L.I. (1977), Biochemistry 16:19, 4217.

Kapicak, L., and Gabbay, E.J. (1975), J. Am. Chem. Soc. 97:2, 403.

Kawawata, J. et al. (1966) in Abstracts of Papers of 9th International Cancer Congress, Tokyo, p. 196.

Kay, C.M., Simmons, and Dounce (1952), J. Am. Chem. Soc. 74, 1724.

Kerstein, H., and Rauen, H.M. (1961), Nature 190, 1195.

Kerstein, H. (1966), Biochemistry 5, 236.

Kinoshita, S., Uzu, K., Nakano, K., Shimizu, M., Takahashi, T., and Matsui, M. (1971). J. Med. Chem. 14, 103.

Kirsh, E.J., in Antibiotics; Gottlieb, D., and Shaw, P.D., Eds., Springer, N.Y., N.Y. (1967), p. 66-76.

Kleinschmidt, A., and Zahn, R. (1959), Z. Natursforsh 14B, 770.

Korn, D., and Weissbach, A. (1962), Biochim. Biophys. Acta. 61, 775.

Krey, A.K. and Hahn, F.E. (1970), FEBS Letters 10, 175.

Krey, A.K., and Hahn, F.E. (1975), Biochemistry 14:23, 5061.

Lang, D., Bujard, H., Wolff, B., and Russell, D. (1967), J. Mol. Biol. 23, 163.

LaRusso, N.F., Tomasz, M., Kaplan, D., and Muller, M. (1978), Antimicrobial Agents and Chemotherapy 13:1, 19.

Lee, C.S., and Davidson, N. (1968), Biopolymers 6, 531.

Lefermine, D.V., Dann, M., Barlatshi, F., Hausman, W.K., Zbinovsky, V., Mannikendam, P., Jadam, F., and Bohonos, N. (1962), J. Am. Chem. Soc. 84, 3184.

LePecq, J.B., and Paoletti, C. (1967), J. Mol. Biol. 27, 87.

Lerman, L.S. (1961), J. Mol. Biol. 3, 18.

Lerman, L.S. (1963), Proc. Natl. Acad. Sci. U.S.A. 49, 94.

Lerman, L.S. (1964), J. Cell. and Comp. Physiol. 64, Supp. 1,1.

Lett, J.T., Parkins, G.M., and Alexander, P. (1962), Arch. Biochem. Biophys. 97, 80.

Lipman, R., Weaver, J., and Tomasz, M. (1978), Biochim. et Biophys. Acta. 521, 779.

Lippard, S.J., Bond, P.J., Wu, K.C., and Bauer, W.R. (1976), Science 194, 726.

Lipsett, M.N., and Weissbach, A. (1965), FEBS Letters 4:2, 206.

Lloyd, R.S., Haidle, C.W., and Robberson, D.L. (1978), Biochemistry 17:10, 1890.

Lown, J.W., Begleiter, A., Johnson, D., and Morgan, A.R. (1976), Can. J. Biochem. 54, 110.

Lyons, J.W., and Kotin, L. (1965), J. Am. Chem. Soc. 87, 1670.

Mandelkorn, L., and Flory, P.J. (1952), J. Chem. Physics 20, 212.

Maniatis, T., Jeffrey, A., and Sande, H.V. (1975), Biochemistry 14:7, 3787.

Marmur, J. (1961), J. Mol. Biol. 3, 208.

Matsumato, I., and Lark, K.G. (1963), Exp. Cell Res. 32, 192.

Mercado, C.M., and Tomasz, M. (1972), Antimicrobial Agents and Chemotherapy 1:1, 73.

Mercado, C.M., and Tomasz, M. (1977), Biochemistry 16:9, 2040.

Mertz, J.E., and Berg, P. (1974), Proc. Nat. Acad. Sci., U.S.A. 71, 4879.

Misra, H.P., and Fridovich, I. (1972), J. Biol. Chem. 247, 581.

Morgan, A.R., Cone, R.L., and Elgert, T.M. (1976), Nuc. Acid Res. 3:5, 1139.

Müller, W. and Crothers, D.M. (1968), J. Mol. Biol. 35, 251.

Müller, W., and Crothers, D.M. (1975), Eur. J. Biochem. 54, 267.

Olivera, B.M., Baine, P., and Davidson, N. (1964), Biopolymers 2, 245.

Otsuji, N., Sekiguchi, M. Iijima, T., Takagi, Y. (1959), Nature 184, 1079.

Otsuji, N., Murayoma, I. (1972), J.Bact. 109, 475.

Parish, J.H. (1972) in Principles and Practices of Experiments with Nucleic Acids; J.Wiley & Sons, N.Y., N.Y.

Peacocke, A.C., and Dingman, C.W. (1968), Biochemistry 7, 668.

Peacocke, A.C., and Dingman, C.W. (1971), Molecular Biology of DNA and RNA; Mosby Isle, Author, p.145.

Povirk, L.F., Wübker,W., Köhnlein, W., and Hutchinson, T. (1977), Nuc. Acid Res. 4:10, 3573.

Pricer, W.E., Jr., and Weissbach, A. (1964), J. Biol. Chem. 239, 2607.

Pricer, W.E., Jr., and Weissbach, A. (1965), Biochem. 4, 200.

Rauen, H.M., and Kerstein, H.W. (1969), Hoppe Seylers Z. Physiol. Chem. 321, 139.

Reich, E., Shatkin, A.J., and Tatum, E.L. (1961), Biochem. Biophys. Acta, 53, 132.

Rosenkranz, H.S. and Rosenkranz, S. (1977), Arch. Biochem. Biophys. 146, 483.

Selker, E., Brown, K., and Yanofsky, C. (1977), J. Bact. 129, 388.

Shiba, et al., (1959), Biken's J. 1, 179.

Skoog, D.A., and West, D.M. (1965), Analytical Chemistry, an Introduction; Holt, Reinert, and Wilson, Publishers.

Small, G., Setlow, J.I., Kooistra, J., and Shapanka, R. (1976), J. Bacteriol. 125, 643.

Stewart, C.R. (1968), Biopolymers 6, 1737.

Strauss, V.P., and Rees, P.D. (1959), J. Am. Chem. Soc. 81, 5295.

Suzuki, H., Nagai, K., Yamaki, H., Tanaka, N., and Umezawa, H., (1969), J. Antibiotics 22, 446.

Szybalski, W. (1958), Ann. N.Y. Acad. Sci. 76, 475.

Szybalski, W., and Iyer, V.N. (1964a), Fed. Proc. 23, 946.

Szybalski, W., and Iyer, V.N. (1964b), Microbiol. Genetics Bulletin 21, 16.

Szybalski, W., and Menningham, H.D. (1962), Analytical Biochemistry 3, 267.

Schuerch, A.R., and Joklik, W.K. (1973), Virology

Taylor, G.I. (1936), Proc. Roy. Soc. London, A157, 546.

Taylor, W.G., and Remers, W.A. (1975), J. Med. Chem. 18, 307.

Tomasz, M., and Lipman, R. , Personnal Communication.

Tomasz, M., Mercado, C.M., Olson, J., and Chatterjie, N. (1974), Biochemistry 13, 4878.

Van Holde, K.E. (1971), Physical Biochemistry; Prentice Hall Publishers, N.J.

Vinograd, J., Lebowitz, J., and Radloff, R. (1965), Proc. Natl. Acad. Sci. U.S. 53, 1104.

Waring, M. (1970), J. Mol. Biol. 54, 247.

Weiss, M.J., Reding, G.S., Allen, G.R. Jr., Dornbush, A.C., Lindsay, H.L., Poleto, J.F., Remers, W.A., Roth, R.H., and Sioboda, A.E. (1968), J. Med. Chem. 11, 742.

Weissbach, A., and Lisio, A. (1965), Biochemistry 4, 196.

Zamanhof, S. (1957), Methods in Enzymology 3, 696.

Zimm, B.H., and Crothers, D.M. (1962), Biochemistry 48, 905.

Zimmer, C.H., Reinert, K.E., Luck, G., Wahnert, V., Lober, G., and Thrum, H. (1971), J. Mol. Biol. 58, 329.

Zimmer, C.H., Triebel, H., and Thrum, H. (1967), Biochim. Biophys. Acta. 145, 742.

Zunino, F. Gambetta, R., Mario, A.D., Velich, A., Zaccarra, A., Quadrifoglio, F., and Crezcenzi, V. (1977), Biochim. Biophys. Acta. 476, 38.